

**ZEOLITE DEACTIVATION DURING
HYDROCARBON REACTIONS:
CHARACTERISATION OF COKE
PRECURSORS AND ACIDITY, PRODUCT
DISTRIBUTION**

BAODONG WANG

**A Thesis submitted for the degree of Doctor of
Philosophy of the University College London**

Department of Chemical Engineering
University College London
London, WC1E 7JE

December 2007

ABSTRACT

The catalytic conversion of hydrocarbons over zeolites has been applied in large scale petroleum-refining processes. However, there is always formation and retention of heavy by-products, called coke, which causes catalyst deactivation. This deactivation is due to the poisoning of the acid sites and/or pore blockage. The formation of coke on hydrocarbon processing catalysts is of considerable technological and economic importance and a great deal of work has been carried out to this study.

The main aim of this work is to understand the deactivation of zeolite catalysts as a result of coke deposition. The deactivation by coke of USHY zeolite was investigated during catalytic conversion of hydrocarbons – 1-pentene, n-heptane and ethylbenzene – as representatives of olefins, paraffins and aromatics respectively, at different reaction temperatures, time-on-streams and composition. Three novel techniques, coke classification, thermogravimetric method for characterising coke precursors and indirect temperature programmed desorption (TPD) for catalyst acid sites characterisation were developed to further study catalyst deactivation mechanism. Product distribution, coke formation, characterisation of coke precursors, as well as the role of strong acid sites on hydrocarbon reactions are presented and discussed.

During catalytic reactions of 1-pentene over USHY zeolite, cracking and hydride transfer were the predominant reactions in initial stage which deactivated rapidly

allowing isomerisation to become the main reaction afterwards. Deactivation studies showed that coke formation was very strong initially which is in good correlation with the initial rapid deactivation. The hydrogen freed during this initial time from the formation of high C/H ratio coke components contributed to the formation of hydride transfer products. The amount of coke precursors decrease with increasing reaction temperature due to the higher desorption of coke precursors into gas phase while hard coke amount increased with temperature as expected from an activated process. The coke amount formed was not proportional to the reactant feed composition, because of a strong pseudo-zeroth-order initial coking on strong acidic sites. The thermogravimetric method provides insight into the chemical character of coke precursor components in terms of the mode of their removal and allows further classification of coke precursors into small and large coke precursors. The concentration and strength of acid sites of coked catalysts were studied by the TPD methodology. Besides, characterisation of coke precursors was also revealed. The initial deactivation preferentially on strong acid sites is very fast. The concentration of free acid sites is inversely correlated well with the total concentration of coke rather than individual coke groups. Coke precursors tend to be more stable at higher reaction temperatures. Furthermore, by selectively poisoning strong acid sites of USHY zeolite, it shows conclusively that strong acid sites are responsible for cracking and hydride transfer reactions as well as strong coke formation while weak acid sites can only catalyse double bond isomerisation.

ACKNOWLEDGEMENTS

I am extremely grateful to my supervisor Dr. George Manos for his guidance, his continual support and encouragement. I have benefited from his many words of wisdom, his high standard of accomplishment and for instilling in me his high ethical standards.

I would like to thank my colleagues, Panos, Seyed and Nnamso for all their help and encouragement. I especially thank Dr Enhong Cao for his assistance of GC set up.

I am greatly appreciative of my parents for their unwavering love and support during my PhD.

The financial support of the Overseas Research Students Awards Scheme and K. C. Wong Scholarship is gratefully acknowledged. The conference grants funded by UCL graduate school and the Royal Academy of Engineering are appreciated.

ABSTRACT	1
ACKNOWLEDGEMENTS.....	3
LIST OF FIGURES	8
LIST OF TABLES	14
1 INTRODUCTION.....	15
2 LITERATURE SURVEY	20
2.1 ZEOLITES	20
2.1.1 <i>History of Zeolites</i>	21
2.1.2 <i>Zeolite Composition and Structure</i>	24
2.1.3 <i>Aluminum Content and Acidity</i>	28
2.1.4 <i>Zeolites X and Y (Faujasites)</i>	31
2.2 ADSORPTION AND DIFFUSION	33
2.3 SHAPE SELECTIVITY.....	38
2.4 HYDROCARBON REACTIONS OVER SOLID ACIDIC CATALYSTS.....	40
2.4.1 <i>Foundations of Catalytic Cracking</i>	41
2.4.2 <i>Cracking of Alkenes</i>	43
2.4.3 <i>Cracking of Alkanes</i>	50
2.4.4 <i>Cracking of Alkylbenzenes</i>	58
2.5 COKING AND DEACTIVATION	59
2.5.1 <i>Coke Characterisation</i>	60
2.5.2 <i>Effects on Coking</i>	62
2.5.2.1 <i>Pore Structure Effect</i>	62
2.5.2.2 <i>Active Sites Effect</i>	64

2.5.2.3	<i>Operating Condition Effect</i>	65
2.5.2.4	<i>Nature of the Feed Effect</i>	68
2.5.3	<i>Modes of Deactivation</i>	68
2.5.3.1	<i>Active Sites Poisoning</i>	69
2.5.3.2	<i>Pore Blockage</i>	71
3	EXPERIMENTAL WORK	72
3.1	EQUIPMENT	72
3.1.1	<i>Reactor</i>	72
3.1.2	<i>Saturator</i>	74
3.1.3	<i>Ten-way Sampling Valve</i>	77
3.1.4	<i>Gas Chromatograph</i>	78
3.1.5	<i>Thermogravimetric Analysis</i>	82
3.1.6	<i>Temperature Programmed Desorption</i>	82
3.2	EQUIPMENT PROCEDURES	85
3.3	CATALYST PREPARATION	87
3.4	CALCULATIONS	88
3.4.1	<i>Components Mole Fraction Calculation</i>	88
3.4.2	<i>Conversion</i>	88
3.4.3	<i>Novel Methods for Coke Characterisation</i>	90
3.4.3.1	<i>Coke Classification</i>	90
3.4.3.2	<i>Coke Precursors Characterisation</i>	91
3.4.3.3	<i>Determination of Activation Energy</i>	95
3.4.4	<i>Acid Site Characterisation</i>	97
4	EXPERIMENTAL RESULTS & DISCUSSION	104
4.1	FIXED-BED REACTOR STUDIES	104
4.1.1	<i>Products Distribution</i>	104

4.1.2	<i>Conversion</i>	111
4.2	THERMOGRAVIMETRIC CHARACTERISATION OF COKE	
	COMPONENTS	112
4.2.1	<i>Coke Content</i>	113
4.2.2	<i>Coke Precursors Characterisation</i>	118
4.2.2.1	<i>Effect of Different Reactants</i>	118
4.2.2.2	<i>Effect of Time-On-Stream (TOS)</i>	121
4.2.2.3	<i>Effect of Reaction Temperatures</i>	125
4.2.2.4	<i>Effect of Reactant Composition</i>	128
4.2.3	<i>Activation Energy (E_A) of Coke Precursors</i>	129
4.3	TPD RESULTS	133
4.3.1	<i>Effect of Different Reactants</i>	133
4.3.2	<i>Effect of Time-On-Stream (TOS)</i>	140
4.3.3	<i>Effect of Reaction Temperature</i>	144
4.4	THE ROLE OF STRONG ACID SITES ON HYDROCARBON	
	REACTIONS	148
4.4.1	<i>Catalyst Preparation</i>	149
4.4.2	<i>Reaction Experiments</i>	152
4.4.3	<i>Results and Discussion</i>	153
4.4.3.1	<i>Product Distribution and Conversion</i>	153
4.4.3.2	<i>Purge with Nitrogen in order to Test Hydrogen Release Delay</i>	160
4.4.3.3	<i>Coke Formation and Acid Site Characterisation</i>	163
5	CONCLUSION AND FUTURE WORK	169
5.1	CONCLUSIONS	169
5.2	FUTURE WORK	172
	REFERENCES	174

APPENDIX 1	189
APPENDIX 2	191
APPENDIX 3	192
APPENDIX 4	193

LIST OF FIGURES

Figure 2-1 Primary building blocks of zeolite	24
Figure 2-2 Pore dimensions of zeolites and critical dimensions of some hydrocarbons	26
Figure 2-3 Formation of a Lewis acid site via dehydroxylation of two Brønsted acid sites by heating zeolites	29
Figure 2-4 Structure of faujasite	32
Figure 2-5 Steps in a heterogeneous catalytic reaction.....	34
Figure 2-6 Diffusivity against pore size.....	36
Figure 2-7A Steps of catalytic reaction.....	37
Figure 2-8 Shape selectivity.....	40
Figure 3-1 The fixed-bed reactor placed inside the furnace (not to scale).....	73
Figure 3-2 Flow chart for nitrogen branches.	76
Figure 3-3 GC system	79
Figure 3-4 Flow chart of Temperature-Programmed Desorption.	85
Figure 3-5 Set up of the fixed-bed reactor equipment.	86
Figure 3-6 Coke precursors and hard coke of a coked sample during thermogravimetric analysis.	91
Figure 3-7 Mass fraction of coke precursors removed from coked catalyst against TGA time.	94
Figure 3-8 Mass fraction of coked precursors removed on coked catalyst against the TGA temperature.....	94

Figure 3-9 Description of free acid sites by the difference of first TPD and TPD without NH ₃ (1-pentene reaction, T = 623 K, TOS = 1 min). For comparison, in the same figure it is shown the acidity of fresh USHY zeolite.....	101
Figure 3-10 Procedure of mild temperature pre-treatment and indirect TPD.....	102
Figure 3-11 TPD temperature programme.....	102
Figure 4-1 Product distribution of 1-pentene reaction over USHY zeolite at 523 K.	105
Figure 4-2 Product distribution of 1-pentene reaction over USHY zeolite at 573 K.	105
Figure 4-3 Product distribution of 1-pentene reaction over USHY zeolite at 623 K.	106
Figure 4-4 Reaction network of 1-pentene reaction.....	107
Figure 4-5 Product distribution of 1-pentene reaction over USHY zeolite at 573 K in short TOS.	110
Figure 4-6 Conversion of 1-pentene reaction over USHY zeolite at various reaction temperatures	112
Figure 4-7 Coke content of 1-pentene reaction over USHY zeolite at 523 K. ...	114
Figure 4-8 Coke content of 1-pentene reaction over USHY zeolite at 573 K. ...	115
Figure 4-9 Coke content of 1-pentene reaction over USHY zeolite at 623 K. ...	115
Figure 4-10 Coke content after 20 min TOS of 1-pentene reaction over USHY zeolite at different reaction temperatures.....	117
Figure 4-11 Mass fraction of coke precursors removed from coked catalyst against the TGA-time for different reactants, reaction temperature is 623 K, TOS=20 min.	120

Figure 4-12 Coke removal rate against TGA-time for samples coked during reactions of different reactants, 1-pentene, n-heptane and ethylbenzene (Reaction temperature = 623 K, TOS=20 min).....	120
Figure 4-13 Mass fraction of coke precursors removed from coked catalyst against the TGA running time at various TOS, reaction temperature = 523 K.....	122
Figure 4-14 Mass fraction of “small” and “large” coke precursors at different TOS.	123
Figure 4-15 Mass fraction of coke precursors removed from coked catalyst against the TGA running time at various reaction temperatures, TOS = 20 min....	125
Figure 4-16 Mass fraction of coke precursors removed from coked catalyst against the TGA running time at various reaction temperatures, TOS = 3 min.....	126
Figure 4-17 Coke percentage at different reaction temperatures (TOS = 3 min).	127
Figure 4-18 Coke content at 20 min time-on-stream of 1-pentene reactant over USHY zeolite at different reactant composition (T = 573 K).....	129
Figure 4-19 Original TGA curve of coke precursor removed over USHY zeolite.	130
Figure 4-20 Coke precursor mass fraction vs. temperature.	130
Figure 4-21 Plots of the decadic logarithm of heating rate against reciprocal temperature.....	131
Figure 4-22 Activation energy vs. residual fraction weight for coke precursor degradation over USHY zeolite.	132
Figure 4-23 TPD without ammonia of deactivated USHY zeolite coked during different reactant systems (T = 623 K, TOS = 20 min).	134

Figure 4-24 First TPD, TPD without NH ₃ and Free acid sites of deactivated USHY zeolite coked during 1-pentene reactions (T = 623 K, TOS = 20 min).	136
Figure 4-25 First TPD, TPD without NH ₃ and Free acid sites of deactivated USHY zeolite coked during n-heptane reactions (T = 623 K, TOS = 20 min).	137
Figure 4-26 First TPD, TPD without NH ₃ and Free acid sites of deactivated USHY zeolite coked during ethylbenzene reactions (T = 623 K, TOS = 20 min).	137
Figure 4-27 Second TPD of deactivated USHY zeolite coked during different reactant systems (T = 623 K, TOS = 20 min).	138
Figure 4-28 TPD without ammonia of deactivated USHY zeolite coked during 1-pentene reactions at different TOS (T = 623 K).	140
Figure 4-29 TGA-measured coke content of deactivated USHY zeolite coked during acid catalytic cracking reaction of 1-pentene at different TOS (T = 623 K).	141
Figure 4-30 1st TPD of deactivated USHY zeolite coked during 1-pentene reactions at different TOS (T = 623 K).	142
Figure 4-31 Free acid sites of deactivated USHY zeolite coked during 1-pentene reactions at different TOS (T = 623 K).	143
Figure 4-32 Second TPD of deactivated USHY zeolite coked during 1-pentene reactions at different TOS (T = 623 K).	144
Figure 4-33 TGA-measured coke content of deactivated USHY zeolite coked during acid catalytic cracking reaction of 1-pentene at different reaction temperatures (TOS = 20 min).	145

Figure 4-34 TPD without ammonia of deactivated USHY zeolite coked during 1-pentene reactions at different reaction temperatures (TOS = 20 min).	146
Figure 4-35 First TPD of deactivated USHY zeolite coked during 1-pentene reactions at different reaction temperatures (TOS = 20 min).	147
Figure 4-36 TPD of fresh catalyst, Free acid sites and Second TPD of deactivated USHY zeolite coked during 1-pentene reactions at different reaction temperatures (TOS = 20 min).	147
Figure 4-37 Acid sites distribution of fresh catalyst, PCS1 (pre-coked catalyst, deactivated at 573 K for 20 min with coke precursors removed- only hard coke remaining) and PCS2 (pre-coked catalyst, deactivated at 623 K for 300 min with coke precursors removed- only hard coke remaining).....	151
Figure 4-38 Deconvolution into weak and strong acid sites distribution of fresh catalyst, PCS1 (coked catalyst, deactivated at 573 K for 20 min with coke precursors removed- only hard coke remaining) and PCS2 (coked catalyst, deactivated at 623 K for 300 min with coke precursors removed- only hard coke remaining).....	152
Figure 4-39 Cracking products ($C_3=$ + iso- C_4) of 1-pentene reaction over different catalyst at 573 K for 20 min.....	154
Figure 4-40 Hydride transfer products (n- C_5 + 2-m- C_4) of 1-pentene reaction over different catalyst at 573 K for 20 min.	155
Figure 4-41 Double bond isomerisation products (trans-2- $C_5=$ + cis-2- $C_5=$) of 1-pentene reaction over different catalyst at 573 K for 20 min.....	156
Figure 4-42 Skeletal isomerisation products (2-m-1- $C_4=$ + 2-m-2- $C_4=$) of 1-pentene reaction over different catalyst at 573 K for 20 min.....	157

Figure 4-43 Conversion over fresh catalyst, PCS1 (coked catalyst, deactivated at 573 K for 20 min with coke precursors removed- only hard coke remaining) and PCS2 (coked catalyst, deactivated at 623 K for 300 min with coke precursors removed- only hard coke remaining).	159
Figure 4-44 Product distribution vs TOS during 1-pentene reactions over fresh USHY catalyst at 573 K.....	162
Figure 4-45 Product distribution vs TOS during 1-pentene reactions over fresh USHY catalyst with purging N ₂ at 573 K.	162
Figure 4-46 TPD without ammonia of deactivated USHY zeolite coked over different catalyst (T = 573 K, TOS = 20 min).	165
Figure 4-47 Acid sites deactivation model.....	165
Figure 4-48 TPD of Total acid sites, Free acid sites and Second TPD of deactivated fresh catalyst coked during 1-pentene reactions at 573 K and TOS = 20 min.....	166
Figure 4-49 TPD of Total acid sites, Free acid sites and Second TPD of deactivated PCS1 coked during 1-pentene reactions at 573 K and TOS = 20 min.	167
Figure 4-50 TPD of Total acid sites, Free acid sites and Second TPD of deactivated PCS2 coked during 1-pentene reactions at 573 K and TOS = 20 min.	167

LIST OF TABLES

Table 2-1 Zeolite History	22
Table 2-2 Some commercial zeolites and their uses	23
Table 2-3 Zeolites and their properties	27
Table 3-1 Residence times at all experimental conditions.....	74
Table 3-2 Nitrogen flow rate and composition at all experimental conditions.....	77
Table 4-1 Coke content of USHY zeolite coked during reactions of different reactants, T = 623 K, TOS = 20min.....	118
Table 4-2 Coke precursors content from different reactants measured by TPD and TGA (T = 623 K, TOS = 20 min).	135
Table 4-3 Coke content of PCS1 and PCS2 under the specified reaction conditions.	150
Table 4-4 Content of coke formed over fresh catalyst, PCS1 and PCS2 at 573 K and TOS=20 min (additionally formed hard coke for PCS1 and PCS2). ...	163

1 INTRODUCTION

Petroleum stock typically contains a large fraction of organic compounds which can not be used effectively due to their large molecular structures. The large organic molecules were first cracked commercially in 1912 by thermal reactions using temperatures in excess of 400 °C (Hatch, 1969). Thermal cracking has been significantly phased out industrially and replaced by a more efficient catalytic cracking process. Catalytic cracking over zeolite-based catalysts is an important reaction in the refining and petrochemical industry (Shuo and George, 2004). The significant breakthrough, introduction of catalysts, was developed in the 1930s. Catalytic cracking quickly replaced thermal cracking in the commercial conversion of crude oil to transportation fuels. Since then, many major improvements have been taken for cracking technology not only in reactor configuration but also in catalyst formulation. The establishment of many industrial and academic research and development laboratories has supported these improvements. However, this research has been largely on an empirical nature. Although the empirical approach has been very successful in terms of the technological advances it has achieved to date, it has left large gaps in the understanding of this important branch of science. Fundamental understanding of the processes underlying the conversion of petroleum distillates into internal combustion-engine fuel has progressed considerably over the years, but still leaves many scientific aspects in the dark (Wojciechowski, 1998).

In the beginning, catalytic cracking involved the use of an acid treated natural clay catalyst, montmorillonite, which greatly improved the efficiency of the cracking process. The natural clays were soon replaced by artificial clays such as amorphous silica-alumina, silica magnesia, and silica zirconia (Wojciechowski, 1998). Although these materials were more costly than the natural clays, they further improved the efficiency of the process. The 1960s saw the evolution of zeolite type materials (crystalline aluminosilicates) which were typically used in an amorphous silica-alumina matrix. Microporous materials, notably zeolites, have replaced corrosive and polluting acids (H_2SO_4 , $AlCl_3$) as catalysts in many refining and petrochemical process. The choice of zeolite catalysts is firmly due to their remarkable acidic properties. Indeed the density and strength of their acid sites can be varied on a large scale and can be adjusted to the desired catalytic reactions. The high thermostability of zeolites is another characteristic, which renders them particularly attractive for processes requiring repetitive regeneration steps at high temperatures. Another major advantage of zeolites is their well-defined pore structure, which apertures and cavities of approximately the size of organic molecules (Guisnet and Magnoux, 1997b). This so-called shape selectivity of zeolites has stimulated research on the synthesis of new molecular sieves, and originated the development of various commercial processes. In more traditional oil refining, zeolite catalysts are involved in the processing of almost every fraction of the crude oil barrel. These materials were found to give excellent products from cracking reactions, in the range of gasoline compounds. Zeolites are widely used catalysts for reactions involving acid catalysts. Their main application, in catalytic cracking, corresponds to the process that consumes the largest amounts of solid catalysts (Costa et al., 1999c).

During the transformation of organic compounds over solid catalysts, there is always formation and retention of heavy side-products, either in the pores or on the outer surface or in both positions (Guisnet and Magnoux, 2001). The formation of these non-desorbed products, generally called coke, is the most frequent cause of catalyst deactivation in industrial processes and is of considerable technological and economical importance to the petrochemical industry (Holmes et al., 1997). Coke is a general name for a mixture of heavy, strongly adsorbed side-products formed on the surface of solid catalysts during organic catalytic reactions. It consists of a large number of non-volatile, low boiling point, low hydrogen content components and is usually the main cause of catalyst deactivation due to the poisoning of the active sites and/or to pore blockage. Coke formation generally occurs via a sequence of elementary reactions which are dependent on the type of reaction, feed composition, type of catalyst used and reaction-reactor environment. The precise mechanism of coke formation is not accurately defined and different precursors, such as styrene, cumene, alkenes, were proposed in the literature (Plank and Nace, 1955). Nevertheless it is more likely that precursors are of various types and that coke is the result of many chain reactions and rearrangements inside the channels and cavities and/or on the external surface. The composition of coke is also affected by a range of factors including the nature of the reactants, time-on-stream, temperature, acid site concentration and naturally the location of coke deposit. Coke will therefore have a broad range of composition dictated by these different factors.

In most commercial processes the cost of catalyst deactivation is very high. Hence, facilitating catalyst stability and optimising regeneration have become at least as

important as controlling the activity and selectivity. Whatever the industrial process, finding ways to limit deactivation by coking and to regenerate catalysts is an important economical objective. Therefore, while industrial laboratories try to find technical solutions, academic laboratories should establish the conceptual background indispensable to the understanding of the related problems (Guisnet and Magnoux, 1997b).

The current study involved the catalytic reactions of 1-pentene, n-heptane and ethylbenzene over USHY zeolite in the temperature range of 523 – 623 K and atmospheric pressure, in a fixed-bed reactor. The study focused on the following objectives:

- Identify the product distribution from 1-pentene catalytic reactions over USHY zeolite.
- Study the mechanisms of catalytic cracking and examine the effect of reaction temperature, time-on-stream and reactant composition.
- Observe coking behaviour during these reactions and study the deactivation mechanisms.
- Introduce coke classification method to study coke precursors and hard coke.
- Further characterise coke precursors by thermogravimetric method.
- Examine the acid sites characterisation of fresh and coked catalysts.
- Examine the role of strong acid sites in hydrocarbon conversions.

This thesis is divided into two main parts, literature survey and experimental results. In the theoretical chapter, the properties of zeolites as catalysts have been

briefly discussed. Moreover, the mechanisms of hydrocarbon reactions over solid catalysts have been explained. Finally, deactivation and coking have been discussed.

In the experimental chapter, the equipment procedure and principle of the apparatuses are described. Furthermore, the results are discussed in four aspects, products distribution (Fixed-bed reactor study), coke classification and characterisation (TGA results), acid sites characterisation (TPD results). Finally, the role of strong acid sites for hydrocarbon conversion is studied.

2 LITERATURE SURVEY

2.1 ZEOLITES

The classical definition of a zeolite is a crystalline, porous aluminosilicate. However, some relatively recent discoveries of materials virtually identical to the classical zeolite, but consisting of oxide structures with elements other than silicon and aluminum have stretched the definition. Most researchers now include virtually all types of porous oxide structures that have well-defined pore structures due to a high degree of crystallinity in their definition of a zeolite (Subhash Bhatia, 1990).

Zeolites are an important class of aluminosilicate crystalline materials, which find many useful applications in the industry. The zeolitic channels (or pores) are microscopically small, and in fact, have molecular size dimensions such that they are often termed “molecular sieves”. This fact has made them a subject of research of increasing importance. Their unique properties find use in such various fields as oil cracking, household detergents and nuclear waste disposal. The reason for their uniqueness is due to their symmetry and their highly specific three-dimensional structure. These properties, referred to as shape selectivity, are just one of the motives for the constant growing attention for zeolites. Their strong acidity is another aspect, as this gives them their catalytic properties. Zeolites are not only theoretically interesting, they are very easy to handle, which means that they are non-toxic, can be regenerated and can withstand temperatures up to 1300 °C, well above temperature limits of previously used catalysts.

Nature has provided us with 34 different zeolites. But among those of interest in industrial applications, only a few are found in abundance, and even fewer are industrially used. The industrial application of zeolites as catalysts depends largely on our ability to synthesise zeolites. The synthesis of known and new structures has made new discoveries in zeolite catalysis possible. Today, more than a few hundreds different aluminosilicate zeolite structures are available (N.Y.Chen et al., 1996).

During the last 20 years, zeolite catalysis has had a revolutionary impact on both fundamental and applied catalysis. The use of zeolite as a catalyst is wide-spread for numerous important processes throughout the chemical and petroleum processing industries (Subhash Bhatia, 1990).

2.1.1 History of Zeolites

In 1756, the Swedish mineralogist A. F. Cronstedt was the first to discover a new class of materials consisting of hydrated aluminosilicates of the alkaline earth. The mineral stilbite was heated and appeared to boil, so it got the name Zeolite (boiling stone) from the Greek “zeo”: boil, and “lithos”: stone (Farooq M.A. and Lemos, 1998).

The first ideas regarding the structure were proposed by Friedel in 1896. The idea of an open framework was based on the observations that various liquids such as chloroform, benzene and alcohols, were retained by some dehydrated zeolites. In

1925, dehydrated chabazite was observed to adsorb water, alcohols and formic acid, but no acetone, ether or benzene. This is the first example of zeolites working as a molecular sieve, and they were defined as porous materials that exhibited selective sorption properties. Only charcoal was known as an alternative to the natural zeolites at the time, but now the term “molecular sieves” also includes metallosilicates – and aluminates, aluminophosphates and other variants.

In 1948, R. M. Barrer produced the first synthetic zeolite, which was an analogue to mordenite. Since then, a large number of zeolites have been synthesized for different purposes, among these ZSM-5, Zeolite-A, X, and Y. At first some of these zeolites were produced commercially for drying natural gas and refrigerants only, but in the early 1960s, they were also applied as catalysts for isomerisation and cracking in the oil industry. In 1974, zeolite has been introduced as detergent additives in washing powders, replacing the environmental harmful phosphates (Farooq M.A. and Lemos, 1998).

Table 2-1 Zeolite History gives an account of zeolite history (Bennett et al., 1983) and Table 2-2 Some commercial zeolites and their uses indicates some synthetic as well as natural zeolites and their respective uses (Smith, 1993).

Table 2-1 Zeolite History

1756	Discovery and naming of first natural zeolite, stilbite
1825	Discovery of natural lecanite
1842	Discovery of natural faujasite
1862	First zeolite synthesis (levynite)
1864	Discovery of natural mordenite

1870-88	First ion exchange studies with zeolites
1890	Discovery of natural erionite
1929	Potential as strong acids described (Pauling)
1930-34	First zeolite structure determinations
1932	Zeolites described as molecular sieving
1942-45	Quantitative separations by molecular sieving
1948	First purely synthetic zeolite
1948	Synthesis of mordenite
1949	Preparation of acid forms of zeolites
1956-64	Synthesis of zeolites A, X and Y (Union Carbide)
1962	Introduction of zeolite-based cracking catalysts (Mobil Oil Corp.)
1975	ZSM-5 catalysts used in ethyl benzene production
1978	ZSM-5 catalysts used in oil dewaxing
1978	Structure of ZSM-5 and ZSM-11
1980	High resolution electron microscopy and NMR applied to zeolite
1985	Methanol to gasoline plant (ZSM-5 catalyst) due to start up
1986	Synthesis of aluminophosphate and highly siliceous zeolites UN-1 and FU-1

Table 2-2 Some commercial zeolites and their uses

Natural Zeolites	Uses	Synthetic Zeolites	Uses
Chabazite	Catalysis and Water Purification	A	Adsorption
Erionite		X	Cracking
Clinoptilolite		Y	Cracking
		ZSM-5	Isomerisation

The range of possible zeolite catalysed transformation has grown steadily in the past few decades, as experimental modifications were explored. By changing the

structure with other metals, changing the pore size and adjusting the acid sites zeolites are incorporated in more and more areas in the world of chemistry.

2.1.2 Zeolite Composition and Structure

The properties of a zeolite are dependent on the topology of its framework, the size, shape, and accessibility of its free channels, the location charge and size of the cations within the framework, the presence of faults and occluded material, the ordering of T-atoms, and the local environment of T-atoms. Therefore, structural information is extremely important in understanding the adsorptive and catalytic properties of zeolite catalysts (Breck, 1974; Rabo, 1976)

The fundamental building block of all zeolites is a tetrahedron of four oxygen anions surrounding a small silicon or aluminum ion. These tetrahedral are arranged so that each of the four oxygen anions is shared in turn with another silica or alumina tetrahedron. Figure 2-1 is primary building blocks of zeolite.

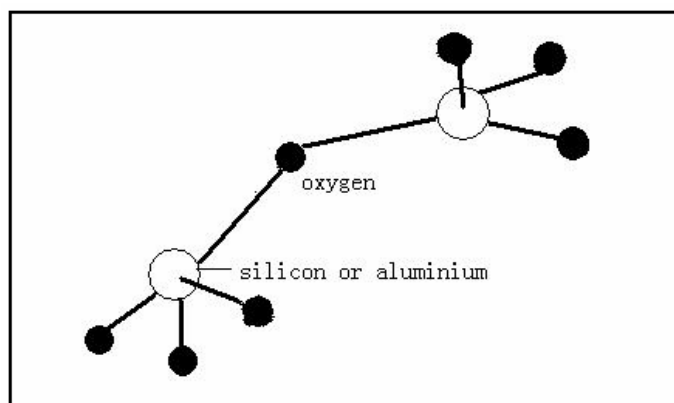
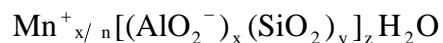


Figure 2-1 Primary building blocks of zeolite

The silica and alumina tetrahedral are combined into more complicated secondary units, which form the building blocks of the framework zeolite crystal structures.

The silica and alumina tetrahedral are geometrically arranged, with Al-O-Al bonds excluded. The unit cell formula is usually written as



where Mn^+ is the cation which balances the negative charge associated with the framework aluminum ions. These metal cations, which neutralize the excess anionic charge on the aluminosilicate framework, are usually alkali metal and alkaline earth metal cations and at least some of them must be able to undergo reversible ion exchange if the material is to be classed as zeolite. Water molecules fill the remaining volume in the interstices of the zeolite.

The tetrahedral are arranged so that the zeolites have an open framework structure, which defines a pore structure with a high surface area. The three-dimensional framework consists of channels and interconnected voids or cages. The cations and water molecules occupy the void spaces in the structure. The intracrystalline zeolitic water can be removed by thermal treatment, usually reversibly. The tetrahedra can be linked together in rings, to form secondary building units (SBU), and by combining them, different zeolite structure are formed. The SBUs are numbered according to the number of atoms in each ring, and number of bonded atoms between them.

The zeolites all contain intracrystalline pores and apertures having dimensions approximately equal to those of many of the molecules converted in catalytic processes. The average channel sizes of zeolites are summarized in Figure 2-2,

along with the sizes of the cavities (supercages) and the critical molecular dimensions of a number of hydrocarbons that are potential reactants in zeolite-catalyzed reactions (Gates B.C., 1992).

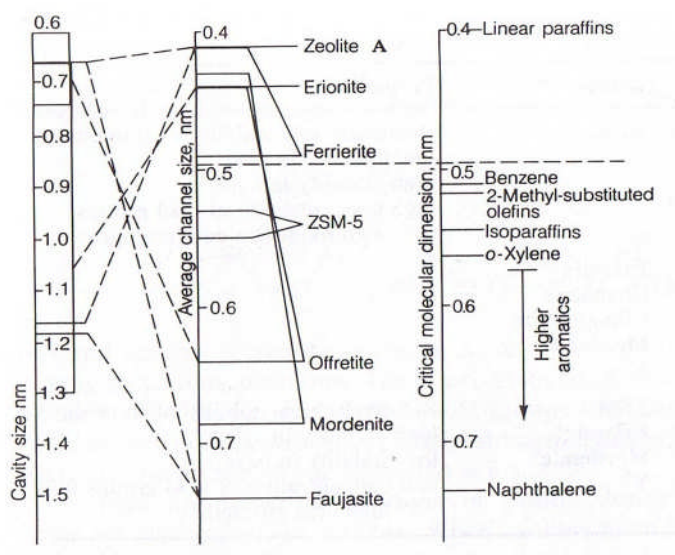


Figure 2-2 Pore dimensions of zeolites and critical dimensions of some hydrocarbons

The zeolites can be broken down into three basic classes according to the sizes of the apertures: small, medium and large. Besides their apertures, which are also referred as channels, some of the zeolites also have cages. Some of the zeolite structures have two sets of cages, the largest one called supercages. As can be seen in the following Table 2-3, the dimensions of the apertures vary according to the number of oxygen in the rings.

Table 2-3 Zeolites and their properties

Zeolite	Number of oxygen atoms in the ring	Dimensions of pore structure	Size of channels (Å)	Typical Si/Al ratio
Zeolite A	8	3	4.1	1-1.5
ZSM-5	10	3	5.4×5.6	>10
	10	3	5.1×5.5	
Mordenite	12	2	6.7×7.0	2-5
	8	2	2.9×5.7	
Faujasite	12	3	7.6	1-1.5 for X 1.5-3 for Y

As can be seen, zeolite A is the one with the smallest channels and has interconnecting channels and supercages. In contrary, faujasites have the biggest channels and supercages, which have made them suitable for cracking in the oil industry, as this allows larger hydrocarbon molecules to enter the pores. The medium pore zeolites, such as ZSM-5, has what is called a pentasil – structure, which does not contain any large supercages. ZSM-5 is usually used for isomerisation of n-butane to isobutane. Mordenite has large channels and is another zeolite with the pentasil structure. Its channel system is practically one dimensional, as the one set of channels has very small dimensions for any molecules to enter (Gates B.C., 1992)

2.1.3 Aluminum Content and Acidity

Zeolites are further grouped into families on the basis of the silicon to aluminium ratio (Si/Al ratio). Since the number of exchangeable cations is proportional to the number of Al^{3+} ions in the framework of the zeolite, the catalyst properties are dependent on the Si/Al ratio. The zeolites with high concentrations of H^+ are hydrophilic, having strong affinities for polar molecules small enough to enter the pores. The highly siliceous zeolites are inherently hydrophobic, taking up organic compounds from water-organic mixtures; the transition occurs at a Si/Al ratio near 10 (Flanigen et al., 1984).

On the other hand, the stability of the crystal framework decreases with increasing aluminium content. Decomposition temperatures range from 700 °C to 1300 °C. Zeolites with high Si/Al ratios are stable in the presence of concentrated acids, but those with low Si/Al ratios are not. Therefore, it is very important to achieve a balance between the catalytic activity of the zeolite and its stability.

The strength of acidity is also dependent on the Si/Al ratio. To understand the acidity, we may consider the simplified representation of the interior regions of the pores as shown in Figure 2-3. Here, the exchangeable cations are placed near AlO_4 tetrahedra because the negative charges are predominantly located here. However, in the actual zeolite, the negative charge is not localized on one or two tetrahedra but is mobile within the framework of oxygen ions. The distribution of negative charge may be important in catalysis in stabilizing cationic intermediates such as carbonium ions.

Zeolites as normally synthesised usually have Na^+ ions balancing the framework charges, but these can be readily exchanged for protons by direct reaction with an acid, giving surface hydroxyl groups- the bronsted sites. (A Bronsted acid is a proton donor whereas a Lewis acid is an electron acceptor). However, some zeolites, such as the faujasites, are unstable in acidic solutions and are activated by forming the ammonium, NH_4^+ , salt, and the heating the structure so that ammonia is driven off and the proton remains. Further heating (in both cases) removes water from the Bronsted site, exposing a tricoordinated Al ion, which has electron-pair acceptor properties, the Lewis acid site. This is shown schematically in Figure 2-3.

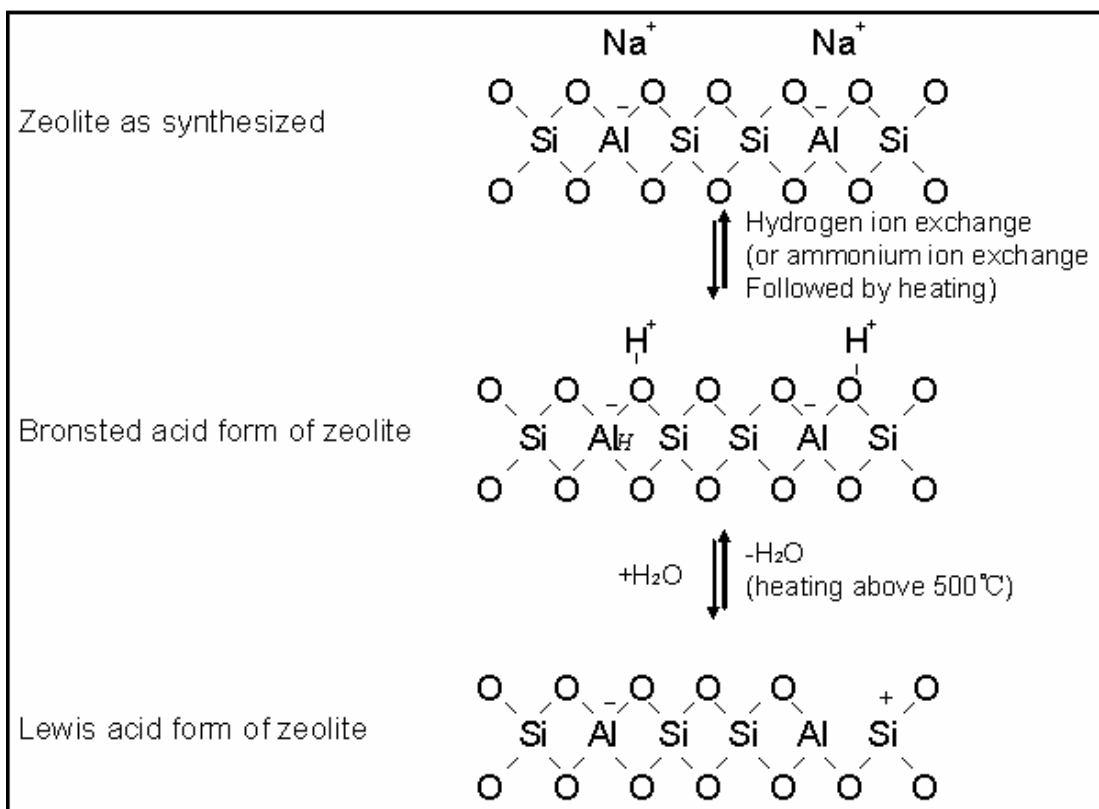


Figure 2-3 Formation of a Lewis acid site via dehydroxylation of two Brönsted acid sites by heating zeolites

There are wide distributions of proton donor strengths among the Bronsted acid groups in zeolites. When zeolites have low densities of proton donor groups, the proton donor strengths are high. For example, HY or HZSM-5 zeolite with a low density of acid group is like an ideal solution of dispersed non-interacting protons in a solid matrix.

Correlation between the acidity of a zeolite and its catalytic properties is a difficult task. Three factors are important: the total number of acid sites, the ratio of Brønsted acid sites to Lewis acid sites, and the acid strength distribution of each each type of site. For Y zeolites, a maximum in strong acid sites and cracking activity occurs at Si/Al ratio from about 7 to 15. In contrast, for ZSM-5, hexane cracking ability increases linearly with increasing aluminum content, leading to the conclusion that the maximum in acidity is a function not only the zeolite structure but also the surroundings of the aluminum atoms in the framework (Humphries et al., 1993).

Since there is one hydrogen per aluminum in the catalyst, as the amount of aluminum increases, the activity of the catalyst should also increase. The relation between aluminum content and activity for paraffin cracking and other reactions over H-Y and HZSM-5 has been noted by many authors (Decanio et al., 1986a; Decanio et al., 1986b; Beyerlein et al., 1988; Marziano et al., 1998; Williams et al., 1999). The catalyst activity dependence on aluminum content does not hold when the Si/Al of most zeolites is less than 10 (Decanio et al., 1986a; Decanio et al., 1986b). Activity is decreasing with a decrease in Si/Al ratio, when the Si/Al ratio is less than 10. It is argued that when the sites become too concentrated within the

catalyst, they interact causing a reduction in their acidity. A maximum activity at the Si/Al ratio of about 10 for most zeolites is observed due to site – site interactions at high activities.

Van Santen (1994) has focused his research on understanding the nature of Brönsted acid sites, which are generated as a result of protons balancing the charge associated with framework substitution of Al³⁺ for Si⁴⁺. Others have proposed methods (Gorte, 1999; Selli and Forni, 1999; Costa et al., 1999a; Costa et al., 1999b), which allow the estimation of the acid site strength distribution, by using temperature programmed desorption (TPD). The possibility of estimating these parameters is of paramount importance in the determination of relationships between activity and acidity.

Variation in acidity also influences the formation rate and composition of coke deposits. As coke is the most important parameter responsible for catalyst deactivation, the detailed characterisation of these deposits is essential. Today, varieties of techniques are available for the characterisation of coke and other related parameters. Although the nature and composition of coke has been extensively studied during various hydrocarbon transformations, the role of acidity is not yet fully understood from the available literature.

2.1.4 Zeolites X and Y (Faujasites)

The zeolites finding the largest-scale application in catalysis belong to the family of faujasites, including zeolite X and zeolite Y. Having 0.74 nm apertures (12-

membered oxygen rings) and a three-dimensional pore structure, they admit even hydrocarbon molecules larger than naphthalene. Their chief application is in catalytic cracking of petroleum molecules (primarily in the gas oil fraction), giving smaller, gasoline-range molecules.

The framework structure of zeolites X and Y is closely related to that of zeolite A. The sodalite cages in faujasites are arranged in an array with greater spacing than in zeolite A. Each sodalite cage is connected to four other sodalite cages; each connecting unit is six bridging oxygen ions linking the hexagonal faces of two sodalite units, as shown in Figure 2-4 (Gates B.C., 1992).

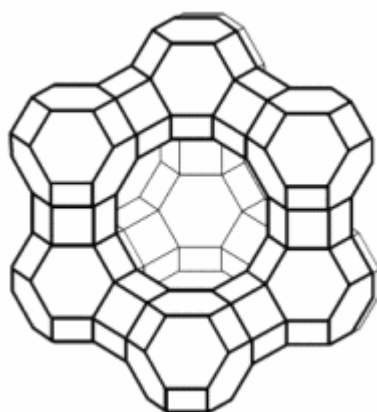


Figure 2-4 Structure of faujasite

Most zeolites are synthesized in the sodium form, the common starting materials for synthesis of zeolite Y being sodium aluminate, NaOH, and silica sol, and the product typically has the approximate composition $\text{Na}_2\text{O} \cdot \text{Al}_2\text{O}_3 \cdot 5.3 \text{SiO}_2 \cdot 5 \text{H}_2\text{O}$. Preparing the hydrogen form of zeolite Y is not so simple, because the faujasite framework collapses when in contact with strongly acidic solutions. This

difficulty can be circumvented by exchanging Na^+ with NH_4^+ and raising the temperature, causing the ammonium ions (now in the zeolite) to decompose into NH_3 gas, which leaves the zeolite, and H^+ ions, which remain in place (Gates B.C., 1992).

Ultrastable Y zeolite is relatively poorer in aluminum atoms and enriched in silicon atoms. Its silicon to aluminum ratio is 4 or more. This means that the aluminum atom density and therefore the acid site density is reduced. This aluminum deficient, or dealuminated, Y zeolite has higher thermal and hydrothermal stability than conventional Y zeolite. The added stability is the reason it is called "ultrastable zeolite". The increased isolation of the aluminum acid sites enhances their acidity and reduces their ability to catalyze reactions involving two or more molecules. These isolated sites give USY zeolite its characteristic ability to increase octane and olefin yield by reducing the effects of a bimolecular reaction called hydrogen transfer. This hydrogen transfer reaction saturates olefins that contribute to the octane potential of the gasoline.

2.2 ADSORPTION AND DIFFUSION

Adsorption and diffusion are two of the most fundamental processes in catalysis. Those molecules with higher rates of diffusion will obviously react preferentially and selectively, while products with higher diffusivity will desorb preferentially.

The overall process by which heterogeneous catalytic reactions proceed can be broken down into a sequence of individual steps as shown in Figure 2-5 and described as followed.

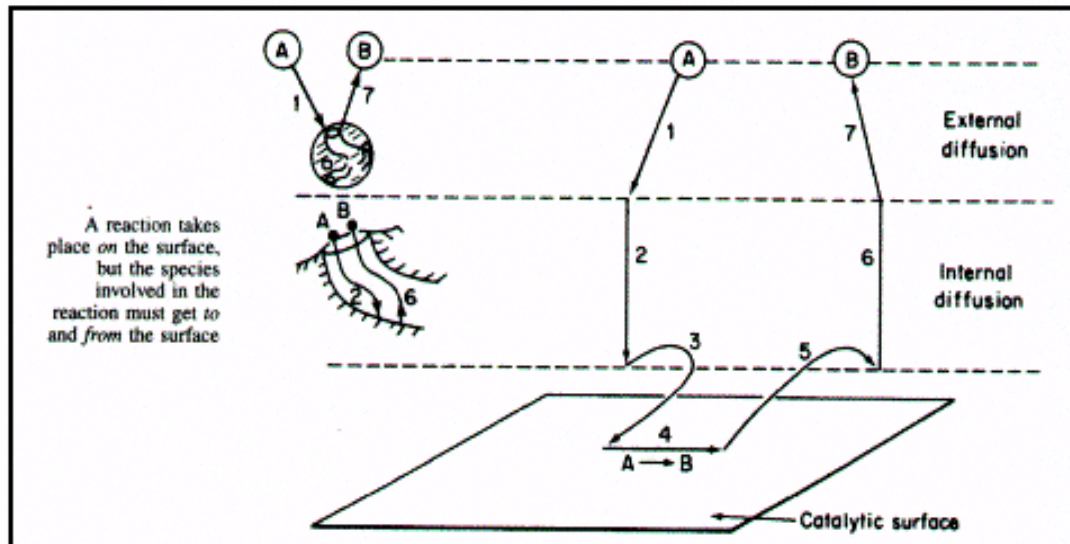


Figure 2-5 Steps in a heterogeneous catalytic reaction

The seven steps in the catalytic reaction:

- 1) External diffusion: mass transfer of the reactant molecules from the bulk fluid to the pore mouth at catalysts external surface
- 2) Diffusion of the reactant molecules into the catalyst pores
- 3) Adsorption and catalyst surface
- 4) Surface reaction to form products
- 5) Desorption of the product from the catalyst surface
- 6) Diffusion of the products from the interior of the pellet to the external surface
- 7) Diffusion of the products into the bulk fluid

The overall rate of a reaction is equal to the rate of the slowest step in the mechanism. When the diffusion steps are very fast compared with the reaction steps, the concentrations in the immediate vicinity of the active sites are indistinguishable from those in the bulk fluid. In this situation, the transport or diffusion steps do not affect the overall rate of the reaction. In other situations, if the reaction steps are very fast compared with the diffusion steps, mass transport does affect the reaction rate.

The diffusion phenomena can be looked at using a plot of diffusivity against pore size as shown in Figure 2-6. Zeolites with pore diameters in the range of 4 to 9 Å are shown to provide a region of diffusivity beyond the regular and Knudsen regions, which has been termed as configurational regime (Satterfield, 1980). This is the region where molecules must diffuse through spaces of near molecular dimensions and is thus of considerable importance in shape-selective catalysis, the effective diffusion coefficient is strongly small so that the mean free path is much greater than the pore size, the interactions with the pore walls predominate and we get Knudsen diffusion. For large pores, the interaction between the molecules is of primary consideration and molecular diffusion describes the transport regime.

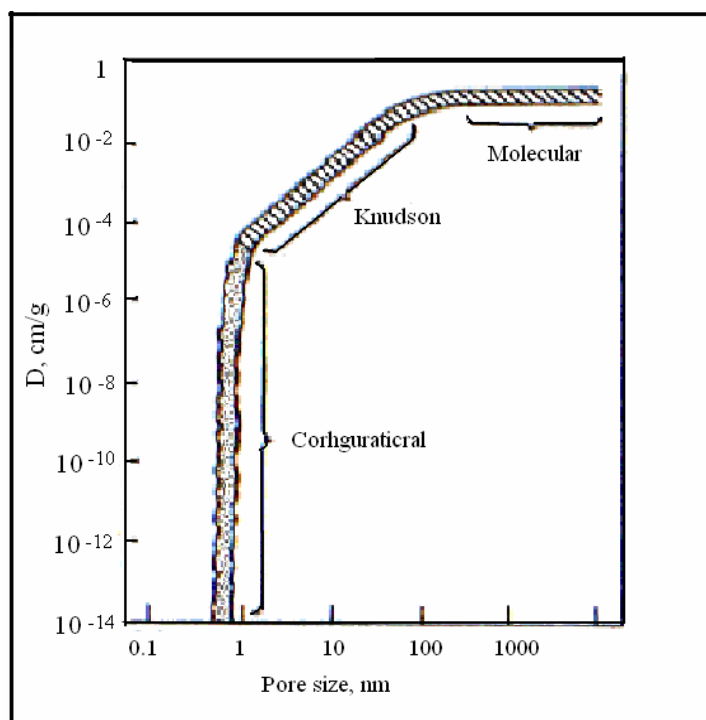


Figure 2-6 Diffusivity against pore size

For a catalytic reaction to occur, at least one and frequently all of the reactants must become attached to the surface. This attachment is known as adsorption and takes place by two different processes: physical adsorption and chemisorption. Physical adsorption represents weak van der Waals forces between the liquid and the solid. The type of adsorption that affects the rate of a chemical reaction is chemisorption. Here, the adsorbed atoms or molecules are held to the surface by valence forces of the same type as those that occur between bonded atoms in molecules. It is believed that the reaction is not catalysed over the entire solid surface but only at certain active sites or centres. An active site is defined as a point on the catalyst surface that can form strong chemical bonds with an adsorbed atom or molecule. The reaction model can be shown Figure 2-7A and Figure 2-7B.

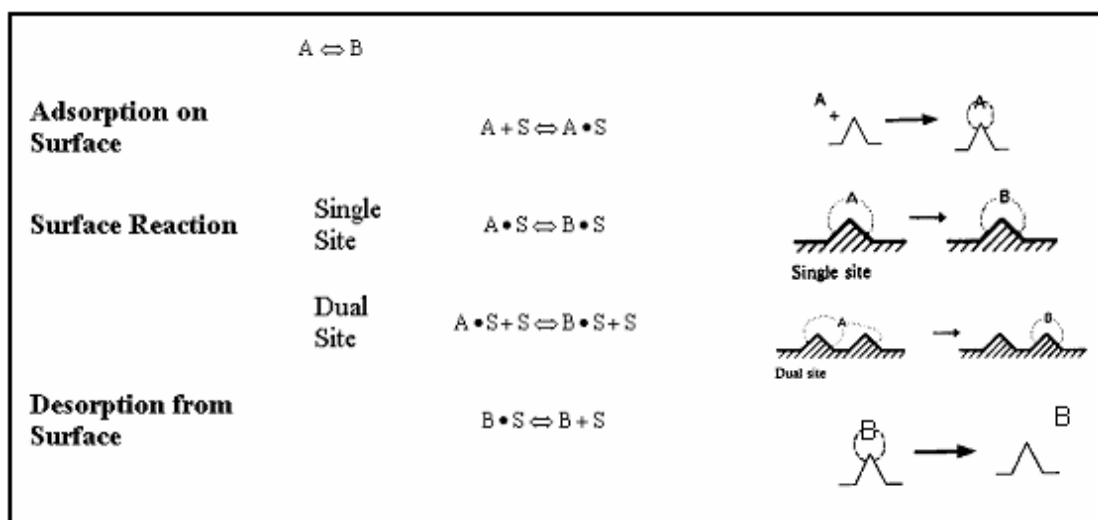


Figure 2-7A Steps of catalytic reaction

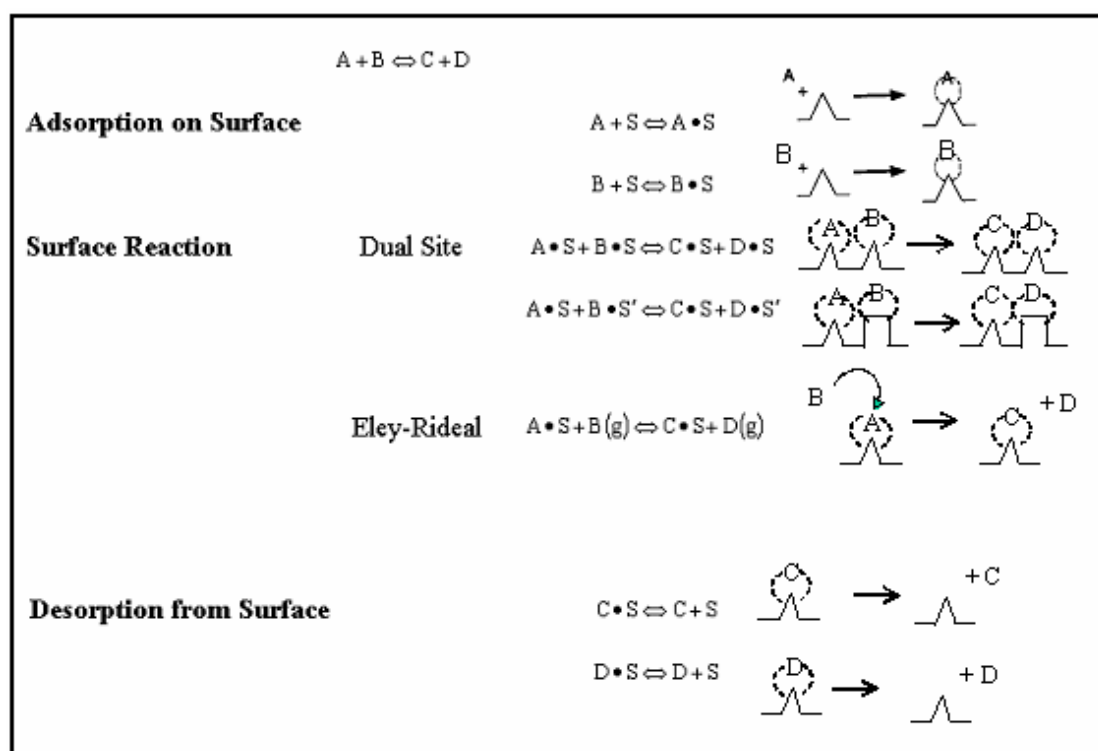


Figure 2-7B Steps of catalytic reaction

The void spaces in the structure of zeolites provide a high capacity for adsorbates, referred to as guest molecules. The sorption capacity is a conveniently measured

property that is used to identify zeolites, and is dependent on molecular size, shape and the topologies of the open framework within which the molecules move. The more condensable the guest molecules (or the lower the temperature), the more rectangular is the isotherm.

However, the transport processes are poorly understood and depend on many factors:

- 1) Intercrystalline channel geometry and dimensions.
- 2) Shape, size and polarity of the diffusing molecules.
- 3) Cation distributions, size, charges and number.
- 4) Concentration of diffusant within the crystals.
- 5) Temperature.
- 6) Lattice defects such as stacking faults
- 7) Presence of impurity molecules in the diffusion pathways.
- 8) Structural changes brought about by penetrants.
- 9) Structural changes associated with physical and chemical treatments.

2.3 SHAPE SELECTIVITY

It is generally accepted that zeolites catalyse via carbenium or carbonium ion intermediates, similar to reactions catalysed by strong acids in homogeneous media. The final product distribution, however, is greatly influenced by steric and

transport restrictions imposed by the narrow zeolite pore structure. The term used to describe these effects is called shape selectivity.

Shape selectivity can be divided into three major classes:

1) Reactant Shape Selectivity:

Only molecules with dimensions less than a critical size enter the pores and reach the catalytic sites, and so react there. In Figure 2-8 A we can see that a straight-chain hydrocarbon is able to enter the pore and react but the branched-chain is not.

2) Product Shape Selectivity:

Only products less than a certain dimension can leave the active sites and diffuse out through the channels. In Figure 2-8 B a mixture of all three isomers of oylene is formed in the cavities but only the para form is able to escape.

3) Transition State shape Selectivity:

This form of shape selectivity can limit or prevent the formation of intermediates in a reaction. The reactions, which require the smallest transition state, will proceed unhindered. This means that a reaction is limited by its mechanism rather than diffusion limitations. As is shown in Figure 2-8 for the trans alkylation of dialkylbenzenes.

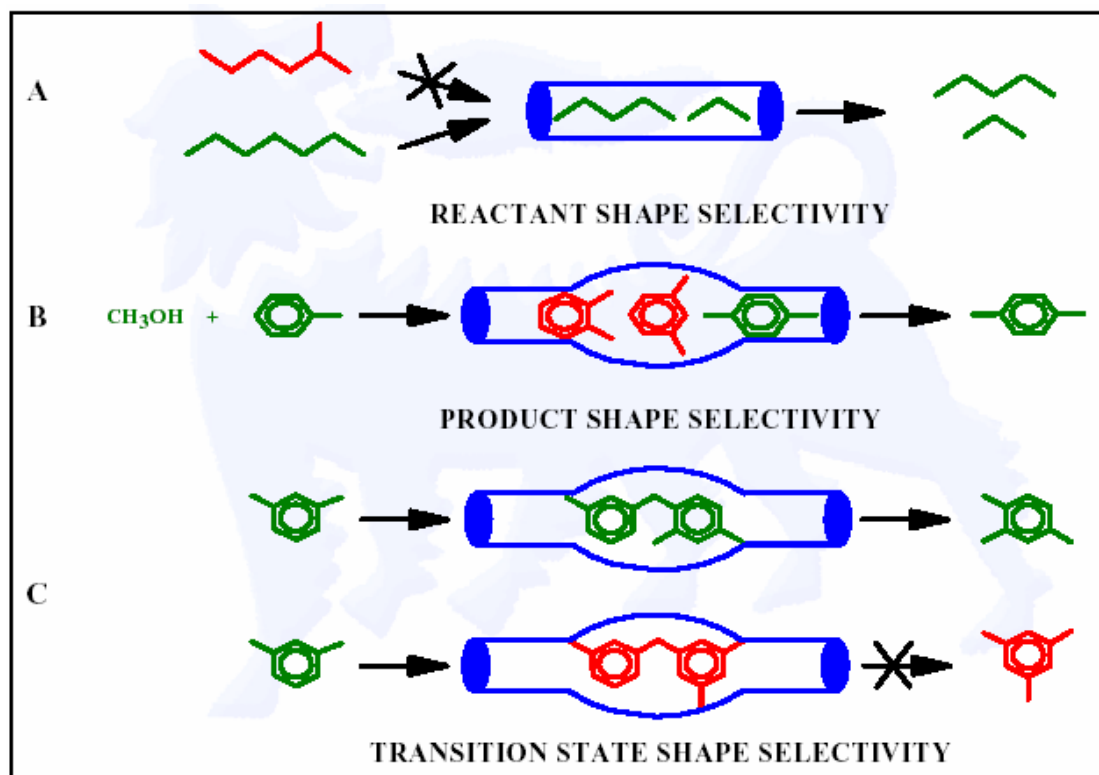


Figure 2-8 Shape selectivity

2.4 HYDROCARBON REACTIONS OVER SOLID ACIDIC CATALYSTS

Industrial applications of cracking catalyst were found well before the catalytic process was understood. When catalytic cracking was introduced, the thermal cracking process was understood to be based upon free radical mechanisms. The products distribution from catalytic cracking was found to be significantly different than the products distribution from thermal cracking. Free radical mechanisms were concluded to not be responsible for catalytic cracking. The

catalytic cracking of molecules is currently understood to be caused by acidic mechanisms relying on carbonium and carbenium ion reactions.

2.4.1 Foundations of Catalytic Cracking

The first information applicable to catalytic cracking was reported in 1933 by Gayer (Gayer, 1933). The polymerization reaction of propylene was investigated over alumina-silica catalyst. The investigation showed an improvement in the polymerization by the addition of hydrochloric acid to the reacting mixture or by acid treating the catalyst before reaction. The polymerization reactions showed the importance of acid characteristics in the formation and decomposition of carbon-carbon bonds. A mechanism was later postulated in 1934 by Whitmore (Whitmore, 1934) indicating how the acidic properties were important in olefin polymerization. The mechanism indicates that any substance that will give up hydrogen ions (H^+) could catalyze the polymerization.

The acidic mechanism of catalytic cracking was established in the late 40's and early 50's. Hansford in 1947 was one of the first to make a detailed study of the cracking of various hydrocarbons on silica-alumina catalyst (Hansford, 1947) along with deuterium exchange reactions. How acidic sites could exist on the catalyst was described. More importantly, a mechanism involving carbenium ions and carbonium ions was explained, while also mentioning that thermal decomposition may be included in the mechanism. The actual properties of the catalyst were taken a step further by Turkevich and Smith in 1948 (Turkevich and

R.K.Smith, 1948) who investigated the isomerisation of 1-butene using sulphuric and phosphoric acid. The idea that the acidic nature was the catalytic important characteristic was substantiated by hydrogen exchange, but the article claims that “the critical demand on the catalyst is that it be able to furnish a hydrogen and accept a hydrogen at a distance of approximately 3.5 Å”. The characteristic 3.5 Å distance being the distance between the first carbon and third carbon in a molecule. This theory is questionable in catalytic cracking since it predicts that silica gel (derived from silicic acid) should be an excellent catalyst and it is known to be ineffective for cracking reactions (Greensfelder et al., 1949).

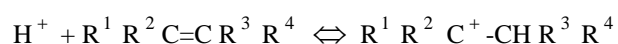
A detailed investigation of the acidic nature of a silica-alumina catalyst was reported in 1949 by Thomas (Thomas, 1949) along with the detailed investigation of the cracking mechanism by Greensfelder, Voge, and Good (Greensfelder et al., 1949) of the same year. Thomas indicated the importance of the presence of alumina in the catalyst and predicted the silica-alumina activity as a function of the acidic level. The silica-alumina activity was dependent on a tetrahedral oxygen structure surrounding each silica and aluminium atom. Greensfelder, et al., also supported Thomas’s work, but emphasized a carbenium ion mechanism and was able to predict the product distribution for cetane cracking over silica-alumina using what was known at the time about carbenium ions. The significant difference in product distribution from thermal cracking and catalytic cracking was evident. Hansford, Waldo, Drake and Honig in 1952 (Hansford et al., 1952) further completed the understanding of cracking by dropping the precious proposed carbene ion portion of Hansford’s theory (Hansford, 1947) due to experiments with deuterium exchange into hydrocarbons. The combination of

these investigations gives unprecedented evidence to an acid catalyzed carbonium/carbenium ion mechanism for catalytic cracking.

2.4.2 Cracking of Alkenes

There are no major disputed issues about the mechanism of alkene cracking over solid acidic catalysts; it is generally agreed that the active centers in these reactions are protic centers on the catalyst surface and that the reactive species are carbenium ions.

All hydrocarbon-cracking catalysts contain protic acidic centers. Thomas first proposed their structure in one of the earliest articles dealing with the mechanism of catalytic cracking (Thomas, 1949) as $[HAlSiO_4]^+$ with a positively charged Al atom. Currently, a similar picture of such centers (traditionally called Bronsted centers) with the hydrogen atom attached to the oxygen atom bridging Al and Si atoms is presented as the most plausible. Generally, reactions of Bronsted acids with alkenes are well known in organic chemistry. The first stage is, most probably, the formation of a complex involving the double bond of an alkene. The next stage is the formation of the carbenium ion in an equilibrium reaction:



The direction of this reaction mostly obeys the stability rule of carbenium ions: primary « secondary « tertiary. As typical for all highly reactive organic intermediates in catalytic reactions, direct observations of carbenium ions derived from alkenes within solid acidic catalysts are difficult and the formation of the

ions is mostly inferred from their subsequent transformations to stable reaction products. Theoretical calculations by Kazansky et al. (Kazansky and Senchenya, 1989) and by Corma et al. (Corma et al., 1998) suggest that the surface of acidic catalysts at high temperatures exerts a strong solvating effect and transforms carbenium ions R^+ into alkoxyaluminum moieties $>Al-O-R$ with a low net positive charge on the carbon atom in the R group. C-O bonds in such alkoxy groups, when vibrationally excited, have an increased charge separation and the R groups act as adsorbed carbenium ions. The most relevant data on the intermediate products formed from a linear alkene, 1-octene, reacted with a crystalline zeolite, H-ZSM-5, were presented by Zamaraev et al. (STEPANOV et al., 1994). Additional important information on the formation of carbenium ions in reaction was produced by Grey et al. (Kao et al., 1998). They studied reactions of several diphenyl-substituted ethylenes over calcined Ca-Y zeolite at room temperature. UV-vis shows that the first stage of the reaction constitutes formation of a brightly colored carbenium ion:



Due to the stabilizing effect of two phenyl groups (Ph), the ions can be observed at room temperature for several hours. Studies with deuterated zeolites show that H^+ in this reaction indeed comes from OH groups in the zeolite. Another technique for observation of carbenium ions in zeolites includes using probe molecules such as deuterated nitrile CD_3CN . IR analysis of zeolites with coadsorbed alkenes and CD_3CN allows identification of nitrile molecules coordinated to secondary and tertiary carbenium ions (BYSTROV, 1992; JOLLY et al., 1994).

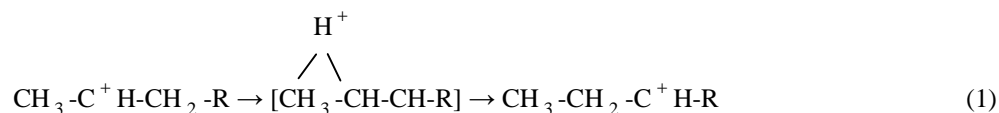
There are three kinds of products in cracking reaction: primary products, secondary products and tertiary products (Kissin, 2001).

A. Primary Products from Carbenium Ions

All products with the same carbon atom number as that of a substrate are called primary products. The primary products may have the same carbon skeleton as that of the substrate or isomerized skeletons.

1. Primary Products with Skeleton preservation

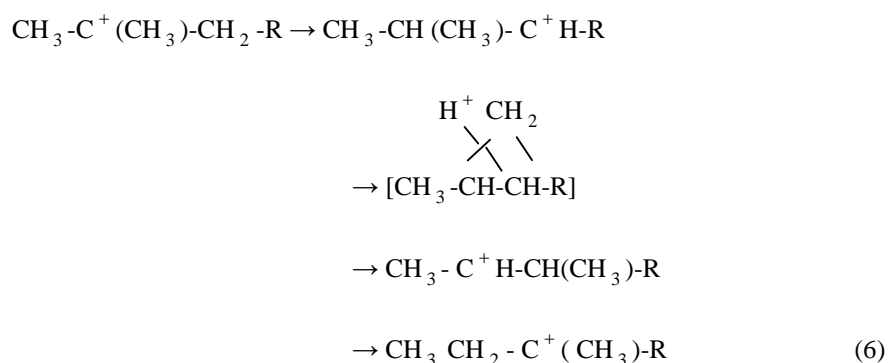
H-Atom Shift



Under normal circumstances, this reaction is unobservable. However, if the catalyst center contains a D atom instead of an H atom, the D atom transferred to the carbenium ion rapidly migrates to any position in the chain. If the C=C bond in the alkene is two- or three-substituted, its steric isomerization takes place readily. Effectively, reaction (1) results in a very rapid scrambling of nearly all H atoms in carbenium ions. Decomposition of the secondary carbenium ion formed in reaction (1) either regenerates the original alkene [reaction (2)] or produces an alkene with an isomerized C=C bond [reaction (3)]:

cyclopropanes; therefore, the protonated cyclopropane structure in reaction (4) should be viewed as a transition state on the reaction coordinate from a linear to a branched carbenium ion rather than a true intermediate (Boronat et al., 1998). Because reactions (4) and (5) result in thermodynamically favorable tertiary carbenium ions, they are usually invoked to explain the chain branching which accompanies alkene reactions over solid acidic catalysts.

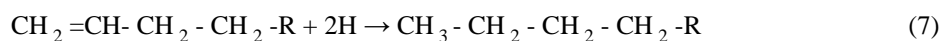
A reaction similar to reaction (3) but involving a carbenium ion derived from a branched alkene results in the methyl group shift along a hydrocarbon chain:



This reaction is called the type-A skeleton rearrangement (Poutsma, 1976); it is the principal reaction responsible for the isomerization of branched alkenes without a change in the number of branches.

2. Formation of Saturated Products

Reactions of alkenes over acidic catalysts are often accompanied by the formation of alkanes with the same skeleton:



Such alkanes are produced, in parallel with isomerized alkenes, relatively easily. For example, yields of n-alkanes in reaction (7) from various 1-alkenes over the same load of aged Y zeolite at 250 °C, normalized to the total yields of all primary products, were as follows: for 1-octene 12.7 %, for 1-decene 17.7 %, for 1-undecene 10.8 %, and for 1-dodecene 12.8 % (Bartley and Emmett, 1984). Acidic catalysts also hydrogenate branched alkenes [reaction (8)], even at 150 °C: trans-3-methyl-2-pentene is converted to 3-methylpentane, 2-methyl-1-hexene and trans-2-methyl-2-hexene to 2-methylhexane, 2,4-dimethyl-1-hexene to 2,4-dimethylhexane, and so forth (Kissin, 1994).

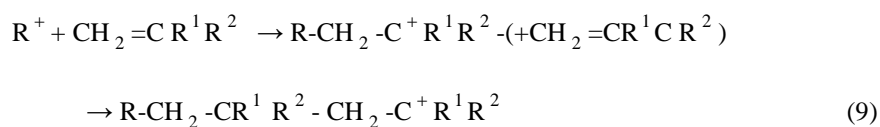
The source of hydrogen in reaction (7) and (8) is not yet known in detail. Analysis of model reactions of diaryl-substituted ethylenes over Ca-Y zeolite (Kao et al., 1998) show that the first hydrogen atom comes from OH groups in the catalyst, whereas the second hydrogen atom can be abstracted from a suitable hydrocarbon substrate (an aromatic solvent, for example)

B. Secondary Cracked Products from Alkenes

All products which are formed in a single reaction, fission of a single C – C bond, or, in the case of alkenes, formation of a single C – C bond in dimerization reactions are called secondary products.

1. Alkene Oligomerization

All alkenes with vinyl and vinylidene double bonds easily oligomerize in the presence of Bronsted acids. This reaction is widely practiced on a commercial scale: synthesis of polyisobutene, synthesis of isobutene dimers, synthesis of basestocks for synthetic lubricants, and so on. Polymerization of alkenes with vinylidene double bonds represents the simplest example. It proceeds through stable tertiary carbenium ions and usually results in the formation of regularly branched polymer chains:

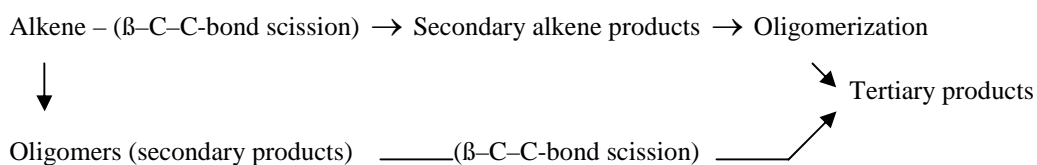


2. C – C-Bond Scission Reactions

The C – C-bond scission reactions in alkenes, which are the principal reactions of all cracking processes, also proceed easily. Cracking reactivity of alkenes increases with an increase of the carbon atom number (Buchanan et al., 1996). Wojciechowcki studied its cracking over H-Y zeolite at 300 °C (Abbot and Wojciechowski, 1987). Although the temperature is too high for model studies, the product distribution still very definitively indicates a single C – C-bond fission reaction: Isobutene amounts for over 98 % of all light cracked products. The reaction proceeds via the well-known β -C – C-bond scission mechanism.

C. Tertiary Products from Alkenes

All products formed from secondary products rather than from substrates themselves are called tertiary products. Tertiary products are required more than one step of the C – C-bond fission or the C – C-bond formation:



2.4.3 Cracking of Alkanes

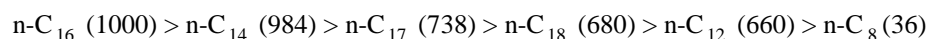
Catalytic cracking of alkanes readily occurs over the same acidic catalysts and approximately under the same conditions as alkene cracking, although cracking rates of alkanes are significantly lower. However, mechanistic understanding of alkane cracking reactions represents a much greater challenge. Although these reactions were studied for over 50 years, several competing mechanisms of alkane cracking still exist in the literature and a unified theory has not yet been formed. The main difficulty in elucidating the alkane cracking mechanism lies in the fact that alkanes, in contrast to alkenes, lack obvious reaction sites for acidic reactions.

A. Reactivities of Alkanes in Cracking Reactions

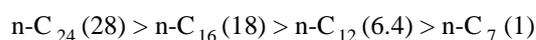
Greensfelder, Voge, and co-workers discovered long time ago that alkane reactivities in cracking reactions strongly depended on the types and the number of various C – H bonds in their molecules (Greensfelder et al., 1949). Tertiary C –

H bonds have the highest reactivity and primary C – H bonds have the lowest reactivity. Two subjects, alkane molecular weight and its chain structure, should be considered separately.

Nace produced the first comprehensive analysis of alkane reactivity as a function of carbon atom number (Nace, 1969). He found that the cracking rate constants of linear alkanes over a zeolite-based catalyst at 382 °C decreased in the following order:



Similar results were produced for cracking of linear alkanes over an amorphous silica-alumina-zirconia catalyst at 500 °C (Sie, 1993) (reactivities are relative to that of n-C₇).



These data indicate that, in general, n-alkane reactivity greatly increases with the increase of the carbon atom number.

Branched alkanes with the same carbon atom number are nearly always more reactive than their linear analogs, both in cracking (Greensfelder et al., 1949; Nace, 1969; Lopez et al., 1977) and in hydrocracking reactions (Goldfarb et al., 1977). n-Alkylcyclohexanes also have a tertiary carbon atom and crack at a higher rate than linear alkanes of the same carbon atom number (Nace, 1969). Two factors responsible for the increased reactivity of branched alkanes versus linear alkanes. The first factor is the direct electronic effect of neighboring alkyl group: molecules with tertiary C – H bonds are more reactive because of the cumulative inductive effect of three alkyl substituents attached to the tertiary carbon atom.

The second factor responsible for the increased reactivity of some branched alkanes is the hyperconjugation effects of methyl substituents (March, 1985), an additional electron-donating property of C – H bonds that is the highest for a methyl group and is absent in a tert-butyl group.

B. Mechanisms of Alkanes Cracking Reactions

Alkane cracking over solid acidic catalysts is clearly a catalytic reaction that takes place on the internal surface of porous catalyst particles, every proposed mechanism should address the following subjects: the main features of active sites on the catalyst surface; the nature of transition species formed as a result of an interaction between active sites and substrate molecules; the mechanism of skeleton isomerization of substrates; the mechanism of C – C fission reactions; the nature of reactions leading to different tertiary products.

1. Carbenium-Ion Mechanism

Carbenium-ion mechanisms are the oldest and, in many respects, still the most popular mechanism invoked for the explanation of alkane transformations in the presence of strong acids (Whitemore, 1932) and, in particular, catalytic cracking of alkanes (Greensfelder et al., 1945; Greensfelder et al., 1949). According to these mechanisms, the surface of solid acidic catalysts contains Lewis centers, very strong aprotic acidic species with vacant orbitals. Earlier carbenium-ion mechanisms assumed that Lewis centers in zeolites are capable, at increased temperatures, of removing H^- from $\text{C}_n \text{H}_{2n+2}$ alkane molecules and converting them to carbenium ions $\text{C}_n \text{H}_{2n+1}^+$:



Such carbenium ions would have the same nature as the carbenium ions derived from alkenes.

Engelhardt and Hall produced an elegant proof that carbenium ions are indeed present in systems containing alkanes and zeolite (Engelhardt et al., 1995). In the case of the isobutyl carbenium ion, $(\text{CH}_3)_3\text{C}^+$, for example, the equilibrium is



If the carbenium ion itself has deuterium labels in any of its methyl groups or if the acid it exists in contains D^+ , a rapid exchange of the labels takes place and all primary hydrogen atoms in the carbenium ion are equally susceptible to acquiring or losing the label.

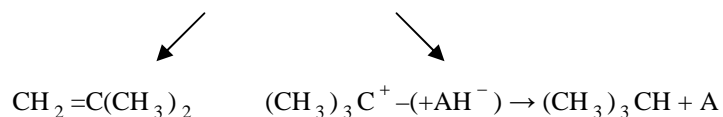
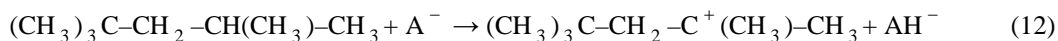
2. Proposed Mechanisms of C – C-Bond Fission in Carbenium Ions from Alkanes

Several ideas about C – C-bond fission in carbenium ions were developed over the years. Most of them represent variations of the similar mechanism proposed for catalytic cracking of alkenes but without oligomerization as an intermediate stage.

β -C – C-Bond Fission in Original Carbenium Ions

It is often assumed that, similar to reactions of alkenes, carbenium ions derived from alkanes undergo C – C-bond fission in the β -position to C^+ . The most convincing example of this C – C-bond fission mechanism in the original carbenium ion derived from an isoalkane is the cracking of 2,2,4-trimethylpentane.

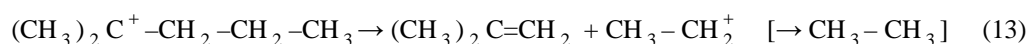
This alkane is the hydrogenated analog of 2,2,4-trimethyl-2-pentene and its cracking is expected to originate with the tertiary carbenium ion and to proceed along the same route as in the case of the alkene:



Indeed, Abbot and Wojciechowski (ABBOT and Wojciechowski, 1988) found that the selectivity of 2,2,4-trimethylpentane cracking over H-Y zeolite at 300 °C and 400 °C with respect to the formation of isobutene and isobutene ranges from 93% to 95%. This can be explained by the consumption of isobutene in oligomerization reactions.

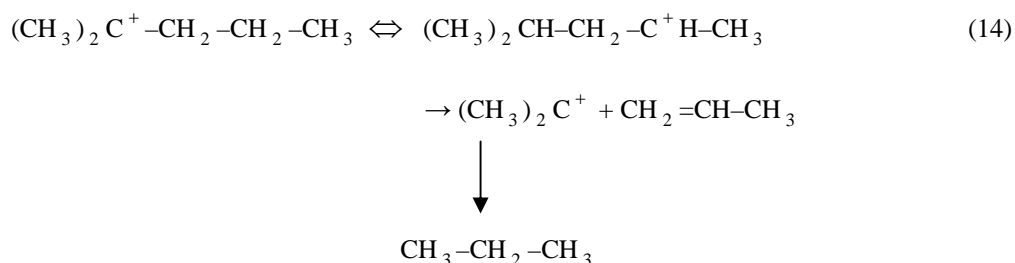
Isomerization of Carbenium Ions Followed by β -C – C-Bond

The cracking reactions produce, as relative minor products, molecules which cannot be derived from original carbenium ions. These difficulties multiply when one attempts to rationalize cracking of linear and monobranched alkanes via the carbenium-ion mechanism. For example, the β -C – C-bond scission in a monobranched carbenium ion derived from 2-methylpentane is expected to proceed as follows:



This reaction requires the formation of a primary carbenium ion, a highly endothermic process. To avoid this difficulty, an alternative cracking route for such carbenium ions was proposed (MARTENS et al., 1986). It includes a charge

shift and the formation of a secondary ion from the tertiary carbenium ion in reaction prior to the C – C-bond scission:



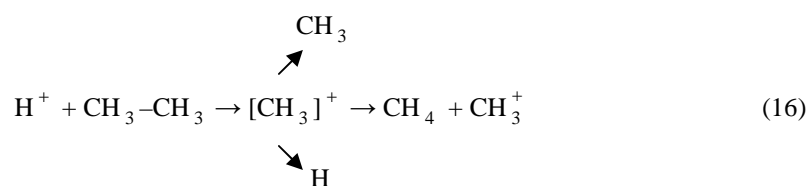
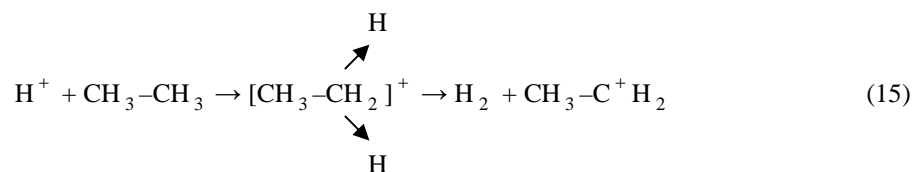
Although the formation of a small secondary carbenium ion in reaction (14) is less endothermic than that of the primary carbenium ion in reaction (13), the equilibrium concentration of the secondary carbenium ion in reaction (14) should be many orders of magnitude lower than that of the tertiary ion, which should make cracking via reaction (14) slow.

3. Carbonium-Ion Mechanisms

Bronsted centers in zeolites are strong protic acidic species. Only zeolites with very strong Bronsted centers cracked the substrate. The main feature of these sites is the tetrahedral-coordinated Al atom that shares an OH group with a neighboring Si atom. These sites account for a few percent of all Al atoms in most zeolites and only ~0.1% in amorphous aluminosilicates (Haag et al., 1984). Bronsted centers in aluminosilicates are nearly universally regarded as the active species in alkene cracking; even relatively weak acids can protonate alkene molecules. However, several researchers claimed that strong Bronsted centers in aluminosilicates could also protonate alkane molecules to nonclassical carbonium ions $\text{C}_n\text{H}_{2n+3}^+$ with

penta-coordinated carbon atoms or that the bronsted centers could even directly protolyze C – C bonds in alkanes and produce smaller alkanes and carbenium ions.

Gas-phase reactions of a naked proton and alkanes with the formation of highly unstable carbonium ions were experimentally established by mass spectrometry. Olah et al. developed the main principles of carbonium-ion chemistry in superacidic solutions in the 1970s. The research of Olah et al. most pertinent to the possible mechanism of catalytic cracking deals with reactions of 21 different alkanes in 2 superacids, $\text{FSO}_3\text{H} \cdot \text{SbF}_5$ and $\text{HF} \cdot \text{SbF}_5$, at temperatures from -78°C to $+20^\circ\text{C}$ (OLAH et al., 1971). The simplest example involves the reaction of the solvated H^+ and ethane. Two parallel reactions take place: Solvated H^+ attacks the main lobe of the C – H or the C – C bond in the ethane molecule with the formation of transient carbonium ions which subsequently cleave:

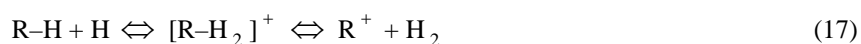


Additionally, CH_3^+ abstracts H^- from the ethane molecule and produces CH_4 and C_2H_5^+ , and the latter ion, in turn, converts to more stable C_4H_9^+ , carbocations. Protolysis of the C – C bond in reaction (16) proceeds at a rate from 8 to 14 times higher than protolysis of the C – H bond in reaction (15). Reactions of ethane with $\text{DF} \cdot \text{SbF}_5$ result in extensive HD exchange in recovered ethane and methane. In

the case of a similar reaction with isobutane, only the tertiary C – H bond undergoes such an exchange due to the predominant formation of the $(\text{CH}_3)_3\text{C}^+\text{HD}$ carbonium ion (Olah et al., 1971). This indicates that the pentacoordinated carbonium ions formed in solution in reactions (15) and (16) are true intermediates rather than transition states, although with very short lifetimes.

4. Reaction Mechanisms Involving Both Carbonium- and Carbenium-Ion Chemistry

Carbonium ions in superacids easily release H_2 or small alkanes and form carbenium ions (Olah and Molnar, 1995). The latter, in turn, react in the same way as carbenium ions derived from alkenes. In general terms, this set of reactions can be represented as follows:

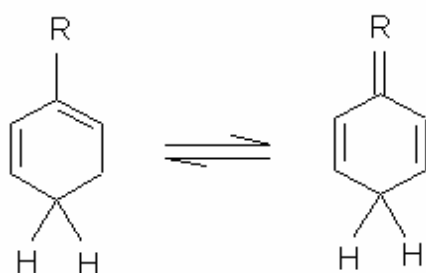


According to this scheme, carbonium ions of substrates convert to carbenium ions and the latter crack according to the standard carbenium-ion mechanism.

Several researchers suggested the bimolecular reactions of carbenium ions derived from carbonium ions. This theory is that small carbenium ions derived from decomposition of carbonium ions could abstract either H^- or alkyl anions from substrate alkane molecules.

2.4.4 Cracking of Alkylbenzenes

The reaction of alkylbenzenes have been studied in superacid media and on solid acids. The results from the super acid experiments are an indication of what may happen in cracking on solid acids. The reaction of small alkylbenzenes in super acids have indicated that the aromatic ring easily forms a carbonium ion (Brown and Pearsall, 1952; Olah et al., 1956; Olah and Kuhn, 1959). The stability of the resulting alkylbenzenium ion is enhanced by ring resonance structures (Mccaulay and Lien, 1951) and can be represented as (Brown and Wallace, 1953):



The cracking of alkylbenzenes has been noted in superacids. The cracking process involves the formation of the alkylbenzenium ion followed by dealkylation (Olah et al., 1972).

Few heterogeneous cracking studies have involved n-alkylbenzenes, but the information available indicates the mechanism over solid acids may depend on the length of the alkyl chain. The cracking of n-butylbenzene over alumina catalysts was investigated by Covini and Pine (Covini and Pines, 1965) where it was concluded that the cracking mechanism begins with aromatic ring protonation forming an alkylbenzenium ion. The resulting complex decomposes by dealkylation to benzene and an adsorbed carbenium ion. Results from

Greensfelder, Voge & Good (Greensfelder et al., 1945) for cracking n-propylbenzene and n-butylbenzene on a silica-alumina zirconia catalyst support this direct dealkylation mechanism. Similarly, Csicsery (Csicsery, 1969) noted direct phenyl cleavage on cracking n-pentylbenzene on alumina catalyst. Contrasting these results, Nace (Nace, 1969) has concluded that cracking of n-dodecylbenzene on zeolite X proceeds by hydride abstraction on the alkyl chain followed by β scission.

The cracking of cumene (isopropylbenzene) has been significantly studied as a model reaction for alkylbenzenes. The major products from cracking cumene on solid acids are observed to be benzene and propylene but other products can form by transalkylation reactions or isomerization reactions (Best and Wojciechowski, 1977; Corma and Wojciechowski, 1979). The benzene and propylene are the products expected from a dealkylation mechanism on a Bronsted site. These products are not formed if cracking only on Lewis sites occur (Corma and Wojciechowski, 1982). The rate limiting step for cumene cracking has been determined to be the decomposition of the surface carbocation into benzene and a propyl-carbenium ion (Campbell and Wojciech.BW, 1971).

2.5 COKING AND DEACTIVATION

During solid catalysed organic reactions, the catalyst always suffers from strong deactivation because of formation and retention of heavy by-products which cause either active sites poisoning and/or pore blockage (Guisnet and Magnoux, 2001).

The formation of these carbonaceous residues on hydrocarbon processing catalysis is of considerable technological and economic relevance to the oil and petrochemical industry (Holmes et al., 1997).

These non-desorbed by-products, called coke, consist of a mixture of high molar mass, hydrogen deficient, low volatility components deposited on the solid catalyst. Coke formation depends mainly on the zeolite pore structure and on the reaction temperature both of which determine the nature of the reactions involved and the retention of coke molecules (through condensation or trapping). The formation of coke molecules begins inside the micropores; however the growth of coke molecules trapped in cavities close to the outer surface of the crystallites leads to highly polyaromatic molecules which overflow onto this outer surface.

In recent years researchers classified coke into two kinds: coke precursors and hard coke. Coke precursors are removed from the catalyst sample simply through volatilisation in inert nitrogen, while hard coke remains on the catalyst even at high temperature (873 K) and is removed by burning (Chen and Manos, 2004).

2.5.1 Coke Characterisation

One technique for “exact” chemical characterisation of coke was developed by Guisnet and co-workers (P Magnoux et al., 1987). With their method, coke is liberated from zeolite by dissolution in hydrofluoric acid solution and extracted by

CH₂Cl₂ as soluble and non-soluble components are recovered. The soluble components can be determined using IR, UV-VIS and GC/MS.

With this method coke formation was investigated by Besset et al. (Besset E. et al., 1999) during n-heptane cracking at 450 °C over a H-MWW zeolite. Coke was found to be constituted of 5 main families:

Family A – mainly naphthalenes

Family B – mainly phenanthrenes

Family C – pyrene, benzophenanthrene, cyclopentapyrene and dibenzophenanthrene derivatives

Family D – indenopyrene, benzoperylene, dibenzochrysene and coronene derivatives

Family E – highly polyaromatic compounds

Shuo classified coke into coke precursors and hard coke during catalytic cracking of n-hexane and 1-hexene over ultrastable Y zeolite. Coke precursors are removed from the catalyst sample simply through volatilisation in inert nitrogen, while hard coke remains on the catalyst even at high temperature (873 K) and is removed by burning (Chen and Manos, 2004).

From the above, it is obvious that in order to optimize catalyst regeneration, information regarding coke characterisation should be obtained because the location and the structure of coke greatly influence catalytic cracking. Coke deposition on zeolites is a complex process that involves several different routes

with different intermediates and several different mechanisms. Despite intensive efforts made by catalyst scientists to study catalyst deactivation, our understanding of the nature of coke and its effect on different functions of the catalyst is still not complete (Liu et al., 1997; Guisnet and Magnoux, 1997b; Besset E. et al., 1999).

A number of studies on hydrocarbon deposits have been carried out by IR spectroscopy. Whatever the catalyst used or the nature of the coking agent, the overall results obtained show the regular presence of aromatic C – H bonds, of methylene group and of aromatic rings in all instances. Extraction of coke with various organic solvents, after dissolving the inorganic matrix of the zeolite, permits its chemical analysis via GC-MS, which confirms its polyaromatic nature (Barbier, 1986; Biswas et al., 1987; Schraut et al., 1987; Henriques et al., 1997a; Guisnet and Magnoux, 1997b; Besset E. et al., 1999).

2.5.2 Effects on Coking

2.5.2.1 Pore Structure Effect

Coke formation is a shape selective reaction. The coking tendency is an intrinsic property of the zeolite pore structure. Since most of the reactions by zeolites are occurring inside the cages (cavities) and in the channel intersections (apertures) where the acid sites are placed, coke is mainly formed inside the pores. Since the size of the intermediates and transition states involved in the formation of coke molecules is close to the size of the space available near the acid sites (cavities,

channel intersections) steric constraints will necessarily limit the formation of these intermediates. The significance of these constraints depends not only on the relative size of the intermediates and cavities but also on their shape. The great coke resistance of ZSM-5 was attributed to its pore structure only, which does not allow the formation of large coke molecules. However, the low density of their acid sites contributes to the low coking rate found with these zeolites (Guisnet M. and Magnoux P., 1992).

However, the effect of the zeolite pore structure is not limited to steric constraints on the formation of coke precursors. Indeed the contact time of the organic molecule with the active sites depends on the rate of diffusion of these molecules, and hence, on the characteristics of the diffusion path inside the zeolite crystallites; the length related to the crystallite size, the size of the pore apertures, the size of the channel intersections and the acid site density (Guisnet M. and Magnoux P., 1992).

The pore structure of the zeolite must therefore be chosen so that firstly, the space inside the vicinity of the acid sites is large enough to allow the formation of the intermediates of the desired reaction and small enough to limit by steric constraints the formation of coking intermediates. Secondly, the diffusion of the desirable molecules must be rapid enough for the reactant transformation to be limited to the formation of the desired product.

2.5.2.2 Active Sites Effect

The acidity plays a significant role in coke formation. The stronger the active sites the faster the reactions and the slower the diffusion of basic intermediates hence the faster the coke formation. The density of the active sites has also a positive effect on coke formation, which can be related to the intervention of many bimolecular reaction (Guisnet, 1990). The rate of reactions occurring through heterogeneous acid catalysis is obviously determined by the characteristics of the acid sites, i.e. their number, strength and density. Coke is formed preferentially on the strongest acid sites and causes their deactivation. Since these sites are the most active, the initial deactivating effect of coke will be more pronounced than if all the active sites were of the same strength. The deactivation effect of coke will decrease when the coke content decreases (Guisnet and Magnoux, 1989), i.e. coke deactivates the coking reactions too. This means that the strongest acid sites will be deactivated first and at a very high rate. In fact, the initial rate of deactivation in a typical cracking process is so rapid that the catalyst is decayed by 99 % within a minute, and this is attributed to the first carbenium ion attached to the pristine acid sites. This adsorbed carbenium ion has a lower activity, i.e. lower strength, than the pristine acid sites, and for that reason the further formation of coke is slower (Butt and Petersen, 1988; Guisnet and Magnoux, 1989).

The formation of high molecular coke takes several reaction steps, so the more times the reactant encounters an active site when diffusing through the zeolite, the higher the risk for converting into coke. Similarly the higher the number of active sites the higher the amount of coke formed will be. Also, some bimolecular reactions require more than one acid site (e.g. hydrogen transfer), which is part of

the coke formation. Therefore, a higher density of acid sites will lead to higher coke content (P Magnoux et al., 1987; Babitz et al., 1997).

2.5.2.3 Operating Condition Effect

1) Temperature

It is widely accepted that the higher the temperature, the higher the formation of carbonaceous compounds. As the Arrhenius equation describes, raising the temperature increases the rate of reaction. Some reactions are more sensitive to changes in temperature than others, and those are the ones with the highest activation energy. Generally, coke formed at higher temperature has a lower carbon to hydrogen (C/H) ratio (Guisnet and Magnoux, 1989). This is because of a higher aromatic content, which at the end leads to graphite or a graphite like structure, formed through alkylation, cyclisation and dehydrogenation. These reactions are favoured at higher temperatures. The physical effect of low temperature is higher adsorption. At high temperatures, the retention of coke is mainly due to trapping in the blocked pores, while at low temperatures because of a stronger adsorption (Guisnet and Magnoux, 1989; Guisnet M. and Magnoux P., 1992) that lowers the volatility of the formed molecules.

However, Cerwueira et al. investigated the influence of coke formed during m-xylene transformation over USHY zeolite at 520 K and 720 K (Cerqueira et al., 2000a). They found that for a short time-on-stream (5 min) the amount of coke was greater at 520 K than at 720 K. the explanation given was that of an easier

retention, at lower temperatures, of coke precursors in the zeolite micropores. All the coke components were located inside the pores. Coke formed at 520 K was mainly constituted by methyl substituted polyaromatic compounds, with three aromatic rings. Coke formed at 720 K was more polyaromatic, methyl pyrenic compounds being the main coke components.

Temperature has a crucial bearing on the chemical nature of the coke produced. Some authors have distinguished the formation of coke between “low-temperature coke” and “high-temperature coke” (Guisnet and Magnoux, 1989; Guisnet M. and Magnoux P., 1992; Guisnet and Magnoux, 1997a). The former is formed at temperature of 300 – 500 K, and consists mainly of branched saturated hydrocarbons with a similar H/C elemental ratio to the reactants, while the later is formed at temperatures above 550 K, and consists of aromatic and polyaromatic species with a lower H/C ratio than the reactants. A simple scheme for the formation of high-temperature coke involves cracking to olefins, followed by oligomerisation, cyclisation and hydrogen transfer reactions, thus (Paweewan et al., 1998)

Paraffins → Olefins → Napthenes → Aromatics → Polyaromatics

As a result of these reactions, it is sometimes difficult to compare formation results from different laboratories when different temperatures are used, even when the so-called high-temperature coke is the only product.

2) Time-On-Stream (TOS) and Residence Time

P. D. Hopkins studied the coke deactivation rate during hexane cracking on H-USY zeolite (Hopkins et al., 1996). Experimentally, the initial coke deactivation of H-USY is rapid and then decreases more slowly with increasing time-on-stream. Similar results were achieved from previous work done by S. Chen and A. Brillis. The amount of both coke precursors and hard coke increases with time-on-stream. Especially at the first 5 min, coke increases fast, from 0.4 % at 1 min to 3.4 % (12.5 kPa, 1-hexane) and from 1.6 % to 6.2 % (22.5 kPa, 1-hexane) at 5 min (Chen and Manos, 2004). From A. Brillis results, it is fairly obvious that coke formation is extremely rapid process at the beginning of the catalyst exposure to the reaction mixture. More than two-thirds of the coke formed during the first 20 min was actually produced in the first minute of TOS. After 1 min, the coke content shows a linear dependence on TOS. The highest coke amount was observed in the experiment with the highest residence time (Brillis and Manos, 2003).

The composition of coke depends very much on the amount of retained on the catalyst. The higher this amount, hence the longer the time-on-stream in flow reactors or the residence time in batch reactors, the greater the complexity and the polyaromaticity of the coke (Guisnet and Magnoux, 2001).

2.5.2.4 Nature of the Feed Effect

It is generally believed that it is the olefins formed from the initial cracking step which are most responsible for coke formation within zeolite catalysts, and so workers have also investigated coke formed from the reaction of olefins within zeolites, rather than the cracking reaction directly (Lange et al., 1988; Moljord et al., 1995).

On acid catalysts coking occurs rapidly from alkenes (Lange et al., 1988) and from polyaromatics (Wolf and Alfani, 1982). In the case of alkenes it is due to their rapid transformation through bimolecular reactions (oligomerization, alkylation, hydrogen transfer) while for polyaromatics it is due to their slow diffusion in the pores owing to the strong adsorption of these basic molecules on the acid sites. Coke formation occurs slowly from the monoaromatics, the alkanes and the naphthenes whose transformation into alkenes and into polyaromatics is slow. The formation of these coke maker molecules is then the limiting step of coking.

2.5.3 Modes of Deactivation

There are two broad categories of catalyst deactivation in acidic zeolites: active site poisoning and pore blockage (Hopkins et al., 1996). The first, site poisoning, is due to irreversible adsorption of poison on the active sites. Because the zeolite pores are only slightly larger than the reactant molecules, only a few atoms of carbon may be required to effectively block pores. For zeolites, site poisoning and

pore blockage are the most commonly observed coke deactivation mechanisms (Mori et al., 1991).

2.5.3.1 Active Sites Poisoning

For active site poisoning, there are three limiting models, uniform site poisoning, selective site poisoning and pore mouth poisoning.

In the uniform site poisoning model, deactivation is assumed to occur uniformly throughout the catalyst particle and the poison deactivates all sites identically. Uniform poisoning is likely to occur if the diffusion rate of the poison in the zeolite is large compared to the rate constant of the poisoning reaction, so that the poison molecule can penetrate deep into the crystal before deactivates a site. For cracking in acidic zeolites, the poison is coke which forms at a site through a series of cracking, polymerization and other hydrocarbon transformation reactions. Thus, uniform poisoning would apply if the cracking reaction itself is not diffusion controlled, i.e., if the Thiele modulus is much smaller than unity (J.B. Butt, 1980). In this case, the uniform poisoning model predicts that the activity would decrease linearly with loss in the number of acid sites.

Selective site poisoning applies if the active sites are inhomogeneous, i.e., some sites are more active than others and the poison deactivates different sites differently. Super acidic sites, for example, have been proposed in zeolites with non-framework Al (Vasques et al., 1989; Goovaerts et al., 1989). Alternatively, the acid strength is thought to be determined by the Si/Al ratio where the acid

strength of isolated acid sites, i.e., those with no second nearest neighbor Al, have higher acid strengths and catalytic activities (Carvajal et al., 1990). If these more active sites are selectively poisoned, then rapid deactivation occurs after only a small fraction of the total active sites is poisoned. Alternatively, selective coking might occur preferentially at one type of acid sites, e.g., Bronsted or Lewis. In the selective poisoning model, the catalytic activity decreases more rapidly than the total number of active sites resulting in a change in the acid strength or acid type distribution upon deactivation.

In pore mouth poisoning, all acid sites are assumed to be uniformly distributed but the rate of reaction is much more rapid than the rate of diffusion. Because of the high rate of reaction, the active sites nearest the external surface of the crystal account for most of the observed activity, while sites at the catalyst interior contribute little. In this model, deactivation begins in a thin shell at the surface of the catalyst particle, where the pore mouths are located. As the outermost sites become poisoned, deactivated zone becomes larger. As this occurs, the reactant molecules must diffuse over a longer distance before they encounter an active site, resulting in a lower apparent activity of the catalyst. In the ideal limit of this model, the poison has no effect on the diffusion of molecules. The pore mouth poisoning model predicts that the activity will decrease more rapidly than loss in the number of active sites.

2.5.3.2 Pore Blockage

One type of pore blockage is pore mouth plugging. In this model, essentially all coke is deposited near the pore mouths and very few of the active sites are covered by coke. The activity declines more rapidly than the number of deactivated sites and the diffusion rate decreases as the pores become increasingly blocked. This model does not assume or require direct poisoning of acid sites. The relationship between cracking activity and measured acidity depends on whether access of the acidity probe molecule is also restricted.

In addition to pore mouth plugging, pore blockage could also occur further inside the crystal, or the coke could block channels or intersections deeper inside the crystal. For a zeolite with a three dimensional channel network, like H-USY, the effect of a blocked pore would be to poison only those sites within the immediate supercage. As a result, the activity would be proportional to the number of remaining and accessible active sites.

3 EXPERIMENTAL WORK

3.1 EQUIPMENT

The equipment used consisted of a fixed-bed tubular reactor, heated by a temperature controlled furnace, a glass saturator that contained the reactant and was situated inside a temperature controlled water bath, two mass flow controllers for the inert gas used namely nitrogen, and a ten-way valve in whose loops samples of the reaction mixture at different TOS were collected. The ten-way valve was connected, after the completion of the experiment, into a gas chromatograph (GC) equipped with a flame ionization detector (FID). It enabled the chromatographic analysis of numerous reaction samples taken in short time-on-stream intervals. The coked samples were analysed by thermogravimetric analysis (TGA) and temperature-programmed desorption (TPD).

3.1.1 Reactor

The fixed-bed reactor, which is shown in Figure 3-1, was a stainless steel tubular reactor, with a total height of 25.5 cm, and an inner diameter of 15 mm. The catalyst bed length averaged 10 mm, was supported by metal sieves of 4 mm thickness. A thermocouple was inserted in a small protection tube, 4 mm in diameter, and placed in the centre of the reactor. This made it possible to measure the temperature along the reactor in order to check isothermicity of the bed. During the first experimental runs, it was observed that there was a temperature

difference between the top and bottom halves of the reactor. To avoid this temperature profile to be developed in the catalytic bed, steel wool was placed just above and below the catalyst bed, which had not any catalytic properties, thereby enduring isothermal conditions (The maximum temperature difference observed was below 1 K).

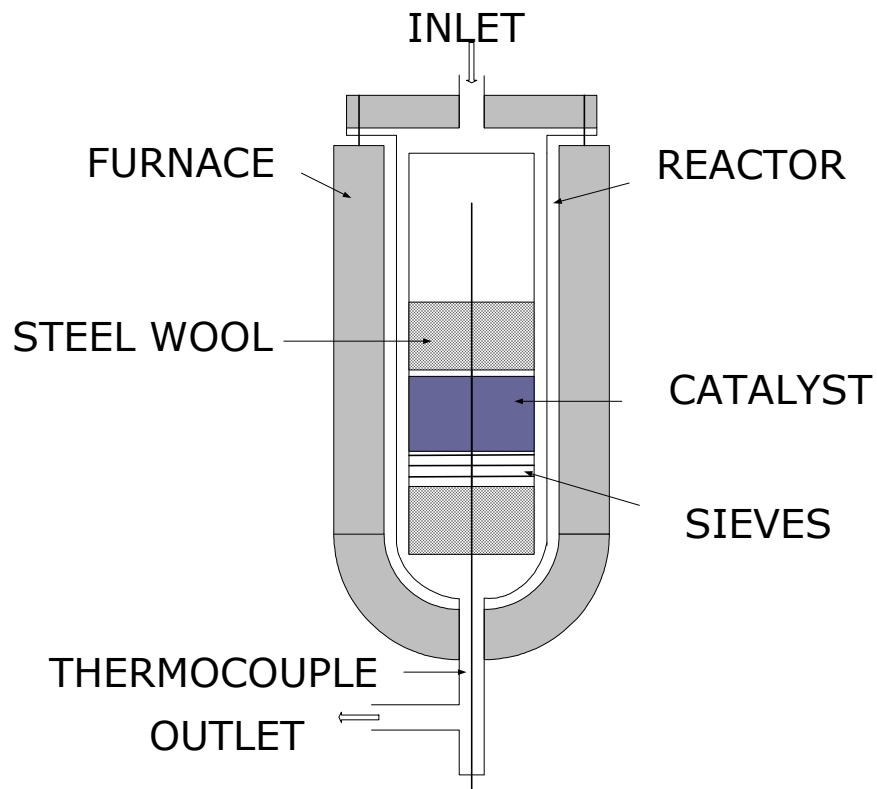


Figure 3-1 The fixed-bed reactor placed inside the furnace (not to scale)

The residence time of the reactor was calculated using the following equation.

$$\tau = \frac{\text{(bed empty volume)}}{\text{(volumetric flow at reaction temperature)}}$$

where: bed empty volume = (bed porosity) \times (bed cross – section area) \times (bed length)

Bed porosity is the void fraction of the catalyst bed and taken equal to a typical value of 0.5 (Brillis and Manos, 2003). Hence with the other parameters' values mentioned, the empty volume of the bed is calculated to be 0.475 ml. The residence times at all experimental conditions are shown in Table 3-1.

Table 3-1 Residence times at all experimental conditions.

	Residence Time (s)		
	1-pentene	n-heptane	ethylbenzene
$V_{N_2}^0$ Temp(K)	50 ml/min		
523	0.066	N/A	N/A
573	0.059	N/A	N/A
623	0.055	0.178	0.239

3.1.2 Saturator

The saturator consisted of a sealed glass tube, containing the reactant along with numerous small glass spheres, to enhance temperature uniformity, as well heat and mass transfer. It was immersed inside a temperature controlled water bath, which achieved temperatures up to 358 K. The reactant vapour formed by the heat produced by the bath was taken along by nitrogen and passed into the reactor. To avoid condensation at some metal pieces (metal tube and four-way valve), two

warm air blower were used to keep them warm. Two connected saturators were used to research desired conditions. The whole set-up was enclosed by aluminum foil.

The water bath temperature was set up to achieve the desired vapour pressure of each reactant. The vapour pressure produced is a function of the adjusted water temperature assuming atmospheric pressure in the system. The correlations were taken from Reid et al. (Robert C.Reid et al., 1987):

$$\ln\left(\frac{P_V}{P_C}\right) = (1-x)^{-1} \times (C_A \times x + C_B \times x^{1.5} + C_C \times x^3 + C_D \times x^6) \quad (1)$$

$$x = 1 - \left(\frac{T}{T_C}\right)$$

and:

$$\ln(P_V) = C_A - \left(\frac{C_B}{T}\right) + C_C \times \ln(T) + \frac{(C_D \times P_V)}{T^2} \quad (2)$$

where: P_V , vapour pressure (bar)

P_C , critical pressure (bar)

T_C , critical temperature (K)

T , saturation temperature (K)

C_A, C_B, C_C, C_D , vapour pressure constants

To achieve the desired composition of the reactant, two branches were set up; one was through the saturator and combined with the other at the end, as shown below:

o

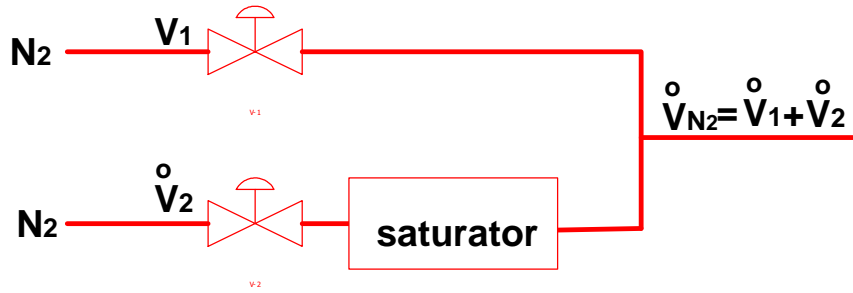


Figure 3-2 Flow chart for nitrogen branches.

By adjusting the nitrogen flow rate of the two branches, the desired reactant composition can be achieved.

$$\overset{0}{V}_1 \rightarrow \overset{0}{N}_1 = \frac{P_0 \overset{0}{V}_1}{RT} \quad (3)$$

$$\overset{0}{V}_2 \rightarrow \overset{0}{N}_2 = \frac{P_0 \overset{0}{V}_2}{RT} \quad (4)$$

$$X_R = \frac{\overset{0}{N}_R}{\overset{0}{N}_{N_2} + \overset{0}{N}_R} = \frac{\overset{0}{N}_R}{\overset{0}{N}_1 + \overset{0}{N}_2 + \overset{0}{N}_R} \quad (5)$$

$$\frac{\overset{0}{N}_R}{\overset{0}{N}_R + \overset{0}{N}_2} = \frac{P_R^{VP}}{P_{latm}} \equiv X_0 \Rightarrow \overset{0}{N}_R = \frac{X_0}{1 - X_0} \overset{0}{N}_2 \quad (6)$$

$$X_R = \frac{\frac{X_0}{1 - X_0} \overset{0}{N}_2}{\overset{0}{N}_1 + \overset{0}{N}_2 + \frac{X_0}{1 - X_0} \overset{0}{N}_2} \Rightarrow X_R = \frac{X_0 \overset{0}{N}_2}{\overset{0}{N}_1 (1 - X_0) + \overset{0}{N}_2} \quad (7)$$

$$\frac{\overset{0}{N}_1}{\overset{0}{N}_2} = \frac{\overset{0}{V}_1}{\overset{0}{V}_2} = \frac{(X_0 - X_R)}{(1 - X_0) X_R} = R \quad (8)$$

$$\overset{0}{V}_1 + \overset{0}{V}_2 = \overset{0}{V}_{N_2} \quad (9)$$

$$V_1^0 = \frac{R}{R+1} V_{N_2}^0$$

$$V_2^0 = \frac{1}{R+1} V_{N_2}^0$$

Table 3-2 Nitrogen flow rate and composition at all experimental conditions

Reactant	Total N ₂ flow rate = 50 ml/min		Composition (%)
	V ₁ (ml/min)	V ₂ (ml/min)	
1-pentene	2.52	47.48	80
n-heptane	7.98	42.02	35
ethylbenzene	34.73	15.27	12

3.1.3 Ten-way Sampling Valve

The ten-way sampling valve was placed in a rectangular temperature controlled box, having ten sample loops. The valve was heated during the experiment and GC-analysis at a temperature of 120 °C. The valve has an entry, which was connected to the exit of the reactor, and an exit, which during the experiment was connected to the waste stream. At specific times during the experiment, samples were taken and kept in the sample loops without any condensation. After the completion of the experiment, the entry was connected to the GC carrier gas line (in this case, helium). Then, a long needle was connected to the exit of the valve and inserted into the injector of GC, enabling injection and analysis of the samples.

3.1.4 Gas Chromatograph

Chromatography is the separation of a mixture of compounds (solutes) into separate components. By separating the sample into individual components, it is easier to identify (qualitate) and measure the amount (quantitate) of the various sample components. There are numerous chromatographic techniques and corresponding instruments. Gas chromatography (GC) is one of these techniques.

The term chromatography covers those separation techniques in which the separation of compounds is based upon the partition, or distribution, of the analytes between two phases in a dynamic system. In gas chromatography we have a gaseous mobile phase and a liquid or solid stationary phase. In gas-liquid chromatography (as used in this research) the stationary phase is a high boiling point liquid and the sorption process is predominantly one of partition. The compounds to be analyzed must be sufficiently volatile for them to be present in the gas phase in the experimental conditions, in order that they may be transported through the column. Samples are introduced into the gas flow via an injection port located at the top of the column. A continuous flow of gas elutes the components from the column in order of increasing distribution ratio from where they pass through a detector connected to a recording system. The basic principle of gas chromatography is that the greater the affinity of the compound for the stationary phase, the more the compound will be retained by the column and the longer it will be take to be eluted and detected. Thus, the heart of a gas chromatography is the column in which the separation of the components takes place. To this must be added the source and control of the carrier gas flow through the column, a means

of sample introduction and a means of detection of the components as they elute from the end of the column. Since temperature will influence the volatility of the analytes, the column is placed in a thermostatically controlled oven. Detectors and some injectors are also heated. A basic system is shown schematically in Figure 3-3.

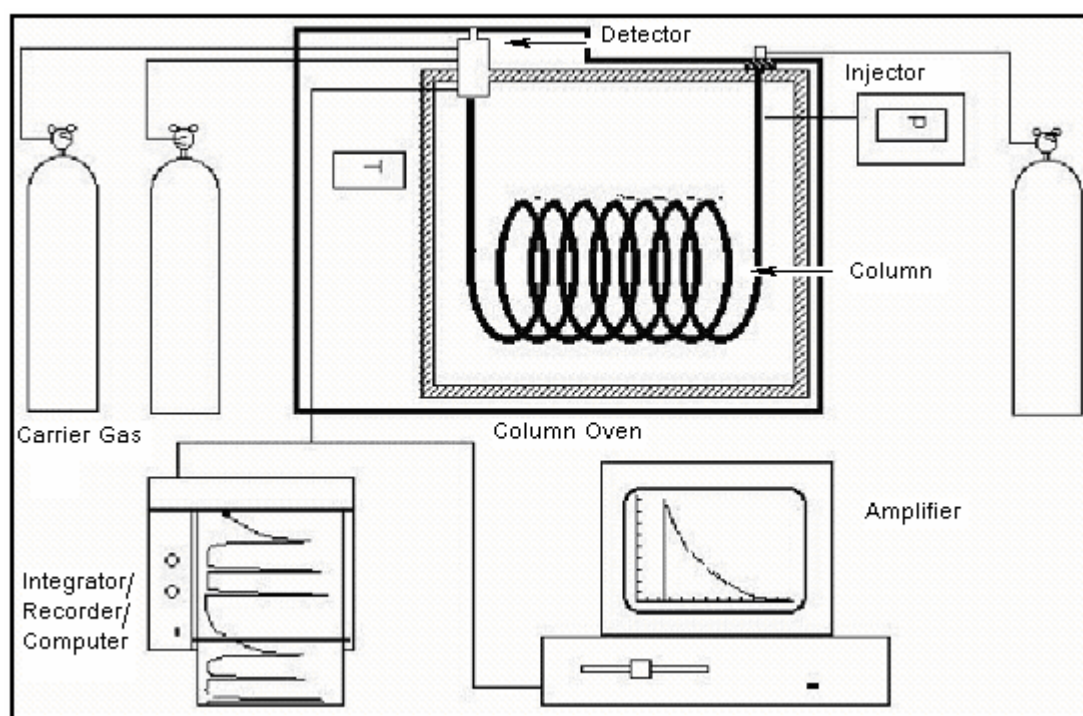


Figure 3-3 GC system

Mobile Phase and Flow Control:

The mobile phase or carrier-gas is He and is supplied from a cylinder via a pressure-reducing head at a pressure of 25 psi. Helium and hydrogen are preferred over nitrogen for capillary columns because chromatographic efficiency diminishes more slowly with increasing flow rate thus facilitating faster separations.

Sample Injection System:

To ensure the best possible efficiency and resolution, the sample should be injected into the carrier-gas stream in as narrow a band as possible. The injector temperature is set at 170 °C. Injections can be either splitless or split. A splitless injection means that the entire sample injected travels through the column. Split injection involves an inlet stream splitter incorporating a needle valve that enables most of the injected sample to be vented to the atmosphere whilst allowing only a small fraction (2 % or less) to pass into the column. Resolution is usually much better in split mode and this is the reason for using it in this analysis.

The Column:

The column being used is a coil of fused silica tubing, 100 m in length with an internal diameter of 0.52 mm. To ensure operation under reproducible conditions, the column is enclosed in a thermostatically controlled oven. The column is a wall coated open tubular one, whereby a thin film of the liquid stationary phase is coated or bonded onto the inner wall of the tube. The exterior of the tube is coated with a layer of a polyamide or aluminium as a protection against cracking or scratching.

The Detector:

The purpose of a detector is to monitor the carrier-gas as it emerges from the column and respond to changes in its composition as solutes are eluted. The detector used here is a flame ionisation detector (FID). H₂ at 15 psi and air at 23 psi are used to fuel the detector.

GC Specifications

System: HEWLETT 5890 PACKED SERIES 2 GC
Column: L&W 100 m WCOT fused silica, CP-SIL-5CB, id: 0.52mm
Carrier-gas: Helium @ 25 psi
Detector: Flame Ionisation Detector – Fuel: H₂ @ 15 psi , Air @ 23 psi
Mode: Split mode – Split Fraction: 1: 50

Operating Conditions

In GC analysis, a temperature program is generally used to ensure adequate separation of the compounds in as short a period as possible. To develop the temperature program, it is necessary to run a sample from an experiment, whereby reactants and products are present.

The temperature programs used for these analyses are as follows:

Oven Temperature 1: 35 °C
Isothermal Time 1: 30 min
Ramp Rate 1: 10 °C/min
Oven Temperature 2: 120 °C
Isothermal Time 2: 5 min

The total run time is 43.5 min.

The injector/detector temperature is 170 °C/ 300 °C.

3.1.5 Thermogravimetric Analysis

Thermogravimetric analysis (TGA) is an analytical technique used to determine a material's thermal stability and its fraction of volatile components by monitoring the weight change that occurs as a specimen is heated. The measurement is normally carried out in air or in an inert atmosphere, such as Helium or Argon, and the weight is recorded as a function of increasing temperature. In addition to weight changes, some instruments also record the temperature difference between the specimen and one or more reference pans (differential thermal analysis, or DTA) or the heat flow into the specimen pan compared to that of the reference pan (differential scanning calorimetry, or DSC). The later be used to monitor the energy released or adsorbed via chemical reactions during the heating process. In the particular case of carbon nanotubes, the weight change in an air atmosphere is typically a superposition of the weight loss due to oxidation of carbon into gaseous carbon dioxide and the weight gain due to oxidation of residual metal catalyst into solid oxides.

In this study, the coked samples were obtained at different reaction conditions and investigated by a novel method developed by our group with a thermal gravimetric analysis (TGA) apparatus, Caln TG 131.

3.1.6 Temperature Programmed Desorption

Temperature-Programmed Desorption (TPD) is one of the most widely used and flexible techniques for characterising the acid sites on oxide surfaces. Determining

the quantity and strength of the acid sites on alumina, amorphous silica-alumina, and zeolites is crucial to understanding and predicting the performance of a catalyst. For several significant commercial reactions (such as n-hexane cracking, xylene isomerization, propylene polymerization, methanol-to-olefins reaction, toluene disproportionation, and cumene cracking), all reaction rates increase linearly with Al content (acid sites) in H-ZSM-5. The activity depends on many factors, but the Bronsted-acid site density is usually one of the most crucial parameters.

TPD of ammonia is a widely used method for characterisation of site densities in solid acids due to the simplicity of the technique. Ammonia often overestimates the quantity of acid sites. Its small molecular size allows ammonia to penetrate into all pores of the solid where larger molecules commonly found in cracking and hydrocracking reactions only have access to large micropores and mesopores. Also, ammonia is a very basic molecule which is capable of titrating weak acid sites which may not contribute to the activity of catalysts. The strongly polar adsorbed ammonia is also capable of adsorbing additional ammonia from the gas phase.

Temperature-Programmed Desorption (TPD) analyses determine the number, type, and strength of active sites available on the surface of a catalyst from measurements of the amounts of gas desorbed at various temperatures. After the sample has been outgassed, reduced, or otherwise prepared, a steady stream of analysis gas flows through the sample bed and reacts with the active sites.

Programmed desorption begins by raising the temperature linearly with time while a steady stream of inert carrier gas flows through the sample. At a certain temperature, the thermal energy overcomes the activation energy; therefore, the bond between the adsorbate and adsorbent breaks and the adsorbed species is liberated from the surface and swept away by the carrier gas. If different active metals are present, the chemical bond between the adsorbed molecule and each metal type will likely be of different energy. Therefore the molecules adsorbed on each active metal will require a different thermal energy level to break the bond and desorb, resulting in distinct peaks on the plot of the TCD output signal vs. temperature. The differential thermal conductivity measured by the detector at any moment is proportional to the instantaneous molecular concentration of desorbed molecules. The volume of the desorbed species obtained from integration of the peak, combined with the stoichiometry factor, yields the number of active sites. Multiple peaks, when they occur, indicate distinct energy differences in active site energies.

In our research, the TPD experiments were carried out in a Micromeritics AutoChem 2910 equipped with a thermal conductivity detector (TCD) and using helium as carrier gas. The flow chart is shown in Figure 3-4.

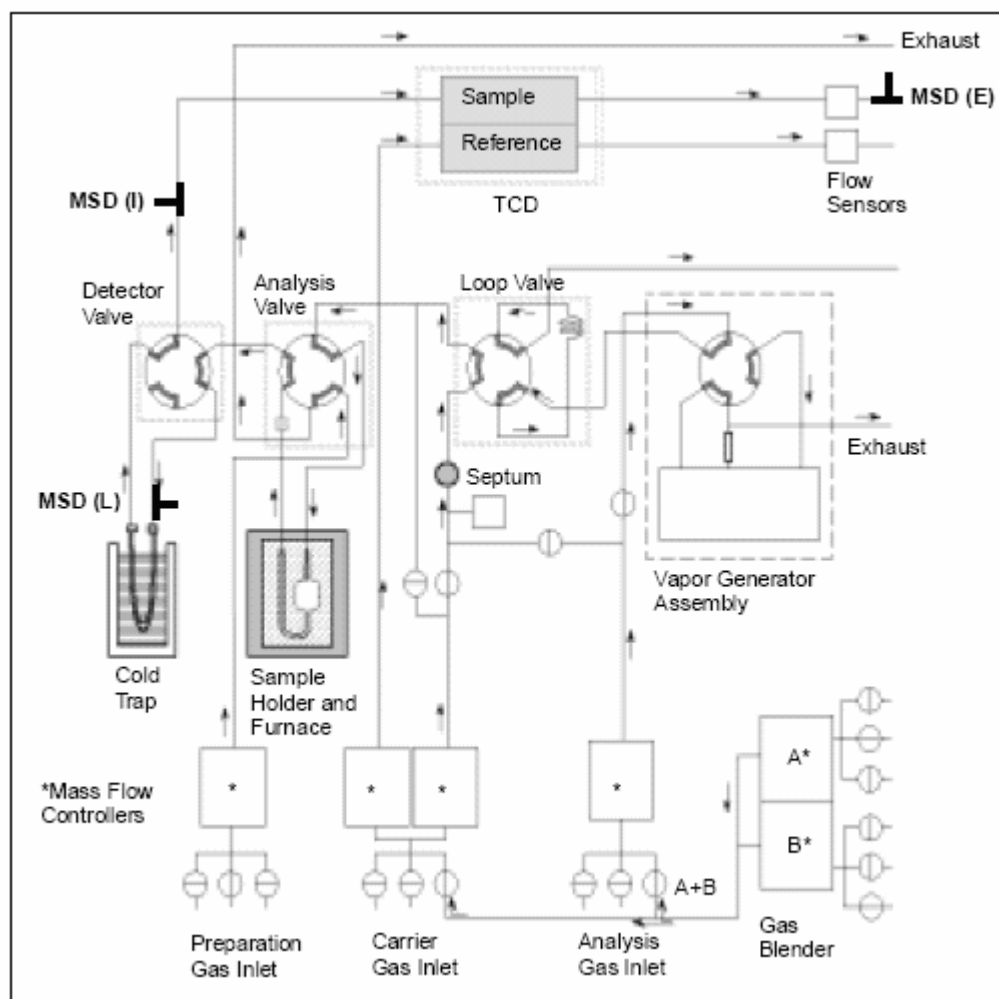


Figure 3-4 Flow chart of Temperature-Programmed Desorption.

3.2 EQUIPMENT PROCEDURES

The equipment set up is shown in Figure 3-5. In order to ensure the feed components had the same steady state composition. Nitrogen was led to the reactor through the upper branch until the reactor was heated to desired temperature. The carrier gas, nitrogen, passed through a saturator containing the particular reactant placed in a heated water bath at specified temperature. After that nitrogen passed through the saturators to fume cupboard by the lower branch

for 15 minutes in order to equilibrate the gas phase. Then the four-way valve was turned and the reaction started. The reaction lasted for 20 minutes which was considered enough time for the catalyst to have been deactivated. Products sample were collected by the ten-way valve at specified times (1, 2, 3, 5, 7, 9, 12, 15 and 20 min).

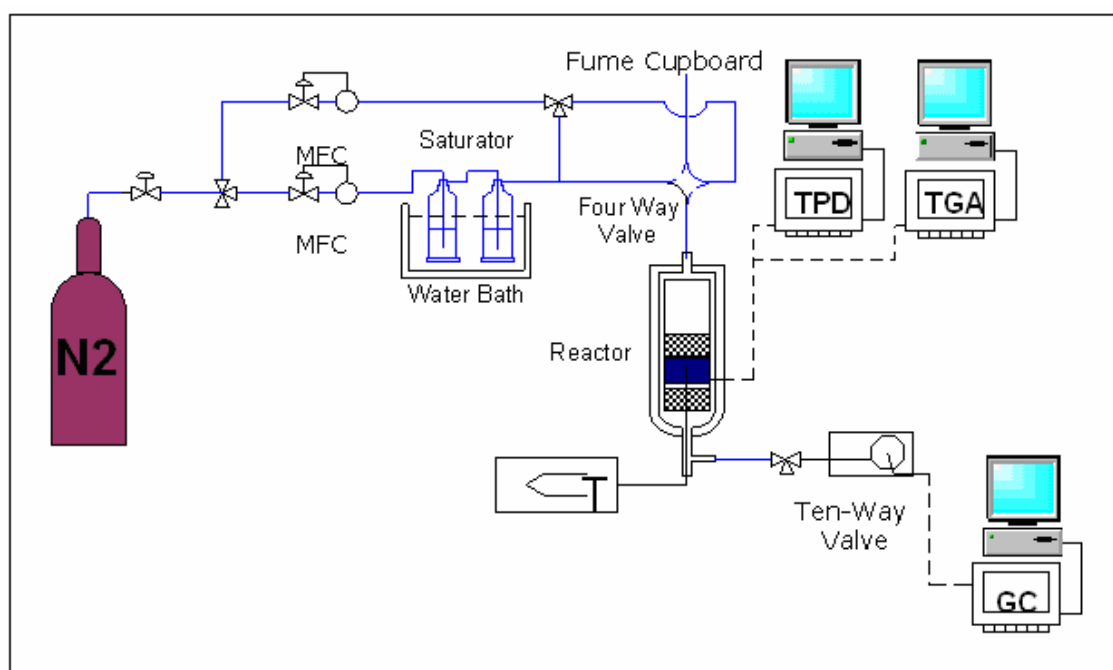


Figure 3-5 Set up of the fixed-bed reactor equipment.

The amount of catalyst used in each experiment was 0.65 gram which was taken in order that the catalyst bed length to be 1 cm. The thermocouple was put inside the reactor and placed exactly at the catalyst bed level, to ensure that the reading was the actual reaction temperature.

Upon completion of the reaction, valves were switched to their initial positions, the saturator was bypassed and the reactor cooled down for 10 min under nitrogen

atmosphere. Then the reactor was disconnected from the rig and put in ice for quick cooling until ambient temperature. Coked samples were obtained at 1, 2, 3, 7, 20 min of time-on-stream and investigated by the novel method with a thermal gravimetric analysis (TGA) apparatus, Caln TG 131 and temperature-programmed desorption (TPD) apparatus, Micromeritics AutoChem 2910.

3.3 CATALYST PREPARATION

The USHY zeolite catalyst was provided by Grace GmbH in powder form with an average particle size of 1 μm , a framework Si/Al ratio of 5.7 and a bulk Si/Al ratio of 2.5. The micropore area was 532.4 m^2/g and the micropore volume was 0.26 cm^3/g . BET surface area was $590 \pm 23.5 \text{ m}^2/\text{g}$.

About 1.5 g USHY zeolite powder was taken and pressed for 1 minute at a weight of 3 tons for 5 times, so as to produce catalyst pellets. The catalyst pellets were crushed and sieved, producing particles in the size range of 1.0-1.7 mm.

Before reaction, the catalyst was calcined in an oven at a rate of 10 K/min to 873 K and maintained there for 12 hours.

3.4 CALCULATIONS

3.4.1 Components Mole Fraction Calculation

The initial calculations from GC reports produce the GC peak area fractions of the main components of the reaction that area equal to the mass fractions. The calculation sequence is as follows:

From the GC outputs the percentage area values – which corresponded to mass fractions (Dietz W.A., 1967) – of all components were divided by their corresponding molecular weights, to produce the number of moles of the components in the sample. The produced mole values were summed up and normalised over the new total, thus the required mole fractions were produced. The above steps were repeated for each of the results, produced for every experiment, and the mole fraction values of the main components were plotted against the time-on-stream.

3.4.2 Conversion

The method was used to calculate the conversion that is based on the mass fractions of the reactant, which are equal to the chromatographic area fraction of the reactant at the reactor outlet (Dietz W.A., 1967). We show the validity of this, starting with the definition of conversion

$$X_A = (\overset{0}{N}_{A0} - \overset{0}{N}_A) / \overset{0}{N}_{A0} = (\overset{0}{m}_{A0} - \overset{0}{m}_A) / \overset{0}{m}_{A0} = 1 - (\overset{0}{m}_A / \overset{0}{m}_{A0}) = 1 - (A_A / A_{TOT})$$

where X_A is the conversion of reactant A, \dot{N}_{A0} is the molar flow of reactant A at the inlet of the reactor, \dot{N}_A is the molar flow of reactant A at the exit of the reactor, \dot{m}_{A0} is the mass flow rate of reactant A at the inlet of the reactor, which is equal to the total mass flow \dot{m}_{TOT} , i.e., the sum of all the hydrocarbon components' mass flow rates at the outlet, \dot{m}_A is the mass flow rate of reactant A at the exit of the reactor, A_A is the GC area of reactant A, A_{TOT} is the total GC area of the hydrocarbon reaction components and (A_A/A_{TOT}) is the GC area fraction of A. This method assumes that the outlet hydrocarbon mass flow is equal to the inlet reactant mass flow. However, it is not strictly valid because some of the hydrocarbons are converted to coke, which can not be accounted for, as it was not a gaseous product and consequently not analyzed by GC. Experiments performed at the very first minute of the reaction indicated that the most of coke were formed during this period. Therefore, the conversion calculated by the above method was not accurate for the first minute. Even for the first minute though, the calculated conversion value represents the fraction of the reactant not converted to coke that reacted to gaseous products. However, it must be said that this conversion estimation was valid after the second minute of reaction, from which the coke formation rate was drastically decreased. We illustrate the above with the following example. At the experimental run with 80 % 1-pentene at 523 K, 50 ml/min N_2 , the mass inlet flow of 1-pentene was 0.5726 g/min, while the coke formed in the first minute was $0.167 \text{ g}_{\text{coke}} / \text{g}_{\text{cat}}$ or 0.1086 g of coke, i.e., its average formation rate was 0.1086 g/min. Hence, in the first minute, 18.97 % of hydrocarbon feed was converted to coke. The coke formation rate drops during

the next two minutes to less than 0.0162 g/min, which is less than 2.8 % of the 1-pentene mass feed rate.

3.4.3 Novel Methods for Coke Characterisation

3.4.3.1 Coke Classification

With the equipment of TGA, about 150 mg coked sample was heated first to 473 K at a rate of 10 K/min and maintained there for 60 min under flowing nitrogen (60 mL N_2 /min) to remove adsorbed water and reaction-mixture components. Secondly the temperature was raised to 873 K at a rate of 10 K/min and kept for 30 min under nitrogen flow (60 mL N_2 /min). During this period coke precursors were removed resulting into a sample weight decrease. By switch from nitrogen to air at the final temperature (873K) and at the same flow rate, the hard coke deposited on the catalyst was burnt off and its weight was measured. The amount of coke precursors in the catalyst was calculated as the difference between the sample mass after drying at 473 K and switching from nitrogen to air at 873 K. The amount of hard coke was estimated by the mass difference of the catalyst sample between before and after switching from nitrogen to air, when the hard coke was completely burnt off (Chen and Manos, 2004). The whole procedure of calculating coke precursors/hard coke is illustrated in Figure 3-6.

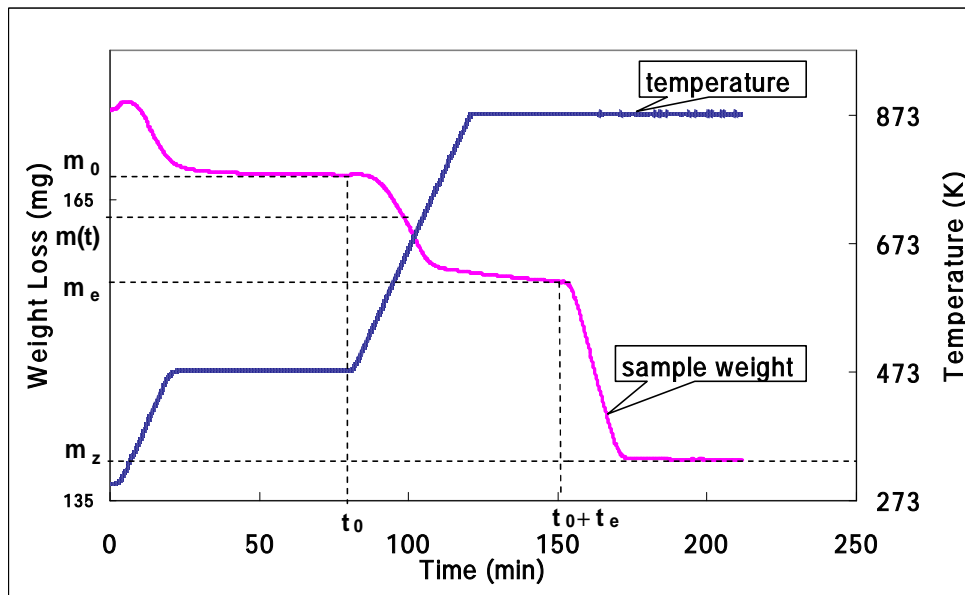


Figure 3-6 Coke precursors and hard coke of a coked sample during thermogravimetric analysis.

All coke concentration, expressed in percent, were estimated by dividing the corresponding coke amounts by the mass of catalyst, which corresponds to the sample mass at the end of TGA procedure after the burning of coke.

$$\% \text{ coke precursors} = \frac{\text{mass of coke precursors}}{\text{mass after burning}}$$

$$\% \text{ hard coke} = \frac{\text{mass of hard coke}}{\text{mass after burning}}$$

3.4.3.2 Coke Precursors Characterisation

An in-depth understanding of the chemical character of coke precursors allows the further study of the catalyst deactivation as well as the development of improved catalysts that generate less coke and are less sensitive to deactivation. Coke characterisation is often limited to determining its amount and bulk elemental

composition. Some studies have been carried out on various aspects of coke character, including C/H ratio and composition (P Magnoux et al., 1987; Moljord et al., 1995; de Lucas et al., 1997). One technique for identifying coke compounds, developed by Guisnet and co-workers (P Magnoux et al., 1987; Moljord et al., 1995; Henriques et al., 1997b), liberates coke from zeolite by dissolution of the framework in hydrofluoric acid and extracted by CH_2Cl_2 . Coke components are recovered as soluble and insoluble coke. The soluble components can be determined using IR, UV-VIS and GC/MS. This characterisation technique is complex and time-consuming. There is an incentive to develop a simple, rapid method to provide some information about the coke precursor's character and, more specifically, its volatility. The methodology presented here is based on determining how easily coke precursors are removed in an inert, non-oxidative atmosphere. The character of coke precursors is evaluated based on its ability to be removed from the catalyst. At each temperature coke precursors are either volatilised or decomposed to smaller fragments that escape from the catalyst.

From the original TGA result (Figure 3-6), the coke precursors contribution is from TGA running time $t = t_0$ to $t = t_0 + t_e$, with a TGA running temperature of 473 – 873 K, where t_0 ($t_0 = 80$ min) is the time at which removal of coke precursors starts, that is, when the TGA temperature begins to increase from $T_0 = 473$ K at a heating rate of 10 K/min and $t_0 + t_e$ ($t_e = 70$ min) is the time of the switch from nitrogen to air after the TGA temperature has remained at the final temperature (873 K) for 30 min. Furthermore, m_0 at $t = t_0$, (i.e., $T_0 = 473$ K) is the sample weight after removing adsorbed water and reaction-mixture components; m_e at $t = t_0 + t_e$, that is, after 30 min at $T = 873$ K, is the sample

weight after removing coke precursors; and $m(t)$ is the sample weight at any time t , $t_0 \leq t \leq t_0 + t_e$. In the figures showing the TGA runs, $t_0 = 80$ min becomes time 0 and $(t_0 + t_e)$ becomes 70 min.

The total mass of pure dry USHY zeolite is m_z . The total mass of coke precursors can be expressed as $m_{cp}^{tot} = m_0 - m_e$.

The mass of coke precursors which have been removed from coked catalyst at time t is $m_{cp}^{removed}(t) = m_0 - m(t)$. The mass of coke precursors which remained on the catalyst at time t is $m_{cp}^{remained}(t) = m(t) - m_e$.

Thus, the total mass concentration of coke precursors in the catalyst (in g/g_{cat}) is:

$$C_{cp}^{tot} = \frac{m_{cp}^{tot}}{m_z} = \frac{m_0 - m_e}{m_z}$$

The mass fraction of coke precursors removed from coked catalyst at any time t is:

$$F_{cp}^{removed}(t) = \frac{m_{cp}^{removed}(t)}{m_{cp}^{tot}} = \frac{m_0 - m(t)}{m_0 - m_e}$$

The mass fraction of coke precursors remaining on the coked catalyst at any time is:

$$F_{cp}^{remained}(t) = \frac{m_{cp}^{remained}(t)}{m_{cp}^{tot}} = \frac{m(t) - m_e}{m_0 - m_e}$$

Figure 3-7 shows the mass fraction of coke precursors removed from the coked catalyst running from 0 to 100 % against TGA time of 0 to 70 min, that is, from t_0 to $(t_0 + t_e)$.

Figure 3-8 shows the mass fraction of coke precursors removed from the coked catalyst running from 0 to 100 % against TGA temperature of 473 – 873 K.

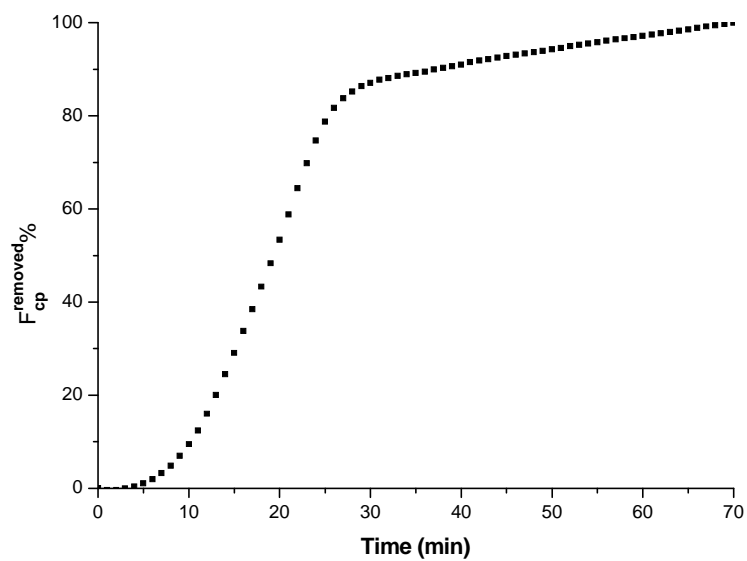


Figure 3-7 Mass fraction of coke precursors removed from coked catalyst against TGA time.

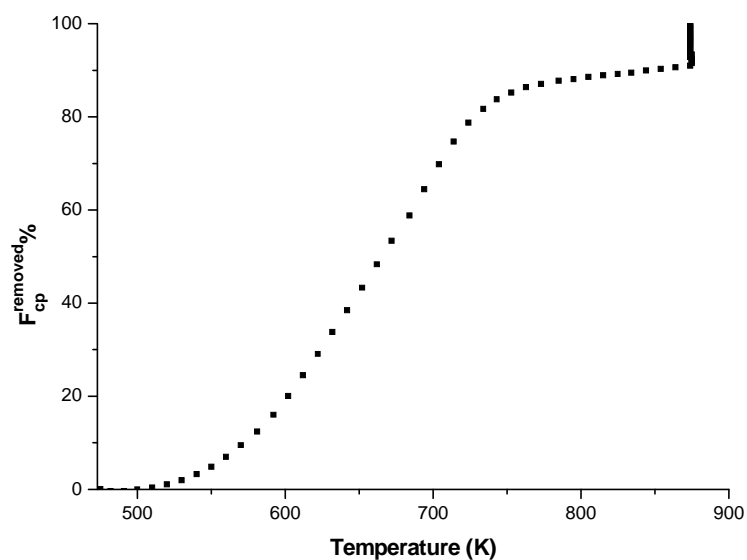


Figure 3-8 Mass fraction of coked precursors removed on coked catalyst against the TGA temperature.

Because the sample was maintained at 873 K for 30 mins during the TGA run, it is not possible to differentiate weight loss during this final 30 min stage, which appears as a vertical jump at the final temperature. Obviously, complementary plots of F_{cp}^{removed} versus temperature, as well as F_{cp}^{remained} versus time, are possible as well. Throughout this thesis, we present results in the form of F_{cp}^{removed} versus time to also capture changes occurring during the last half hour at 873 K. Each graph also gives a temperature versus time plot to connect weight loss with temperature.

3.4.3.3 Determination of Activation Energy

The Ozawa method (Ozawa T., 1965) was chosen to determine the activation energy of coke precursors. An advantage of this method is that it allows the estimation of the activation energy independently of the assumed reaction order. The Ozawa method estimates the activation energy of the overall decomposition process from experimental runs at different heating rates. From the TGA curve at each heating rate, the temperature is estimated for specific conversion levels, e.g. 10, 20,90 %. The plot of the decadic logarithms of the heating rates against the reciprocals of the corresponding values of the absolute temperatures should produce a straight line whose slope is proportional to the activation energy. By repeating this procedure for various conversion levels an activation energy value is determined for each conversion level. The average of these values is taken as the activation energy for coke precursors over USHY zeolite. The Ozawa methodology is briefly explained in the following paragraphs.

Although the catalytic cracking process is a complex one often the kinetic model used for interpretation of TGA data assumes that the overall degradation rate (r) can be expressed by a simple kinetic equation (Ozawa T., 1965).

$$r = -\frac{dw}{dt} = kw^n = A\exp\left(-\frac{E_A}{RT}\right)w^n$$

where w is the fractional residual weight of the sample, t is the time, n is the overall reaction order, k is the reaction rate constant, E_A is the activation energy, R is the universal gas constant and T is the absolute temperature.

In a TGA run the temperature increases linearly with time with a constant heating rate α

$$T = T_0 + at$$

By integration and using Boyle's approximation (Doyle C D, 1961) the above rate equation becomes

$$\int_{w_0}^w -\frac{dw}{w^n} = \frac{A}{a} \int_{T_0}^T \exp\left(-\frac{E_A}{RT}\right) dT = \frac{A}{a} \frac{E_A}{R} p\left(\frac{E_A}{RT}\right)$$

where p is a function whose decadic logarithm is approximated by Doyle as

$$\log p\left(\frac{E_A}{RT}\right) = \lambda + \mu\left(\frac{E_A}{RT}\right)$$

where λ and μ are constants whose values are estimated by Doyle (Doyle C D, 1961). For our method the value of μ is needed and it is equal to -0.4567.

For a given value of fractional residual weight, i.e. a given value of conversion, the integral of the left hand side of the above equation is constant and symbolised by $F(w)$. By taking the decadic logarithms of both right and left hand sides of the equation we get

$$\log F(w) = \log A + \log E_A - \log R - \log \alpha + \lambda + \mu \left(\frac{E_A}{RT} \right)$$

or

$$\log \alpha = v + \left(\mu \frac{E_A}{R} \right) \frac{1}{T}$$

where v is a constant incorporating all the other terms of the above equation

$$v = \log A - \log F(w) + \log E_A - \log R + \lambda$$

Hence, plotting of the decadic logarithms of the heating rates against the reciprocals of the temperatures at which the fractional residual weight reaches the same specified value should produce a straight line with slope equal to

$$\text{Gradient} = \mu \frac{E_A}{R}$$

From the gradient then the activation energy value can be estimated as

$$E_A = (\text{Gradient}) \frac{R}{\mu}$$

This estimated activation energy value corresponds to a specific coke precursors fractional residual weight, i.e. a specific conversion level. From the estimated values at different conversion levels the average value can be estimated and is accepted as the activation energy for coke precursors.

3.4.4 Acid Site Characterisation

The coke formation on zeolites and the effect of coke on acidity of catalyst were studied by several methods, such as IR, NMR, UV-VIS, and temperature

programmed desorption (TPD) (Cavell et al., 1982; Hopkins et al., 1996; Dedecek et al., 2006; Gil et al., 2007). Among them NH_3 -TPD seems to be one of the most applicable and efficient ones, providing not only the amount of acid sites but also their strength distribution. However, the regularly used Thermal Conductivity Detector (TCD) can not differentiate the signal of ammonia and other gas-phase components such as desorbed coke precursors. Hence, in the case of nonavailability of a component-specific detector, the normal NH_3 -TPD method can not be applied to coked catalysts because of falsification of the TPD signal by coke precursors removed at high temperatures. In this research, we adopted an indirect TPD method with mild temperature sample pretreatment to study the acidity of coked zeolites.

The coked samples were investigated by the novel method with a temperature programmed desorption (TPD) apparatus, a Micromeritics AutoChem 2910. The common method of acidity estimation using TPD needs sample pretreatment at relatively high temperatures. Furthermore the temperature programme itself causes coke precursors to volatilise and/or decompose into smaller volatile fragments (Cerqueira et al., 2000a). This decomposition might also leave nonvolatile fragments on the catalyst surface. These nonvolatile fragments are accounted for as hard coke. Current work is further looking into the exact mechanism of removal of coke precursors through thermal treatment. In both cases these coke components cause a falsification of the TPD signal that does not represent the ammonia amount desorbed. To avoid this falsification due to the chemically active character of coke precursors, we adopt indirect TPD methods with mild temperature sample pretreatment to study the acidity of coked zeolites.

With this method the free acid sites of coked zeolites as well as acid sites inhabited by hard coke can be quantitatively determined. Furthermore, the character of coke precursors can be studied.

The TGA (Thermogravimetric Analysis) temperature programme for classification of coke precursors and hard coke (Wang and Manos, 2007b) was applied to the TPD analysis. A blank TPD analysis was carried out in absence of catalyst in order to verify if ammonia retained in the apparatus set up was significant. As the TCD (Thermal Conductivity Detector) signal during this analysis did not increase above the base line, one can conclude that the amount of ammonia retained by the system itself is negligible. Around 50 mg coked catalyst sample was placed in a U-shaped quartz cell. It was then preheated at 10 K/min to 473 K where it stayed for 1 h. During the process, reagents adsorbed on the catalyst surface and most of water molecules were removed. After cooling to 353 K, adsorption of ammonia was carried out in He stream (10% NH₃, 20 mL/min). After the catalyst surface became saturated, the loaded sample was heated to 383 K by 10 K/min for physisorbed NH₃ to be desorbed. The linear temperature program (10 K/min) was then started from 383 K to 873 K and remained at 873 K for 30 min. The desorbed ammonia and coke precursors were monitored continuously with a thermal conductivity detector. This is called First TPD. The fresh zeolite was also analysed by this method to measure the total free acid sites. The total number of acid sites could be found quantitatively by driving the desorbed ammonia from NH₃-TPD experiments to a standard HCl solution of a specified concentration, e.g. 0.1 M, and subsequent titration.

The same TPD was carried out initially without preceding ammonia adsorbed. This was called TPD without ammonia. Furthermore, availability of GC/MS or HPLC/MS instruments coupled to the TPD rig could characterise the molecular composition of the coke components removed. A Second TPD with ammonia was carried out with 873 K for preheating 30 min instead of 473 K. During this period of preheating, coke precursors as well as water adsorbed and reaction mixture components were removed. The First TPD contains both ammonia and coke precursors adsorbed on the zeolite. However, the TPD without ammonia only contains coke precursors. Comparing the signal of TPD without ammonia with that of First TPD, it is obvious that they overlap at the high temperature zone (right side) for any coking system due to removal of coke precursors and the strong acid sites, which contribute at high temperature (above 600 K) ammonia signal, being deactivated. By subtracting the signal of TPD without ammonia from the signal of First TPD, the free acid sites of coked sample inhabited by both coke precursors and hard coke can be calculated as presented in Figure 3-9.

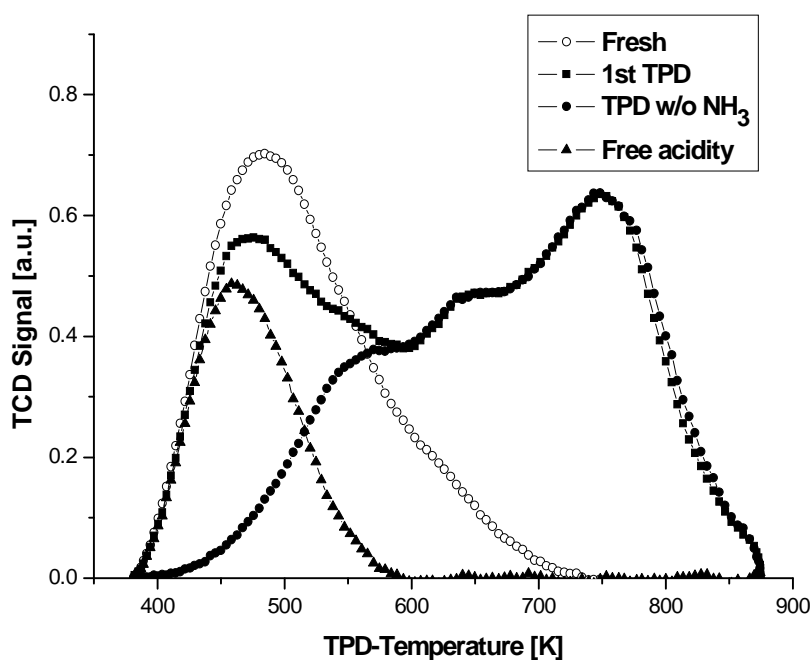


Figure 3-9 Description of free acid sites by the difference of first TPD and TPD without NH₃ (1-pentene reaction, T = 623 K, TOS = 1 min). For comparison, in the same figure it is shown the acidity of fresh USHY zeolite.

First TPD of fresh zeolite determines directly the total acid sites of fresh zeolite which is also shown in Figure 3-9. Since coke precursors have been removed after the pre-treatment at 873 K in He stream during Second TPD, only hard coke remained deposited on the coked catalyst. Therefore, the signal of Second TPD detected by TCD is due exclusively to desorbed ammonia and reveals the free acid sites of coked zeolite samples inhabited only by hard coke, after complete removal of coke precursors. All these TCD signals were normalized by the zeolite weight excluding coke components. These calculation processes can be clearly illustrated in Figure 3-10. With these methods, not only the amount of acid sites but also the acid sites strength distribution of coked zeolites can be determined.

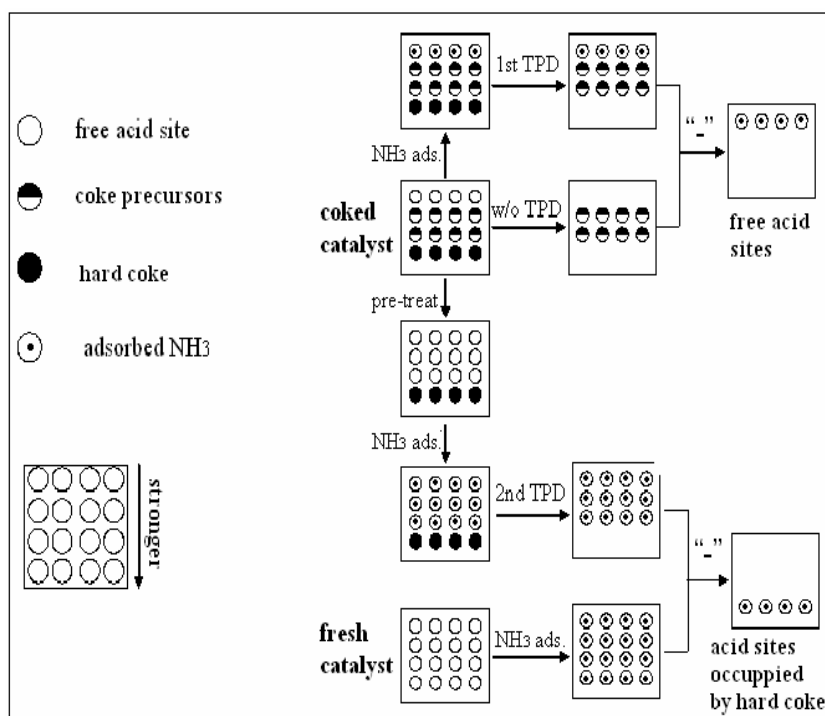


Figure 3-10 Procedure of mild temperature pre-treatment and indirect TPD.

In order to make the temperature treatment very clear, we also present the whole temperature programme in Figure 3-11.

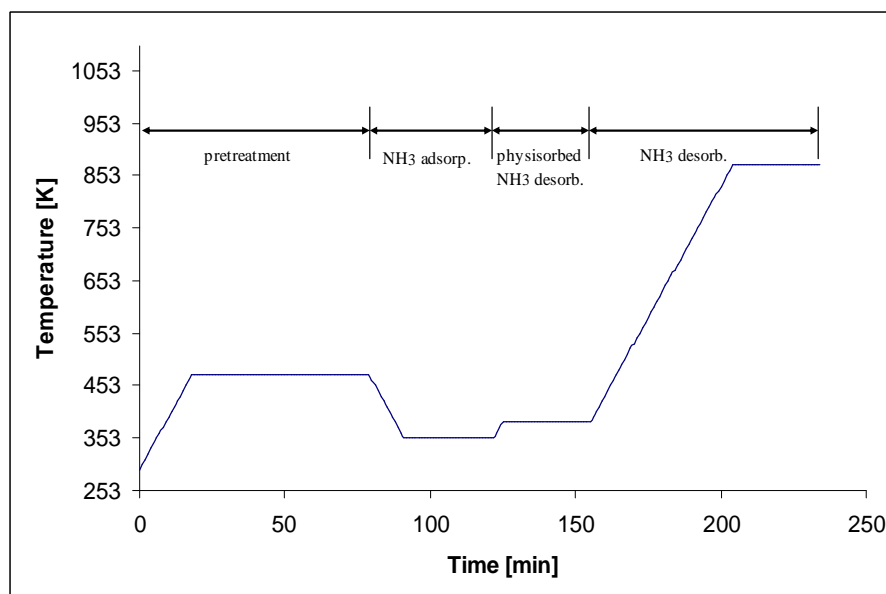


Figure 3-11 TPD temperature programme.

Since the samples used were exposed to high temperature cycles, in order to test their thermal stability the acidity of a regenerated catalyst was also measured. The NH_3 -TPD curve of the regenerated catalyst after removal of all coke components at 873 K in air was exactly the same as this of the fresh sample. The structure of the fresh catalyst samples being ultrastabilised zeolite and having been calcined at 873 K stays intact at exposure at high temperatures.

4 EXPERIMENTAL RESULTS & DISCUSSION

4.1 FIXED-BED REACTOR STUDIES

In this chapter we report about catalyst deactivation during reactions of 1-pentene over USHY zeolite in a fixed-bed reactor. The effects of reaction temperature and time-on-stream (TOS) on product distribution and conversion are discussed. Cracking and hydride transfer were the predominant reactions in the first minute of TOS which deactivated rapidly allowing isomerisation to become the main reaction afterwards. The hydrogen freed during this initial time from the formation of high C/H ratio coke components contributed to the formation of hydride transfer products.

4.1.1 Products Distribution

Experiments in the absence of catalyst at different reaction temperatures (523 – 623 K) did not produce any detectable amounts of any products. The product distribution of 1-pentene reactions over USHY zeolite at various reaction temperatures is presented in Figure 4-1, Figure 4-2 and Figure 4-3. The major products grouped according to main reaction formed were:

- Double bond isomers (DbI): trans-2-pentene (t-2-C₅=) and cis-2-pentene (c-2-C₅=);
- Skeletal isomers (SkI): 2-methyl-1-butene (2-m-1-C₄=) and 2-methyl-2-butene (2-m-2-C₄=);
- Cracking (Cr) products: isobutene (i-C₄=) and propene (C₃=);

- Hydride transfer (HT) products: n-pentane (n-C₅) and 2-methylbutane (2-m-C₄).

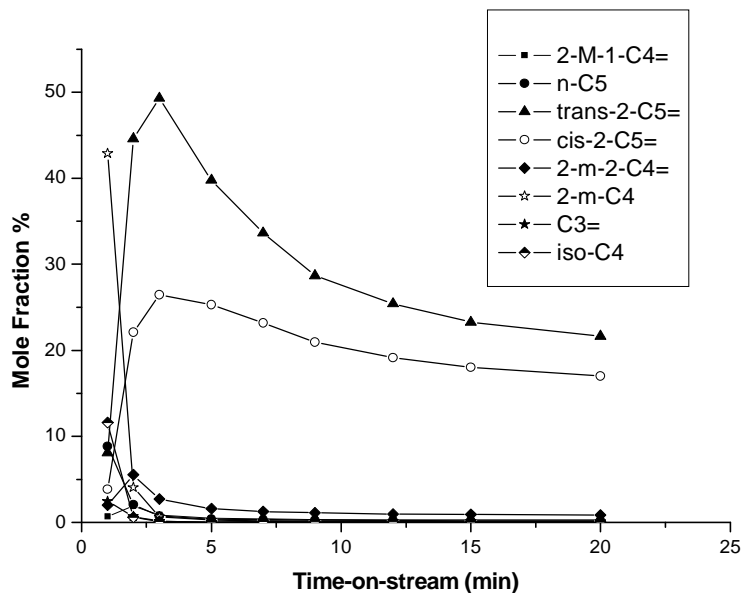


Figure 4-1 Product distribution of 1-pentene reaction over USHY zeolite at 523 K.

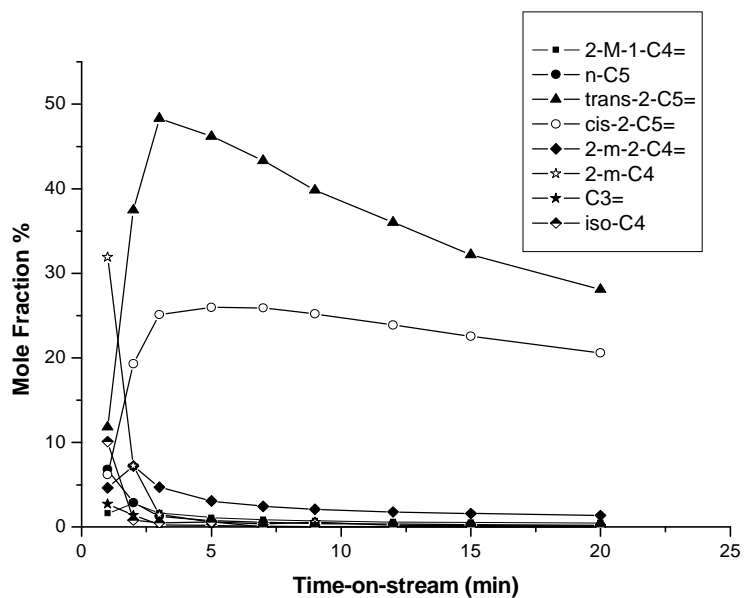


Figure 4-2 Product distribution of 1-pentene reaction over USHY zeolite at 573 K.

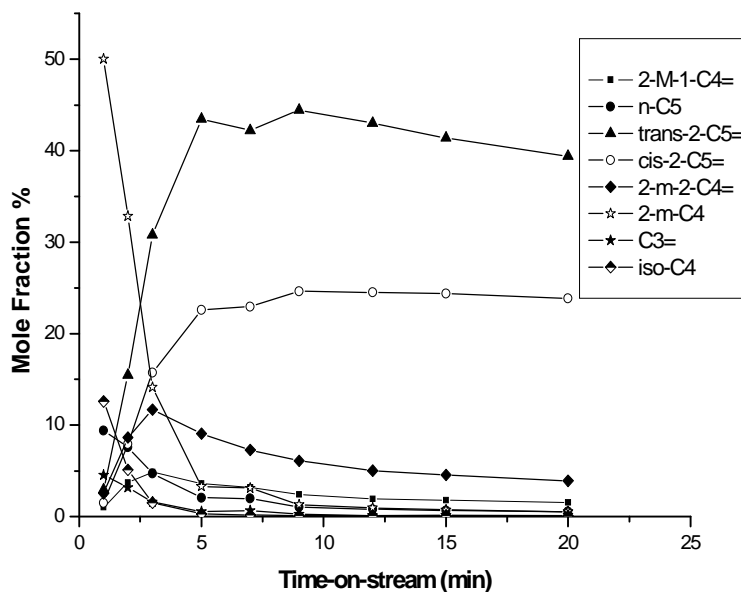


Figure 4-3 Product distribution of 1-pentene reaction over USHY zeolite at 623 K.

GC analysis detected other hydrocarbons in amounts much less than 1 %. Based on the product distribution, a reaction network was suggested as shown in Figure 4-4 (Hochtl et al., 2001). Since ethene is very easy to form coke (Paweewan et al., 1998), octene (Brillis and Manos, 2003) and hexene (Chen and Manos, 2004) are easy to further crack, they were not detected more than 1 % even at initial stage of the reaction.

Initially, hydride transfer and cracking were the predominant reactions rather than isomerisation. At 1 min TOS and 523 K, the products by hydride transfer and cracking reaction account for 51.7 % (2-m-C₄: 42.9 %, n-C₅: 8.8 %) and 14.1 % (i-C₄: 11.6 %, C₃: 2.5 %) respectively. Correspondingly at 573 K, hydride transfer and cracking products account for 38.7 % (2-m-C₄: 31.9 %, n-C₅: 6.8 %) and 12.8 % (i-C₄: 10.1 %, C₃: 2.7 %), while 59.5 % (2-m-C₄: 50.1 %, n-C₅: 9.4

%) and 17.1 % (i-C₄=: 12.6 %, C₃=: 4.5 %) at 673 K. However, these products decreased drastically during the initial stage, indicating a fast deactivation of these hydride transfer- and cracking-reactions. These observations concerning the decrease of hydride transfer can be ascribed to a very rapid formation of coke at the initial stage of the reaction. Since coke components are hydrogen poor with a carbon to hydrogen ratio (C/H) much larger than this of the reactant, hydrogen is transferred during coking from coke precursors to olefinic surface species which desorb as paraffinic products. Formation of paraffins – n-pentane, 2-methyl-butane (isopentane) and isobutane– in these reactions, is enhanced by hydride transfer at initial TOS. As this hydrogen was consumed in conjunction with a sharp decrease of coking rate, no more hydrogen was available for hydride transfer to form paraffins resulting in a sharp drop of the yield of n-pentane, 2-methyl-butane and isobutane from 1-pentene.

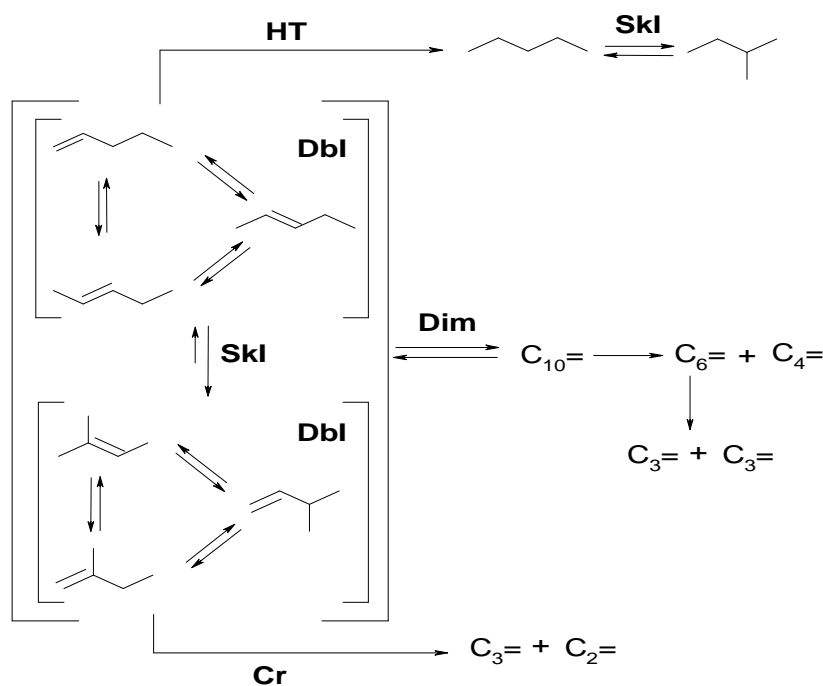


Figure 4-4 Reaction network of 1-pentene reaction.

As explained above, hydride transfer and cracking products experienced a steep decline at 1 min of TOS, while isomer mole fractions increased followed by a slow deactivation. This initial increase of double bond isomers, trans- and cis-2-pentene, is indicative of the behaviour of intermediate products. It suggests that at the initial stage trans- and cis-2-pentene react further to cracking products at a much higher rate than the rate they are formed from the reactant 1-pentene. After 3 min of TOS, the only remaining products in significant amounts were 1-pentene isomers, i.e. trans-2-pentene, cis-2-pentene and small amounts of branched isomers, 2-methyl-2-butene and 2-methyl-1-butene. We would like to emphasise that the blank experiments in the absence of catalyst did not produce any pentene isomers. The only reactions taking place after 3 min at the three different temperatures were isomerisations and mainly double bond isomerisations rather than skeletal ones. Furthermore, the thermodynamically favoured trans-2-pentene was formed in larger amounts than cis-2-pentene at all conditions. Cis-2-pentene mole fraction however was nearer to the equilibrium value and showed a much slower decline than trans-2-pentene. Chemical reaction equilibrium calculations with Gibbs energy of formation data taken from (Robert C. Reid et al., 1987) result into the following compositions:

At 523 K; 1-pentene: 3.6 %, cis-2-pentene: 19.4 %, trans-2-pentene: 77.0 %.

At 573 K; 1-pentene: 3.9 %, cis-2-pentene: 18.2 %, trans-2-pentene: 77.9 %.

At 623 K; 1-pentene: 4.1 %, cis-2-pentene: 17.3 %, trans-2-pentene: 78.6 %.

Although strong coking took place in the first minute that resulted into all strong acid sites being occupied by coke, the rest of the acid sites were enough to catalyse double bond isomerisation at high extent. Over strong acid sites the selectivity towards hydride transfer/cracking reactions compared to isomerisation

was very high. Hence, almost all 1-pentene which comes into contact with strong acid sites converts to corresponding products with almost no isomers formed, as they undergo further cracking reactions. However, the selectivity picture over weak acid sites reverses converting 1-pentene exclusively to isomers. Hence, isomerisation yields showed a drastic increase. The product distribution profiles with TOS (Figure 4-1, Figure 4-2 and Figure 4-3) show a remarkable synchronisation between the decline of hydride transfer/cracking and the raise of isomerisation reactions. Comparing cracking and hydride transfer products at three different reaction temperatures, it can be observed that the initial time interval where the rapid decline takes place decreases as the reaction temperature decreases. Considering the coking in the first three minutes of TOS (Figure 4-7, Figure 4-8 and Figure 4-9), the amount of total coke increased slower at high temperatures than that at lower temperatures mainly due to slower hard coke increase indicating slower deactivation rates at higher temperatures.

In order to study the reaction product distribution in more details, 1-pentene reaction over USHY zeolite at 623 K was carried out only for much shorter time-on-stream, 3 min, allowing more often sampling. Products were sampled at every 20 seconds in the first 180 seconds TOS. The product distribution is presented in Figure 4-5. It can be clearly seen that the hydride transfer products decreased rapidly, 2-methyl-butane decreased from 46.3 % at 20 s TOS to 1.6 % at 180 s TOS and n-pentane decreased from 7.5 % at 20 s TOS to 1.7 % at 180 s TOS. This observation confirms the above explanation of limitation of hydrogen from transformation of hydrogen rich reaction components to hydrogen poor coke components. The cracking products also decreased, isobutane decreased from 22.7

% at 20 s TOS to 0.2 % at 180 s TOS and propene decreased from 7.5 % at 20 s TOS to 1.7 % at 180 s TOS respectively. The decrease for cracking products can be explained by the fast catalyst deactivation. The fast coke formation induced poisoning of the acid sites, especially the strong ones. In addition, the deposited coke would decrease the accessibility of alkenes to part of the acidic sites and would reduce the free space around the acid sites available for the formation of the bulky bimolecular reaction intermediates (Zhu et al., 2005). However, during the initial TOS during which hydride transfer and cracking experienced a steep decrease, double bond isomerisation products, trans-2-pentene and cis-2-pentene increased. On the other hand, higher reaction temperature favoured higher formation of double bond isomerisation products whose decline was much slower for the same reason that the overall conversion shows an apparent lower deactivation at higher temperatures (see following section 4.1.2). All acidic solids, regardless of their cracking ability, isomerise alkenes (Kissin, 2001). Cracking and Skeletal isomerisation need stronger acid sites which are deactivated faster.

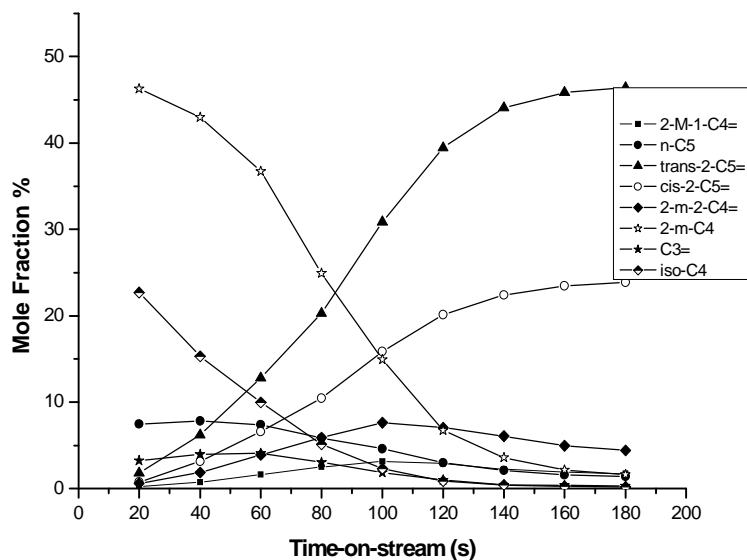


Figure 4-5 Product distribution of 1-pentene reaction over USHY zeolite at 573 K in short TOS.

4.1.2 Conversion

The conversion of 1-pentene versus TOS is shown in Figure 4-6 for three different reaction temperatures. The conversion eventually decreased at all temperatures. As expected the conversion levels were higher at higher temperatures although initially the conversion was almost 100 % at all reaction temperatures. As discussed above, during the first minute of TOS the conversion was exclusively due to hydride transfer/cracking reactions, while later it was due to isomerisation reactions. During the initial period, the catalyst underwent through a rapid deactivation phase, which was steeper at lower reaction temperatures. Although the catalyst was deactivated at different levels at different reaction temperatures at 1 min TOS (Figure 4-7, Figure 4-8 and Figure 4-9), the conversions were not much different. This suggests that at 1 min there were enough free acid sites for the isomerisation to take place. On the other hand, similar amounts of total coke were formed at different temperatures (Figure 4-7, Figure 4-8 and Figure 4-9) indicating similar catalyst activity levels. Hence, the higher conversions are simply due to the Arrhenius relationship. Similar amounts of acid sites result at higher reactivity and hence conversion at higher temperatures. This led to an apparent slower deactivation at higher temperatures (Figure 4-6).

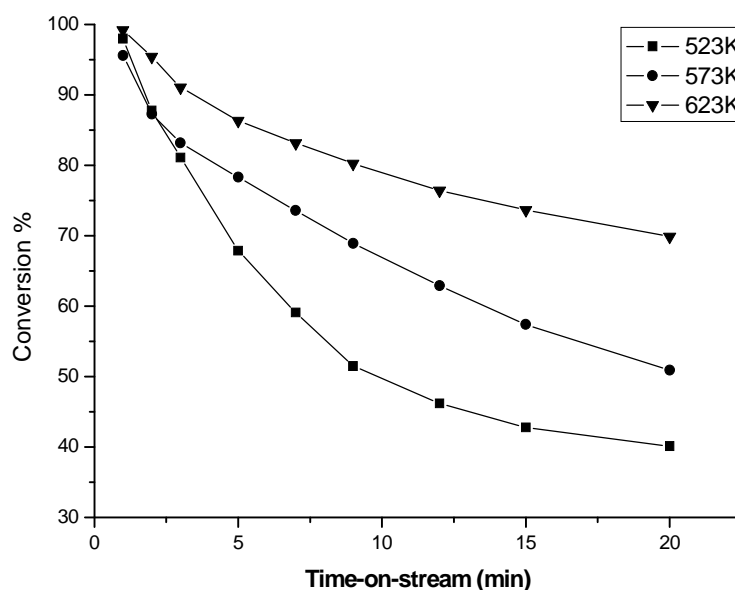


Figure 4-6 Conversion of 1-pentene reaction over USHY zeolite at various reaction temperatures

4.2 THERMOGRAVIMETRIC CHARACTERISATION OF COKE COMPONENTS

Coke is classified into coke precursors, which are removed from the catalyst sample simply through volatilisation in inert nitrogen, and hard coke, which remains on the catalyst even at high temperature (873 K) and is removed by burning. Furthermore, coke precursors are characterised by the thermogravimetric methodology (described in chapter 3.4.3.2). The effect of different reactants, time-on-stream and reaction temperature on coke precursors formation and chemical characterisation was investigated. The method allowed us to classify coke precursors into “small” and “large” ones. Coke precursors are formed

preferentially on the strongest acid sites with a rapid rate with fast further transformation to other coke species. Furthermore, the method revealed a maximum of large coke precursors with time-on-stream due to the fast transformation of them into hard coke over strong acid sites compared to the much slower formation from small coke precursors over weak acid sites.

4.2.1 Coke Content

Since the initial deactivation effect of coke is most important for the catalyst deactivation study, the effect of reaction time (TOS) in the first 20 min on the coking behaviour of 1-pentene reaction over USHY zeolite at different reaction temperatures was investigated. As we can see from Figure 4-7, Figure 4-8 and Figure 4-9, presenting the total coke content of 1-pentene reaction over USHY zeolite at 523 K, 573 K and 623 K, the coke content at all these three reaction temperatures was quite high, about 21 % at 20 min of TOS. Furthermore, it is fairly obvious that coke formation is an extremely rapid process at the beginning of catalyst exposure to the reaction mixture. The total coke formation rate is extremely high during the first minute, whereas it becomes much lower afterwards, similarly to 1-octene reaction (Brillis and Manos, 2003). After 3 min, the total coke content shows a linear dependence on TOS which is also in good agreement with previous work (Brillis and Manos, 2003). In the first minute, 16.7 %, 13.2 % and 13.1 % ($g_{\text{coke}}/g_{\text{cat}}$) content of total coke were produced at 523 K, 573 K and 623 K respectively. The total coke content formed in the first minute decreases with increasing reaction temperature. Although the total coke amount at 523 K was quite higher than at the other two temperature levels, the initial conversion was extremely high at all three reaction temperatures suggesting that the available

catalytic acidic sites are sufficient for cracking. Hence, the cracking ability seemed unaffected by reaction temperature during initial TOS. However, the temperature has an effect on the condensation of coke components resulting to coke precursors volatilising and/or desorbing more easily at higher temperatures. Although the amount of coke at the end of the reaction (20 min) was almost the same, the initial coking rate at high temperatures was a little lower than that at low temperatures because of the lower condensation of coke components at high temperatures. For example, at 2 min TOS, coke content was 19.2 %, 18.5 % and 16.7 % for 523 K, 573 K and 623 K. Less coke at higher reaction temperature results in higher conversion. Since coke is formed preferentially on the strongest acid sites and causes their deactivation, the initial deactivation effect of coke is more pronounced than it would be if all of the acid sites were of the same strength (Brillis and Manos, 2003; Wang and Manos, 2007a; Wang and Manos, 2007b).

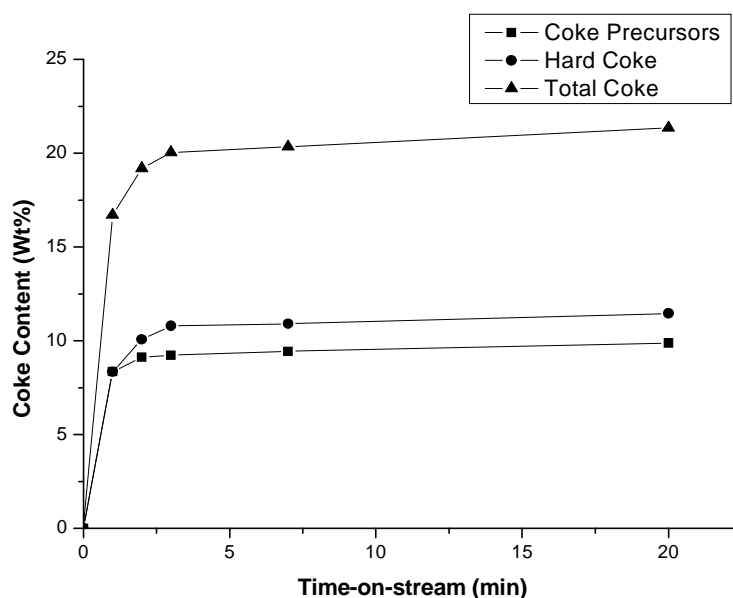


Figure 4-7 Coke content of 1-pentene reaction over USHY zeolite at 523 K.

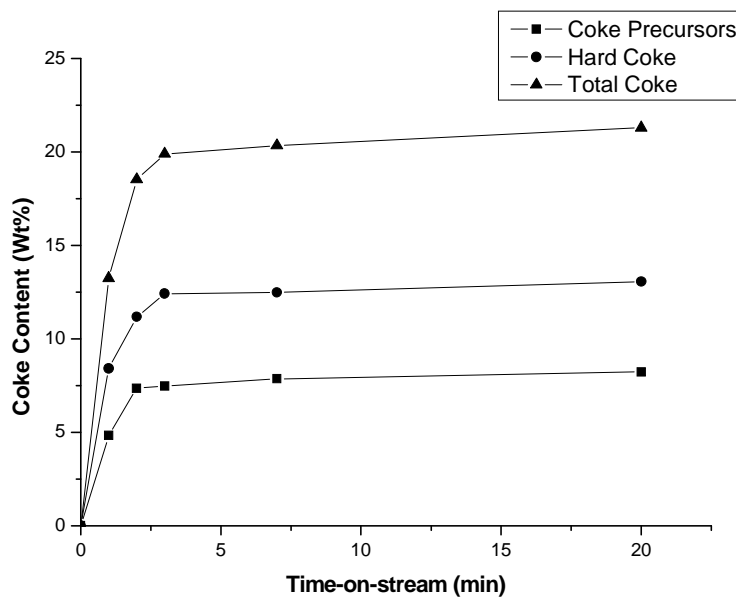


Figure 4-8 Coke content of 1-pentene reaction over USHY zeolite at 573 K.

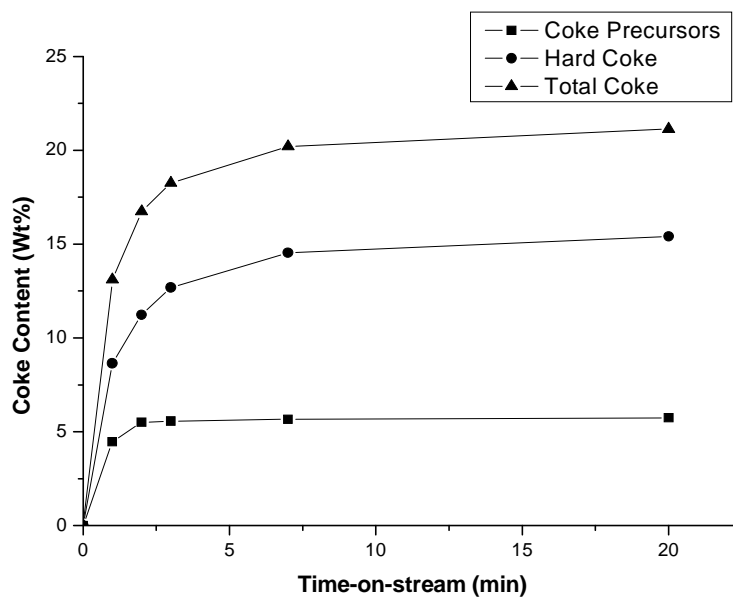


Figure 4-9 Coke content of 1-pentene reaction over USHY zeolite at 623 K.

Classification of coke into coke precursors and hard coke was carried out in order to gain an insight into the coking effects on catalyst deactivation (The method is

described in chapter 3.4.3.1). As shown in Figure 4-7, Figure 4-8 and Figure 4-9, both coke precursors and hard coke increased with increasing TOS. Both showed a fast coke formation in the first minute TOS and linear time dependence after the first minute especially for hard coke. It can be assumed that hard coke has a saturate character. By comparing the colour of coke precursors and hard coke, we found coke precursors were brown while hard coke was black indicating that the latter is more aromatic than coke precursors. Regarding coke colour studies, we observed the following: the originally brown coked catalyst was heated to 873 K with 10 K/min in nitrogen flow and then cooled down to room temperature, i.e. it underwent the treatment where coke precursors have been removed leaving only hard coke. The colour of the final catalyst state, i.e. hard coke, was black. This can be explained as following. Coke precursors continuously grow larger surface causing the size of the surface oligomers to continue to grow and eventually form polyaromatic hard coke. Hard coke being very aromatic in character has a black colour, while coke precursors containing much less polyaromatics have a much lighter colour. The ratio of coke precursors to hard coke in a coked catalyst sample determines the overall sample colour. The original brown coloured coked catalyst (sample from 1-pentene reaction over USHY zeolite at 523 K, TOS = 20 min) consists of almost equal amounts of coke precursors and hard coke (Figure 4-7). This is confirmed by the coked catalyst samples from different reaction temperatures, 523 K and 623 K; brown and dark gray colour respectively. The ratio of hard coke/coke precursors is almost 1.2 at 523 K compared to 2.7 at 623 K.

From Figure 4-7, Figure 4-8 and Figure 4-9, it can be also observed that hard coke content is higher than coke precursors during the whole reaction process at all

three different reaction temperatures. At 523 K and 573 K, after 1min TOS, both coke precursors and hard coke were formed by the very similar rate while the formation rate of hard coke is slightly higher than coke precursors at 623 K. Moreover, the difference in coke content between coke precursors and hard coke increases with increasing reaction temperature although the amount of total coke is similar. It shows that the individual amounts of coke precursors and hard coke is more influenced by reaction temperature rather than the amount of total coke. The effect of reaction temperature on the amount of coke precursors, hard coke as well as total coke is shown in Figure 4-10. These results indicate that the total amount of coke nearly stays the same with reaction temperature, the amount of coke precursors decreases with increasing reaction temperature while the amount of hard coke increases. This behaviour can be explained by the higher volatility of coke precursors with increasing reaction temperature and their removal into gas phase (Chen and Manos, 2004). The hard coke formation, however, increases with temperature as an activated reaction process as predicted by Arrhenius behaviour.

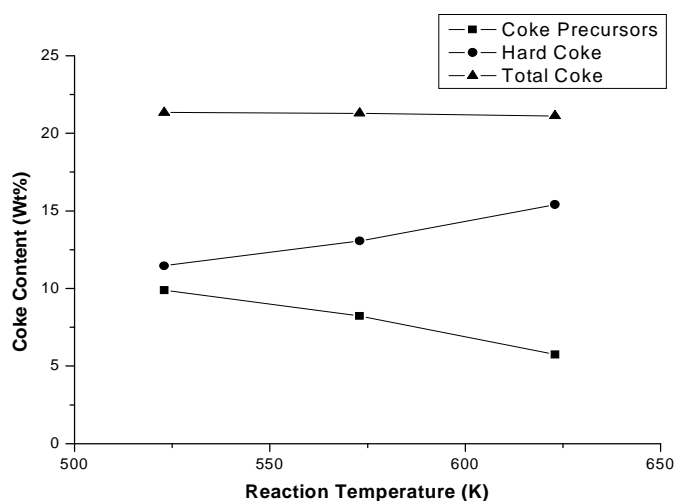


Figure 4-10 Coke content after 20 min TOS of 1-pentene reaction over USHY zeolite at different reaction temperatures.

4.2.2 Coke Precursors Characterisation

4.2.2.1 Effect of Different Reactants

To investigate the application of this TGA method (chapter 3.4.3.2) for coke precursors characterisation, we used different reactants: an alkane (n-heptane, 35 % in N₂, residence time = 0.178 s, WHSV = 59.579 h⁻¹), an alkene (1-pentene, 80 % in N₂, residence time = 0.055 s, WHSV = 86.211 h⁻¹) and an aromatic hydrocarbon (ethylbenzene, 12 % in N₂, residence time = 0.239 s, WHSV = 25.886 h⁻¹). Unfortunately, achieving the exact same experimental conditions with all three reactants was not possible, due to the huge volatility differences among these components. The reaction temperature (623 K) and TOS (20 min) of analysed sample were the same for all reactants, however. Different coking mechanisms occur with the three different reaction systems, resulting in different compositions of coke precursors (Cerqueira et al., 2000b; Chen and Manos, 2004) as well as different ratios of coke precursors to hard coke, as shown in Table 4-1.

Table 4-1 Coke content of USHY zeolite coked during reactions of different reactants, T = 623 K, TOS = 20min.

$\% = \frac{g_{\text{coke}}}{100g_{\text{zeolite}}}$	Coke Precursors %	Hard Coke %	Total Coke %
n-Heptane	1.74	0.78	2.52
Ethylbenzene	3.37	1.03	4.50
1-Pentene	5.73	15.40	21.13

Figure 4-11 plots the mass fraction of coke precursors removed from coked zeolite of these reactions against the TGA running time. We see that coke precursors in the n-heptane and ethylbenzene systems are removed at relatively the same rate during the entire TGA-run, indicating a uniform distribution of coke precursors. With 1-pentene, however, several changes in the removal rate occur during the run. In the first 5 – 15 min, the removal rate of 1-pentene coke precursors is quite low. During this time, removal of the 1-pentene coke precursors is more difficult than removal of the paraffin/aromatic systems. The rate of removal increases rapidly between 15 min (620 K) and 25 min (720 K), then slows considerably at 25 – 30 min (720 – 770 K) until the end of the TGA-run. This phenomenon becomes clearer by looking at another way of plotting the results. From the original Figure 4-11 by differentiation we can estimate and plot the coke precursor removal rate against time, as shown in Figure 4-12. Here the 1-pentene coke precursors show a relatively high peak at around 22 min, followed by a plateau at a considerably lower level until the end of the TGA run. With both other systems, the rate is spread out uniformly at a much lower level. Figure 4-11 and Figure 4-12 indicate a considerable variation in the chemical character of coke precursors, as evident from the mode of their removal in an inert atmosphere.

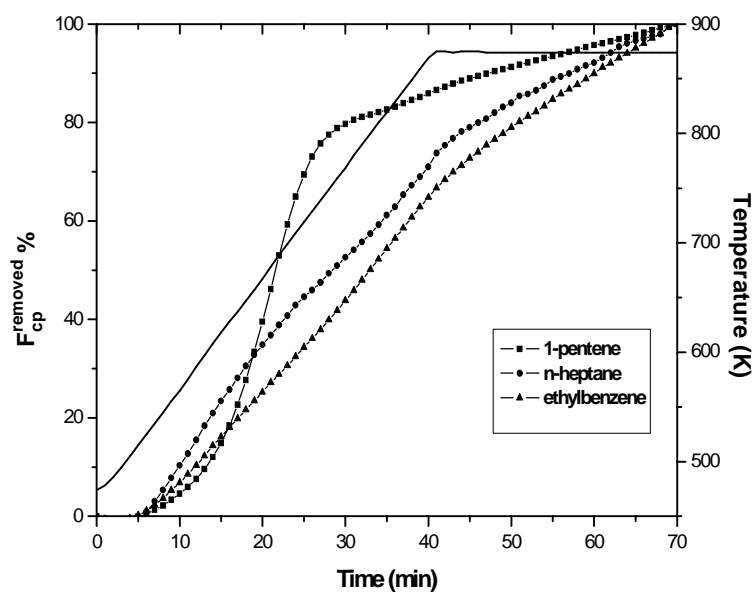


Figure 4-11 Mass fraction of coke precursors removed from coked catalyst against the TGA-time for different reactants, reaction temperature is 623 K, TOS=20 min.

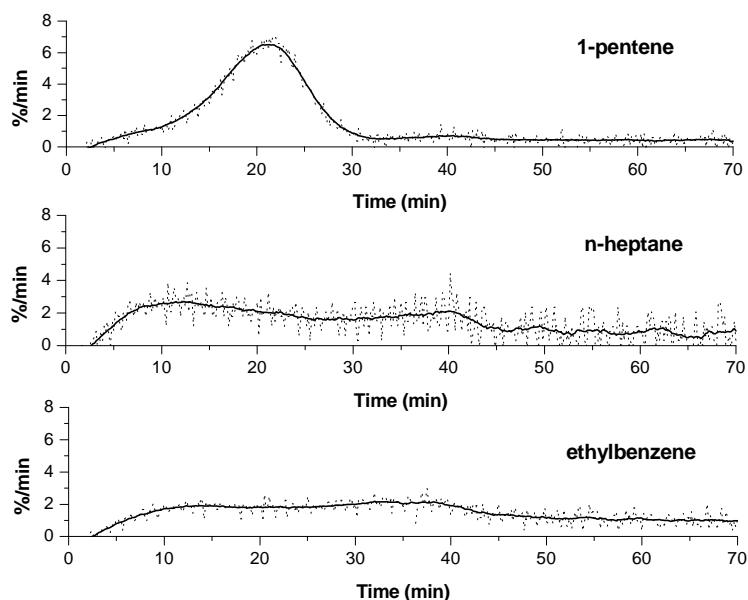


Figure 4-12 Coke removal rate against TGA-time for samples coked during reactions of different reactants, 1-pentene, n-heptane and ethylbenzene (Reaction temperature = 623 K, TOS=20 min)

1-Pentene cracking occurs according to carbenium mechanism (Kissin, 2001). It easily forms a carbenium ion when it is adsorbed on a Brönsted proton. These carbenium ions can be transformed into coke precursors through bimolecular reactions, such as oligomerization, alkylation and hydrogen transfer (M Guisnet and P Magnoux, 1994). From the 1-pentene curve in Figure 4-11, the ability to remove coke precursors decreases at 25 min indicating that either the composition of coke precursors is not uniform and/or the stability of coke precursors differs greatly. For the alkylbenzene reaction on solid acids, an aromatic ring easily forms a carbonium ion (Olah and Kuhn, 1959). The reaction process involves formation of the alkylbenzenium ion, followed by dealkylation (Olah et al., 1972). During this kind of reaction, polyaromatic coke precursors are formed by accumulation of fused and/or bridged aromatic rings. Their diffusion into the pores is slow due to the strong adsorption of these basic character molecules on the acid sites, which is smoother than that of alkene (M Guisnet and P Magnoux, 1994), resulting in almost linear removal of the coke precursors with time. The chemical character of coke precursors from n-heptane, a paraffin, is between that of 1-pentene and ethylbenzene. In both cases, coke formation occurs slowly from the monoaromatics and alkanes, the transformation of which into alkenes and polyaromatics is slow. The formation of these coke-making molecules is then the limiting step of coking (M Guisnet and P Magnoux, 1994).

4.2.2.2 Effect of Time-On-Stream (TOS)

Figure 4-13 presents the mass fraction of coke precursors removed at various TOS from coked USHY zeolite during 1-pentene cracking (1-pentene, 80 % in N₂,

residence time = 0.066 s, WHSV = 86.211 h⁻¹) at 523 K. It can be clearly seen that coke precursors are removed rapidly in the first 25 min of TGA time (473 K – 720 K, 0 – 25 min), followed by much slower removal (720 K – 873 K, 25 – 70 min). For all samples, coke precursors removal slows considerably at around 25 min (720 K), indicating the existence of two coke precursors types. The first group contains coke precursors removed at the first stage of the TGA procedure (0 – 25 min). Judging from their removal rate and lower temperature, this group comprises coke precursors that are more easily removed than those of the latter group. We call these “small coke” precursors, in contrast to “large coke” precursors, which are removed after 25 min. During the entire TGA run, the order of the curves remains the same: $F_{cp}^{removed}$ (TOS=20 min) > $F_{cp}^{removed}$ (TOS=7 min) > $F_{cp}^{removed}$ (TOS=3 min) > $F_{cp}^{removed}$ (TOS=2 min) > $F_{cp}^{removed}$ (TOS=1 min).

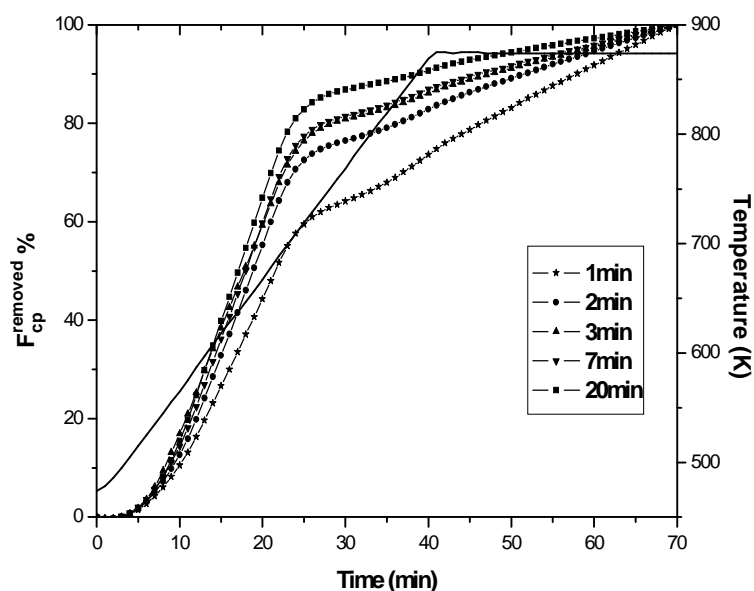


Figure 4-13 Mass fraction of coke precursors removed from coked catalyst against the TGA running time at various TOS, reaction temperature = 523 K.

The mass fraction ratio of small coke to large coke precursors increases with TOS, which is counterintuitive finding. On the other hand, plotting the corresponding mass fractions (including the mass fraction of hard coke) with TOS (Figure 4-14) shows a maximum in the large coke precursors curve, which is indicative of reaction schemes in series: reaction mixture components \rightarrow small coke precursors \rightarrow large coke precursors \rightarrow hard coke. Figure 4-14 clearly shows that the decreased amount of large coke precursors is accompanied by a significant increase of the amount of hard coke and a much slower increase in the amount of small coke precursors. By itself, however, this reaction scheme does not explain the observed TOS run for the two coke precursors groups. The role of strong and weak acid sites must be taken into account.

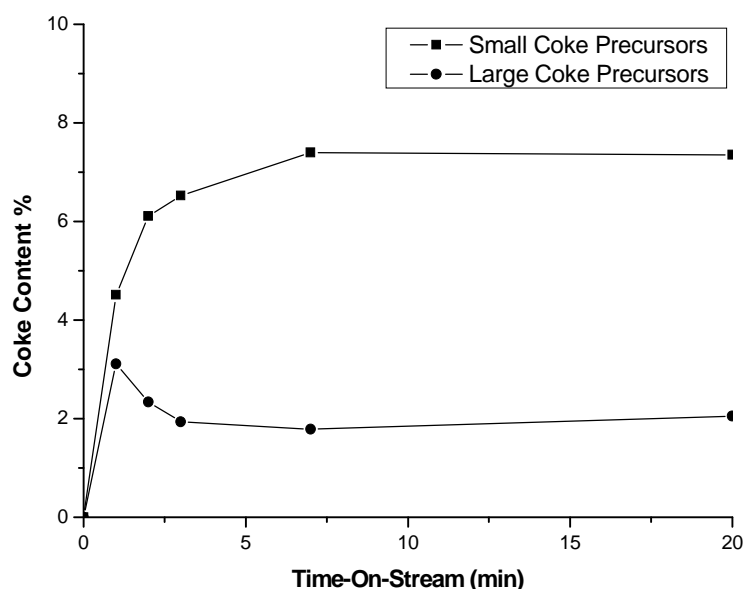


Figure 4-14 Mass fraction of “small” and “large” coke precursors at different TOS.

During alkene reactions on USHY zeolite, the main reaction as well as coke formation occurs first at strong active sites. At TOS = 1 min, GC analysis of the

reaction mixture revealed considerably greater formation (in both number and size) of cracking/hydrogen transfer products than occurred later. Similar results have been reported previously (Brillis and Manos, 2003; Bjorgen et al., 2003). With further increases in the number and size of coke precursors, they begin to be deposited on weak acid sites, while the precursors on strong acid sites grow larger. The results presented in Figure 4-13 suggest that coke precursors deposited on strong acid sites, i.e. at earlier TOS, are more stable than those formed on weak acid sites. Soon all strong acid sites are occupied by coke precursors. Hence, at longer TOS, a large proportion of coke precursors on weak acid sites are lighter. The rate of coke precursors removal is faster at later TOS compared with earlier TOS, because the fraction of coke compounds on strong acid sites decreases with TOS. About 60 % (TOS = 1 min) to 82 % (TOS = 20 min) of coke precursors were removed in weak acid sites. The maximum mass fraction of large coke precursors is due to the rapid transformation of these precursors into hard coke over strong acid sites compared with the much slower formation from small coke precursors over weak acid sites.

Coke is formed preferentially on the strongest active sites. Because these sites are the most active, the initial deactivating effect of coke is more pronounced than it would be if all of the active sites were of the same strength (Brillis and Manos, 2003). Through aromatization, coke deposits become larger and more aromatic with increasing TOS and coke content (Hopkins et al., 1996; Holmes et al., 1997; Cerqueira et al., 2000b). This is also demonstrated by the colour of coked catalyst. The 20-min TOS sample is black, indicating strong aromatic character, whereas the 1-min sample is brown, indicating a less-unsaturated bond character. In the

strong acid sites of the coked sample at 20 min TOS, more coke precursors of greater stability were formed. In the weak acid sites part, because of the long TOS, more coke precursors were formed as well. The most likely explanation for this phenomenon is that strong acid sites are more deactivated for 1-pentene cracking and coking. The reaction may be initiated at a few, very strong acid sites, as suggested by the observed product distribution.

4.2.2.3 Effect of Reaction Temperatures

Figure 4-15 and Figure 4-16 display the mass fraction of coke precursors removed from coked catalyst at various reaction temperatures and two different TOS, 20 min and 3 min, against the TGA running time respectively.

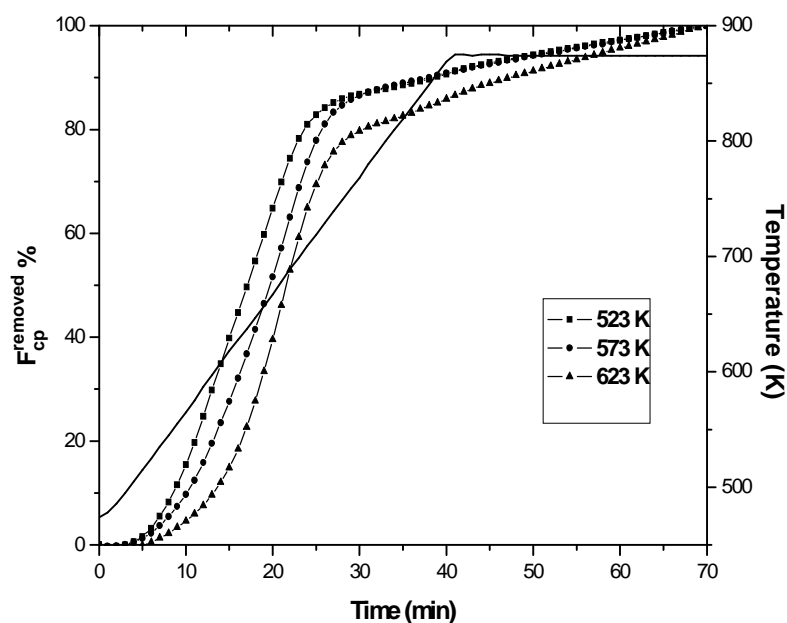


Figure 4-15 Mass fraction of coke precursors removed from coked catalyst against the TGA running time at various reaction temperatures, TOS = 20 min.

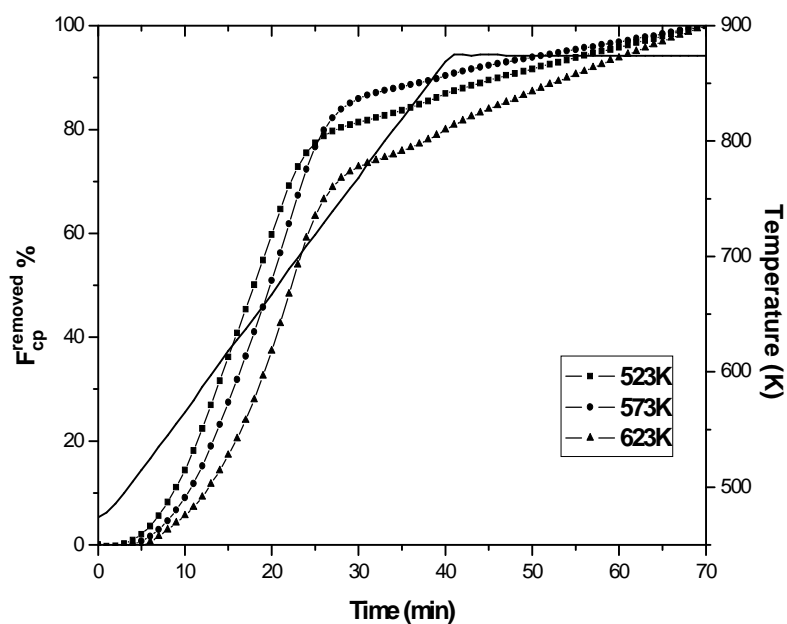


Figure 4-16 Mass fraction of coke precursors removed from coked catalyst against the TGA running time at various reaction temperatures, TOS = 3 min.

It is obvious that coke precursors from the sample of low reaction temperature are more easily removed than those from the sample of high reaction temperature. This can be explained by the higher desorption of the coke precursors into the gas phase and/or faster transformation of coke precursors to hard coke with increasing reaction temperature (Chen and Manos, 2004). Furthermore, coke precursors are more aromatic and stable at high reaction temperature than at low reaction temperature. Figure 4-17 plots all coke groups against reaction temperature for TOS = 3 min. Coke precursors content decreases with increasing reaction temperature, due mainly to the significant decrease of small coke precursors. Large coke precursors remain almost constant, indicating almost equal rates of formation from small coke precursors and rates of disappearance into hard coke. Hard coke exhibits the opposite tendency, increasing slightly with increasing

temperature. The total coke content decreases slightly with increasing reaction temperature due to the slightly greater temperature dependence of coke precursors compared with hard coke. Because it is a reaction-activated process, transformation of coke precursors into hard coke is likely faster at high reaction temperature (Moljord et al., 1995), confirming the above explanation.

At strong acid sites (25 – 70 min, 720 – 873 K), the $F_{cp}^{removed}$ values are closer to one another at different reaction temperature (523 K, 573 K and 623 K) at TOS = 20 min, (Figure 4-15) than at TOS = 3 min (Figure 4-16). This finding is in good agreement with the foregoing results; long TOS results in strong acid sites deactivation rather than weak acid sites deactivation. Consequently, from Figure 4-15 and Figure 4-16, $F_{cp}^{removed}$ versus time, some information on coking mechanism can be derived.

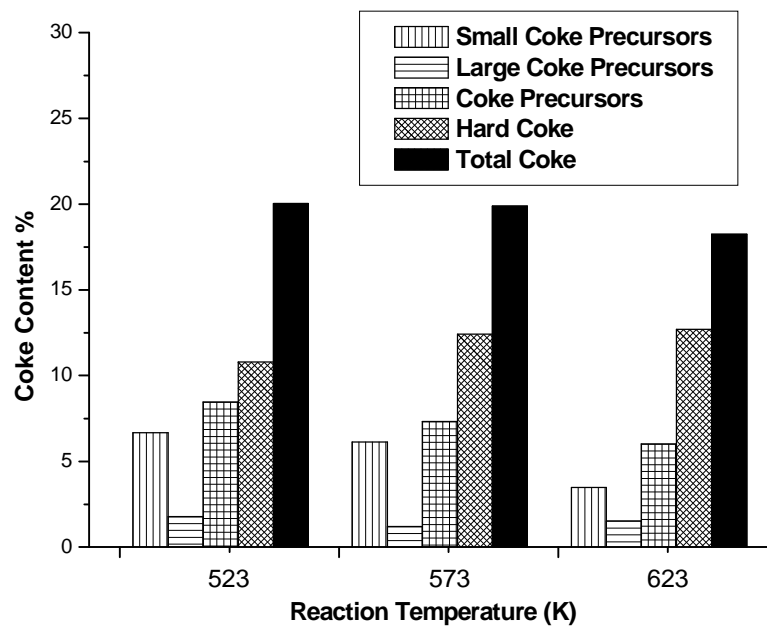


Figure 4-17 Coke percentage at different reaction temperatures (TOS = 3 min).

4.2.2.4 Effect of Reactant Composition

The amount of coke produced during 1-pentene cracking at different reactant composition over USHY zeolite is presented in Figure 4-18. It can be observed that, even though the two reactant compositions were in a ratio of 4:1, the coke content was only slightly higher for the high composition reaction. For all kinds of coke, the differences in coke content between the higher and lower reactant compositions were only 8.8 % (coke precursors), 15.8 % (hard coke) and 13.1 % (total coke). The reaction for this little difference in coke content is the preferential initial coking of the strong acid sites, which shows pseudo-zeroth-order behaviour with regard to the reactant composition. Coking occurs on active catalyst sites, and coke formation rate increases with the strength of these active sites (Manos and Hofmann, 1990). Zeolites contain strong active sites that promote coking tremendously. It is in good agreement with the above explanation, fast initial coking rate.

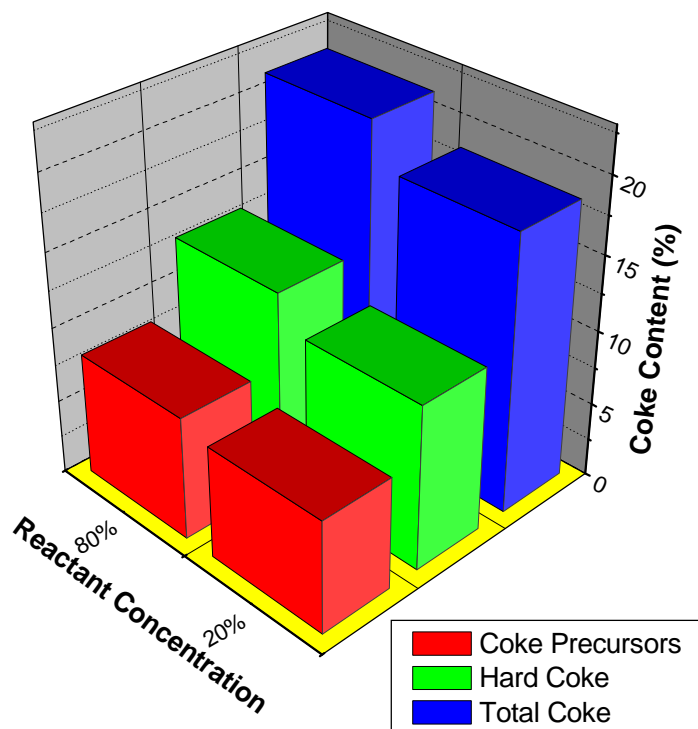


Figure 4-18 Coke content at 20 min time-on-stream of 1-pentene reactant over USHY zeolite at different reactant composition ($T = 573$ K).

4.2.3 Activation Energy (E_A) of Coke Precursors

As explained in chapter 3.4.3.3 the original TGA curve recording the change of the total mass of coke and catalysts had to be transfer to a curve showing the change of the coke precursors mass fraction with temperature. This was done by subtracting from the recording TGA total mass the catalyst mass, which did not change during the experiment. In the example of the 1-pentene reaction over USHY zeolite (80 % in N_2 , reaction temperature = 623 K, TOS = 20 min, residence time = 0.055 s, WHSV = 86.211 h^{-1}), Figure 4-19 and Figure 4-20

present this transformation. Figure 4-19 shows the original TGA curves at all the three heating rates while Figure 4-20 shows the corresponding curves of the coke precursors mass fraction vs. temperature during the coke precursors removal.

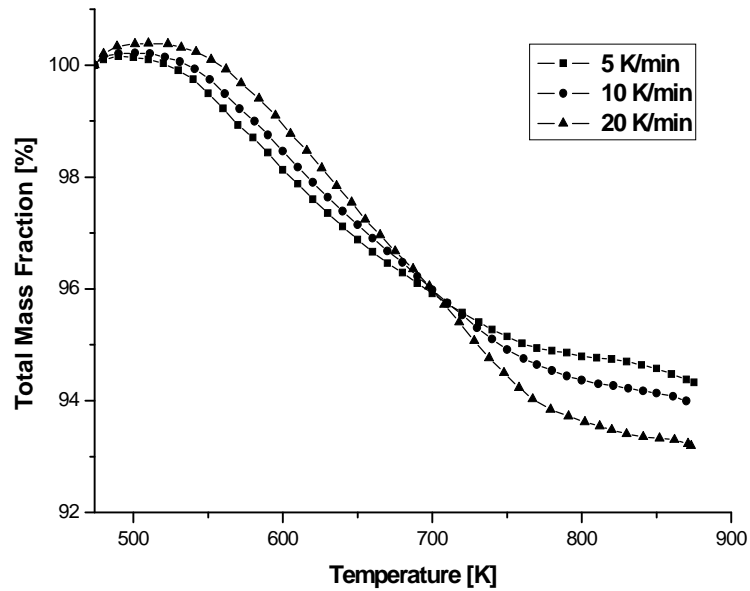


Figure 4-19 Original TGA curve of coke precursor removed over USHY zeolite.

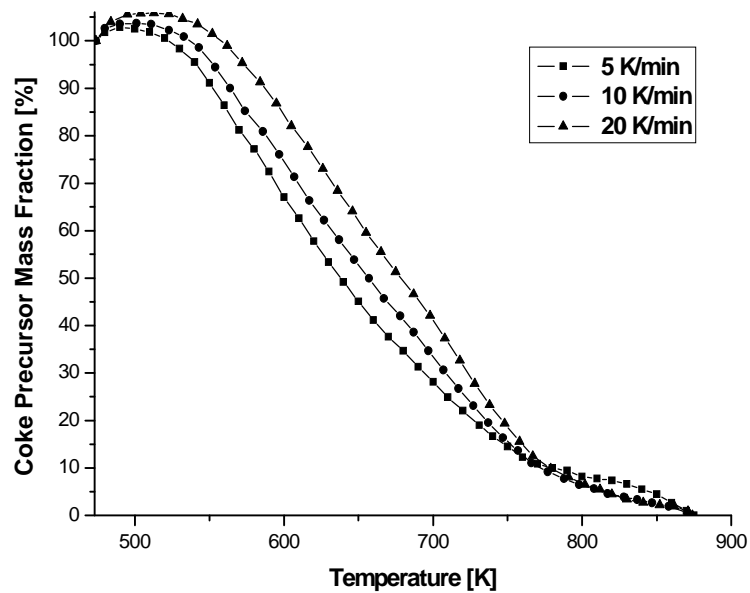


Figure 4-20 Coke precursor mass fraction vs. temperature.

Figure 4-21 presents the corresponding logarithmic plots for various coke precursor fractional residual weights i.e. plots of the logarithm of heating rate vs. the reciprocal of temperature of temperature at which by this heating rate the coke precursor fractional residual weight corresponding to a specific conversion level was reached.

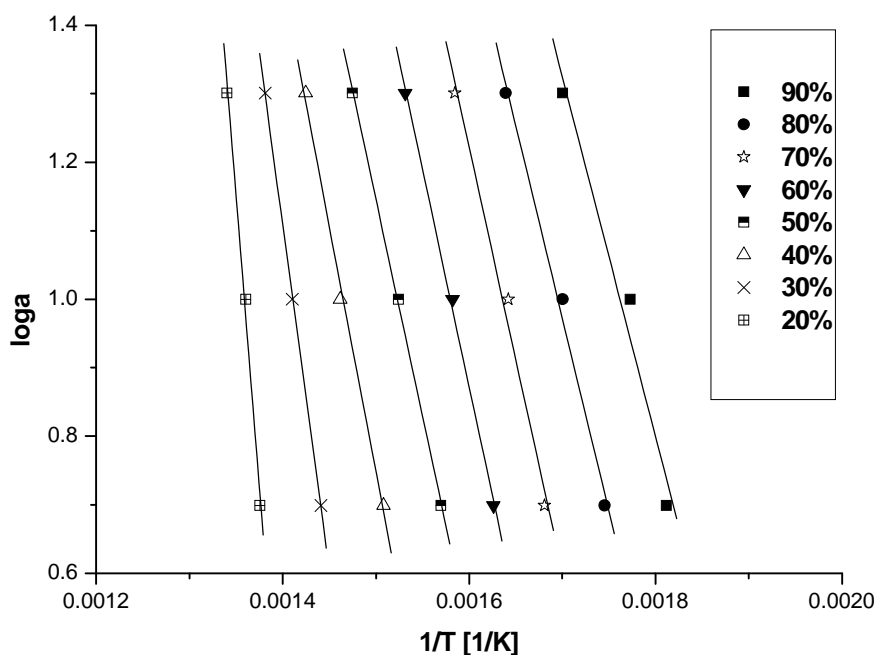


Figure 4-21 Plots of the decadic logarithm of heating rate against reciprocal temperature.

A tendency of the gradients of the various lines decreasing with increasing residual weight fraction was observed.

From the gradients of these curves the activation energies at the corresponding coke precursor fractional residues over the catalysts of this study were determined and are presented in Figure 4-22.

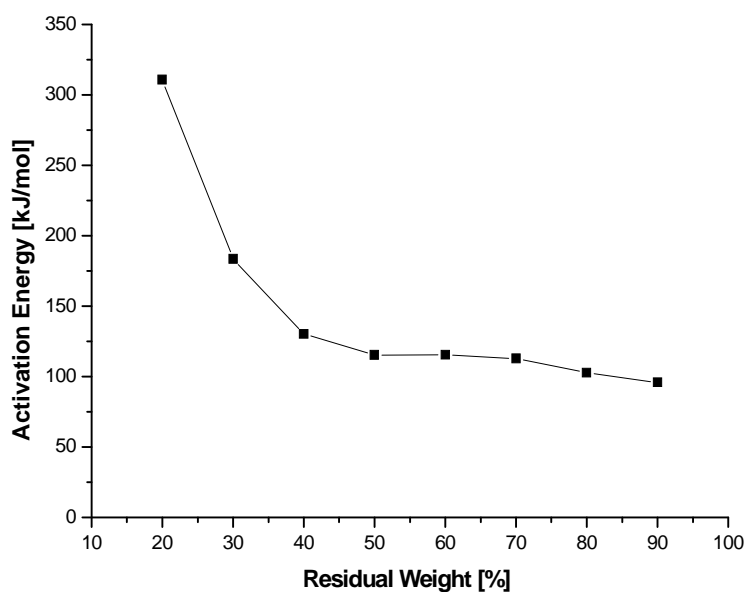


Figure 4-22 Activation energy vs. residual fraction weight for coke precursor degradation over USHY zeolite.

It presents the apparent activation energy values as function of the fractional residual weight. The values of apparent activation energy at the fraction residual weight from 90 – 40 % show relatively uniform and low at about 110 kJ/mol suggesting the group of small coke precursors which can be removed more easily, while E_A increase to 310 kJ/mol with decreasing residual weight fraction from 30 – 20 % indicating the existence of another group of coke precursors – larger ones. Additionally, mass and heat transfer could be accounted for the deviation of deactivation energy values.

4.3 TPD RESULTS

A novel NH_3 -TPD methodology was applied to study the amount as well as strength of acid sites of coked catalysts. Conventional Temperature Programme Desorption (TPD) of ammonia can not be applied to coked catalyst as coke precursors removed during the temperature programme falsify the ammonia signal. The effects of coke formation from different reactants, time-on-stream and reaction temperatures on acid sites deactivation were investigated. Besides acid sites deactivation, characterisation of coke precursors can also be revealed. The initial deactivation preferentially on strong acid sites is very fast. The concentration of free acid sites is inversely correlated well with the total concentration of coke rather than individual coke groups. Coke precursors tend to be more stable at higher reaction temperatures.

4.3.1 Effect of Different Reactants

The indirect TPD method was applied to deactivated catalysts coked by different reactants, an alkane (n-heptane, 35 % in N_2 , residence time = 0.178 s, WHSV = 59.579 h^{-1}), an alkene (1-pentene, 80 % in N_2 , residence time = 0.055 s, WHSV = 86.211 h^{-1}) and an aromatic hydrocarbon (ethylbenzene, 12 % in N_2 , residence time = 0.239 s, WHSV = 25.886 h^{-1}). Because of the huge volatility difference of these reactants, it was not possible to have the same experimental conditions with them. With all reactants the reaction temperature (623 K) and TOS (20 min) of analysed samples were the same. With these three different reaction systems,

different coking mechanisms take place resulting in differences in deactivation of acid sites and composition of coke precursors (Cerqueira et al., 2000b). TPDs without ammonia of deactivated USHY zeolite coked by 1-pentene, n-heptane and ethylbenzene at reaction temperature of 623 K and 20 min of TOS are displayed in Figure 4-23.

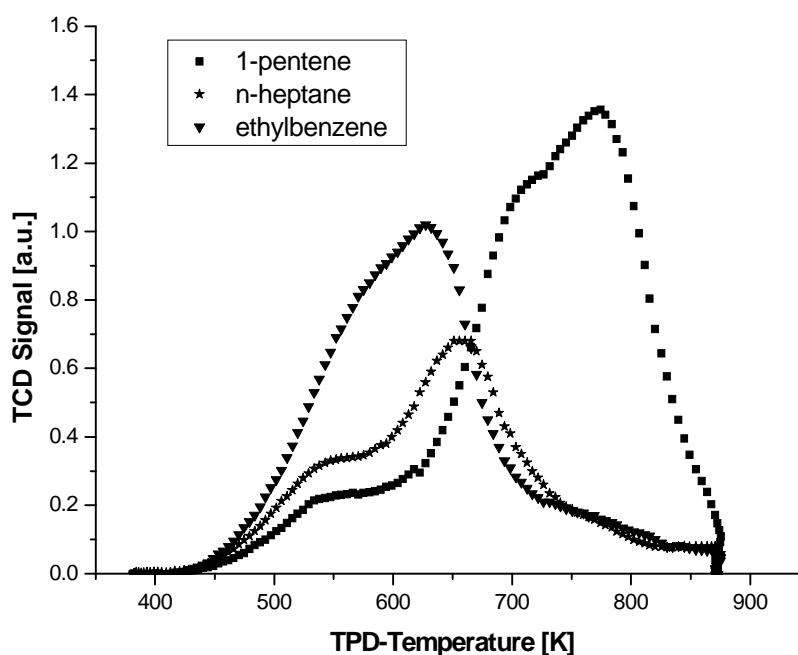


Figure 4-23 TPD without ammonia of deactivated USHY zeolite coked during different reactant systems ($T = 623$ K, TOS = 20 min).

The peaks in the TCD output are due to coke precursors in the carrier gas. The area below TPD thermograms would be proportional to the amount of coke precursors if the composition of different coke precursors had the same TCD signal response factor. These three TPD integrals and the corresponding amounts of coke precursors content measured by thermogravimetric analysis are presented in Table 4-2.

Table 4-2 Coke precursors content from different reactants measured by TPD and TGA (T = 623 K, TOS = 20 min).

	1-pentene	ethylbenzene	n-heptane
TPD-area [a.u.*K]	333	205	121
TGA-weight [mg/g _{cat}]	65.1	38.2	19.8
TPD-area/ TGA-weight	5.1	5.4	6.1

The fact that the ratios of the TPD area to the corresponding coke TGA weight are similar indicates that the TCD signal response factors are not profoundly different. From both methods, TPD and TGA, the order of formation of coke precursors is 1-pentene > ethlybenzene > n-heptane.

From Figure 4-23, it can be clearly seen that most of coke precursors from 1-pentene reactions were removed at high temperatures. There are two coke precursors desorption peaks from 1-pentene reactions: a small one located at 540 K and a large one located at 760 K. This suggests that a small part of coke precursors can be removed at low temperature while most of coke precursors are more stable and can be removed at higher temperatures. As for n-heptane, a small peak at 540 K is contributed to the easy removal of coke precursors and a relative large peak at 650 K is attributed to stable coke precursors. There is only one coke precursors peak for ethylbenzene residing at 627 K, indicating that it is much more easily removable than in the case of 1-pentene. Coke precursors produced by 1-pentene are more difficult to remove than those by the n-heptane/ethylbenzene systems at low temperature and need much higher temperatures for that. This is

possibly due to the faster progress of coking during 1-pentene reactions. Coking is not a static process, and transformations between coke components take place continuously. Coke precursors transform to more stable ones, which convert further to hard coke. Not only the amount of coke precursors with 1-pentene is a lot higher than with the other reactants, but also the hard coke with 1-pentene is an order of magnitude higher than the hard coke with ethylbenzene or n-heptane.

The estimated, by the method described in section 3.4.4, acid sites of deactivated USHY zeolites coked during 1-pentene, n-heptane and ethylbenzene reactions respectively are presented in Figure 4-24, Figure 4-25 and Figure 4-26.

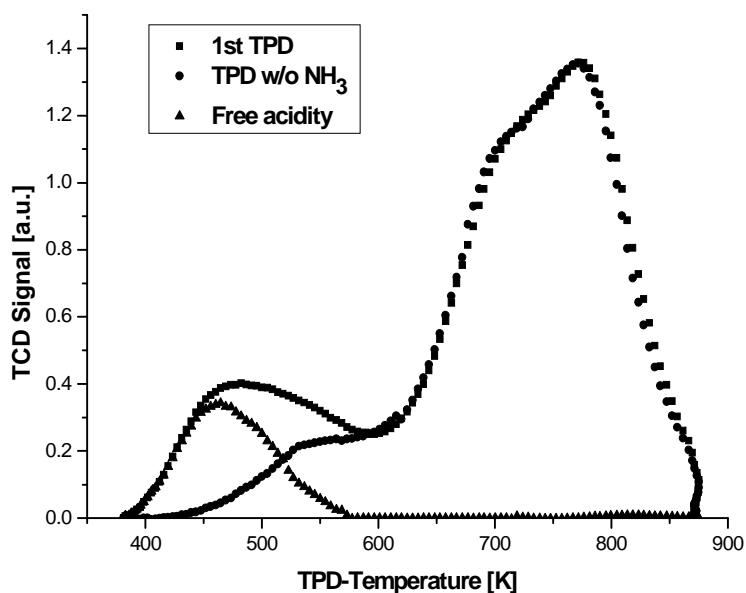


Figure 4-24 First TPD, TPD without NH₃ and Free acid sites of deactivated USHY zeolite coked during 1-pentene reactions (T = 623 K, TOS = 20 min).

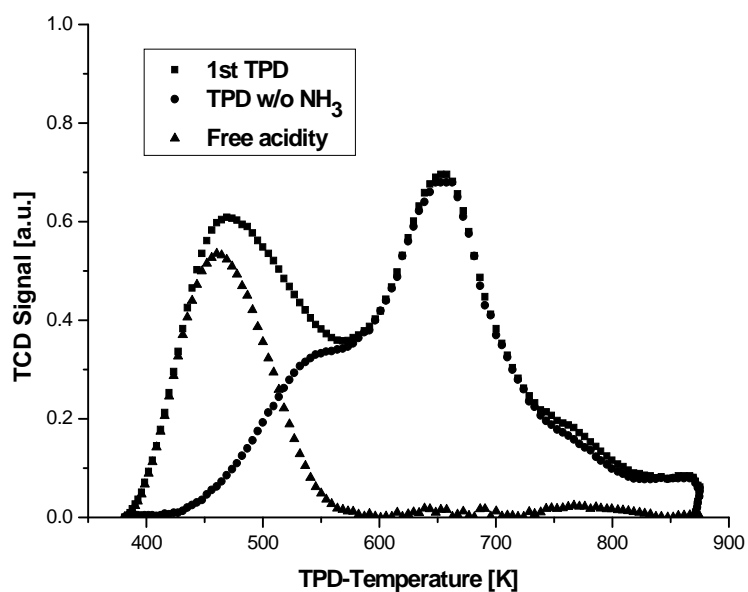


Figure 4-25 First TPD, TPD without NH₃ and Free acid sites of deactivated USHY zeolite coked during n-heptane reactions (T = 623 K, TOS = 20 min).

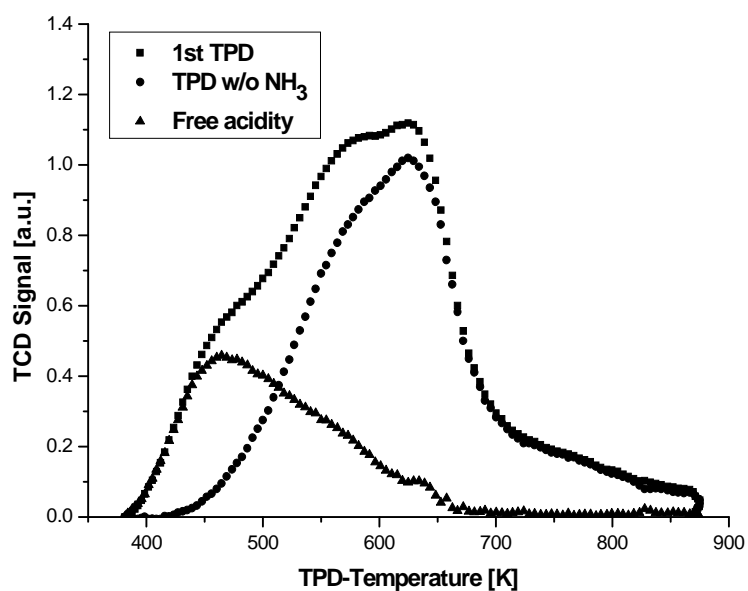


Figure 4-26 First TPD, TPD without NH₃ and Free acid sites of deactivated USHY zeolite coked during ethylbenzene reactions (T = 623 K, TOS = 20 min).

For 1-pentene and n-heptane systems, the signals of TPD without ammonia and the first TPD overlap from 590 – 873 K, while for ethylbenzene system the two signals overlap from 650 – 873 K. This suggests that less strong acid sites have been poisoned during ethylbenzene reactions compared to 1-pentene/n-heptane systems. The area in the low-temperature range obtained from the difference in TPD curves between the TPD without ammonia and the first TPD is due to the ammonia adsorption. In all cases strong acid sites are occupied by coke first and deactivated. Hence, ammonia can only be adsorbed at weak acid sites (showing maxima around 500 K) left after coking. The phenomenon confirms that coke preferentially deactivates the strongest acid sites (Moljord et al., 1995).

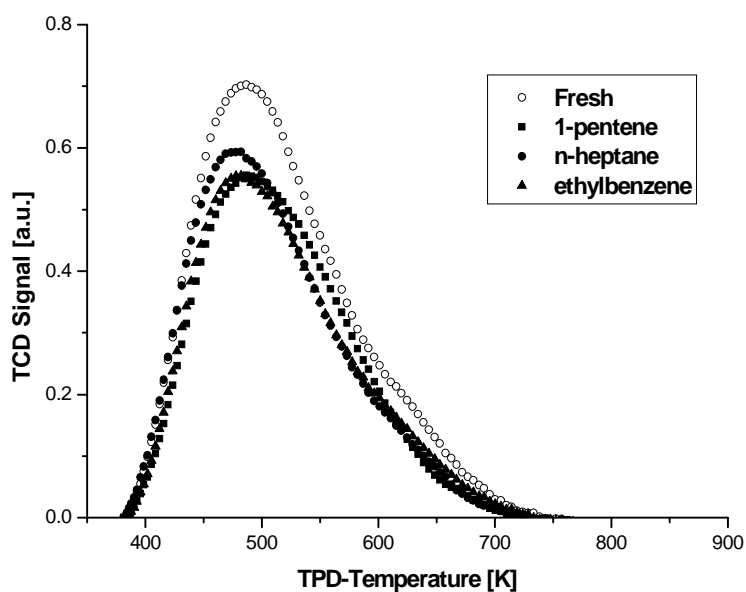


Figure 4-27 Second TPD of deactivated USHY zeolite coked during different reactant systems (T = 623 K, TOS = 20 min).

Figure 4-27 shows the second TPD for coked catalyst samples from 1-pentene, n-heptane and ethylbenzene reactions. Since coke precursors had been removed through pretreatment at 873 K in inert flow, only hard coke remained on the catalyst before the second TPD. The second TPD signal presents the free acid sites not occupied by hard coke. They include acid sites which were occupied by coke precursors but have been freed through the removal of coke precursors during the pretreatment. Although hard coke contents from thermogravimetric analysis (TGA) results are quite different, $0.78 \text{ g}_{\text{coke}}/100\text{g}_{\text{zeolite}}$ for n-heptane, $1.03 \text{ g}_{\text{coke}}/100\text{g}_{\text{zeolite}}$ for ethylbenzene and $15.40 \text{ g}_{\text{coke}}/100\text{g}_{\text{zeolite}}$ for 1-pentene, respectively, the free acid sites not coked by hard coke for these three different reactants are nearly the same. This also means that the acid sites blocked only by hard coke are almost the same. The number of acid sites occupied or blocked by hard coke is not proportional to the content of hard coke. If we set

$$\alpha = \frac{\text{Number of acid sites occupied by hard coke}}{\text{concentration of hard coke}} \propto \frac{\text{Area of Fresh} - \text{Area of 2nd TPD}}{\text{g}_{\text{hard coke}}/100\text{g}_{\text{zeolite}}}$$

, then $\alpha_{\text{1-pentene}} (1.45) \ll \alpha_{\text{ethylbenzene}} (23.09) \approx \alpha_{\text{n-heptane}} (26.01)$.

Hard coke is formed on strong acid sites where the adsorbates are strongly adsorbed (chemisorbed) and possess intense acid site catalytic properties for cracking reactions. For 1-pentene system, coke is formed during cracking reaction through a sequence of reaction steps, such as protonation, alkylation, isomerisation, hydride transfer, deprotonation and ring closure (Guisnet and Magnoux, 2001). This kind of hard coke molecule on each strong acid site seems to be much larger and heavier than that from ethylbenzene and n-heptane systems. Another possible explanation for the very different α -values might be the very different amounts of hard coke concentrations; around 1% for n-heptane and ethylbenzene compared to 15% for 1-pentene. The initially formed coke

molecules might be able to spread further apart, deactivating proportionally a larger number of acid sites. Larger coke amounts lead to a denser packing in the narrow zeolitic pores which decreases the number of acid sites deactivated per coke.

4.3.2 Effect of Time-On-Stream (TOS)

The TPDs without ammonia of coked USHY zeolite during 1-pentene cracking at 623 K at various TOS are presented in Figure 4-28.

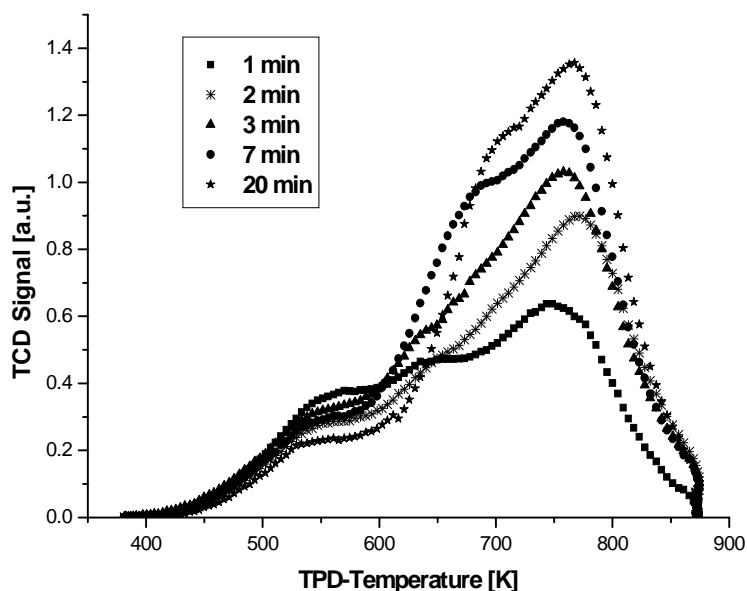


Figure 4-28 TPD without ammonia of deactivated USHY zeolite coked during 1-pentene reactions at different TOS ($T = 623$ K).

The integral area of TPD curve increases with TOS indicating the amount of coke precursors increases with increasing TOS although slightly stronger than TGA results indicate (Figure 4-29).

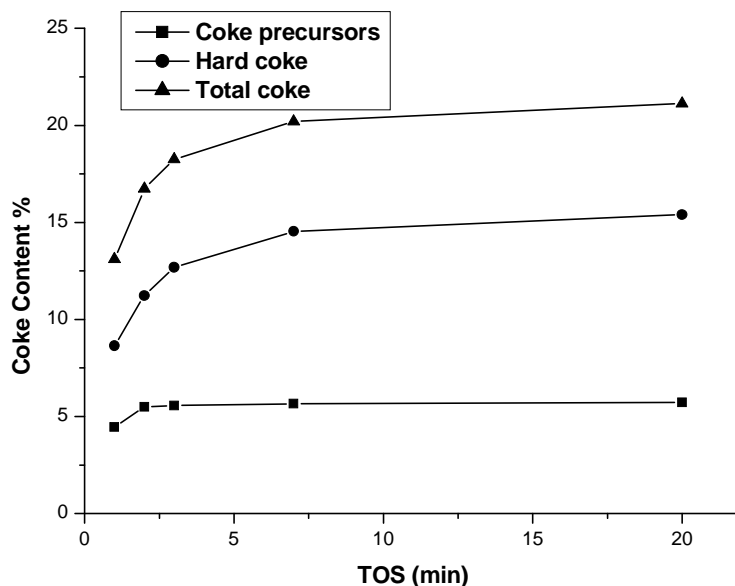


Figure 4-29 TGA-measured coke content of deactivated USHY zeolite coked during acid catalytic cracking reaction of 1-pentene at different TOS ($T = 623$ K).

This might be due to differences in TCD response factors especially as the composition of the coke precursors change as shown below. The corresponding TPD-area/TGA-weight values are nonetheless inside the ± 10 % error indicated in Table 4-2. It can be also observed that there are two peaks in TPD signal resulting in two types of coke precursors. The first small peak located at relatively low temperature represents the coke precursors which can be removed more easily, while the second stands for more stable coke precursors. The first peak becomes smaller with TOS while the second peak becomes larger, indicating a transformation of coke precursors from one type to another. Through aromatization, coke deposits become larger and more aromatic with TOS and coke content (Holmes et al., 1997; Matsushita et al., 2004). Since coke formation

is an extremely fast process at the beginning of catalyst exposure to the reaction mixture, most of coke precursors are formed in the first minute TOS. Although the amount of coke precursors increases slowly, their composition still changes via solid surface reactions of coke component. The unstable coke precursors convert to stable coke precursors with TOS resulting in the decrease of the amount of unstable coke precursors and the corresponding increase of the amount of stable coke precursors.

Figure 4-30 shows the first TPDs of deactivated USHY zeolite samples coked at 623 K reaction temperature at different TOS. The first peaks are larger at each TOS than the corresponding ones in Figure 4-28 due to the additional adsorption of ammonia on the weak acid sites. The corresponding second peaks at different TOS in both figures overlap due to saturation of coke on strong acid sites leading in complete poisoning of strong acid sites.

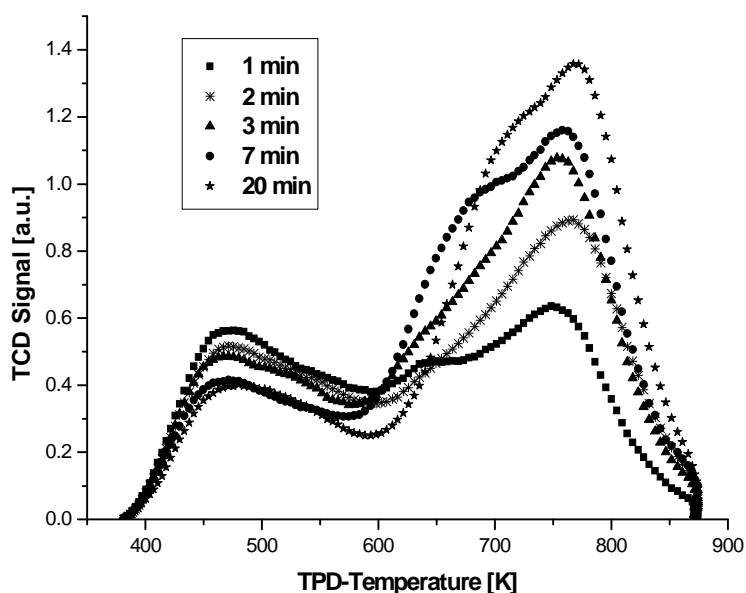


Figure 4-30 1st TPD of deactivated USHY zeolite coked during 1-pentene reactions at different TOS ($T = 623$ K).

The free acid sites of coked USHY zeolites from 1-pentene reaction at 623 K from different TOS are shown in Figure 4-31. Compared with the fresh catalyst, the amount of free acid sites of coked catalyst decreases with TOS. It is obvious that the first minute of TOS sample suffers a very fast strong initial acid sites deactivation with a relative slow acidity deactivation afterwards. After 7 minutes, the acid sites almost do not decrease any more. Furthermore, the acid sites deactivation is correlated with the content of total coke. Also, acid sites distribution can be illustrated with Figure 4-31. The loss of acid sites is more pronounced at strong acid sites than at weak acid sites, which confirms the higher contribution of strong acid sites on coke deposition.

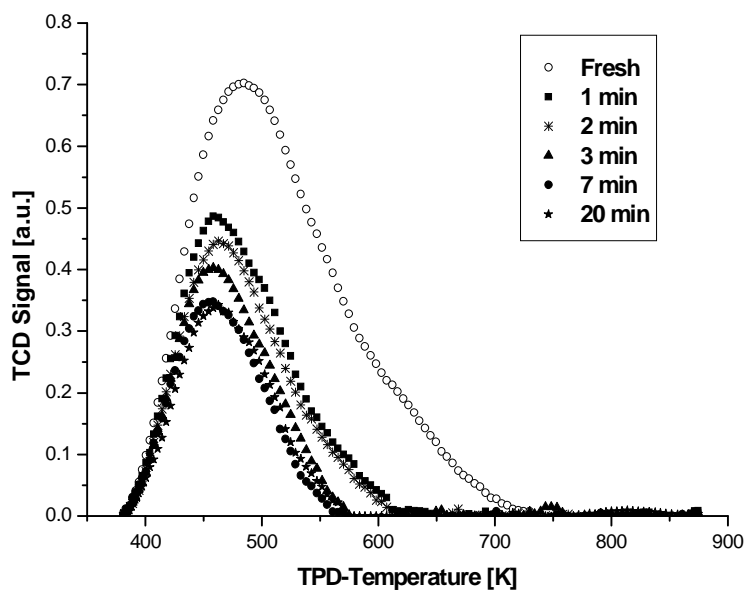


Figure 4-31 Free acid sites of deactivated USHY zeolite coked during 1-pentene reactions at different TOS ($T = 623$ K).

From Figure 4-32 we can see that the acid sites deactivated by hard coke at different TOS periods are not profoundly different as the content of hard coke

increases slightly with increasing TOS (Figure 4-29). This could be explained by the rapid initial coking on strong acid sites causing their full deactivation. The amount of strong acid sites decreases rapidly at the start of exposure of catalyst to the reaction mixture. After the strong acid sites have been deactivated in a very short time, coke continues to deposit on weak acid sites with a much lower rate. At the same time, hard coke still continues to accumulate and grows up on these strong acid sites at a lower rate.

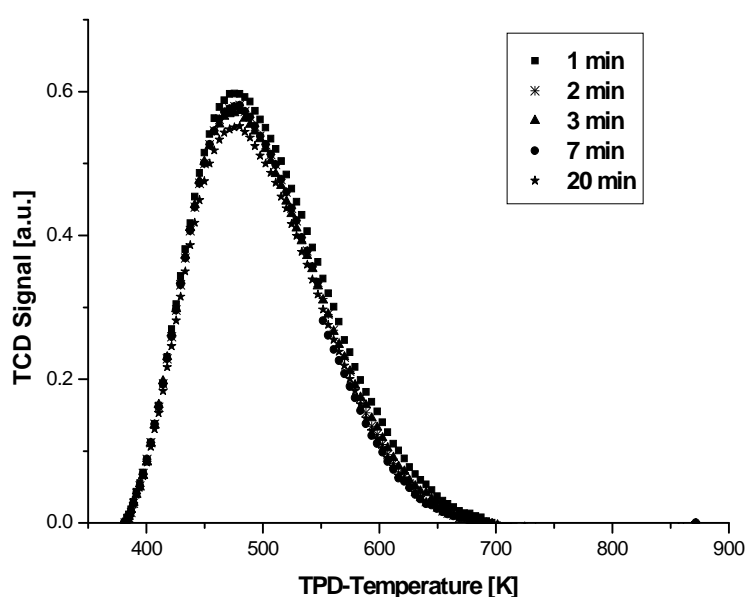


Figure 4-32 Second TPD of deactivated USHY zeolite coked during 1-pentene reactions at different TOS ($T = 623$ K).

4.3.3 Effect of Reaction Temperature

As shown in Figure 4-33 (data obtained by TGA measurements), the amount of hard coke increases with increasing reaction temperature while the amount of coke precursors decreases. This can be explained by the fact that coke precursors can transform to hard coke faster at high temperatures. However, the amount of

total coke almost does not change with reaction temperatures. Figure 4-34 displays the TPD without ammonia at various reaction temperatures (TOS = 20 min) against TPD temperature. The integral area of TPD without ammonia curve decreases with increasing reaction temperature; that is correlated well with the amount of coke precursors from TGA results. Taking into account the thermal conductive detector (TCD) working principle, it seems reasonable to assume that coke precursor molecules are removed from the catalyst without decomposition. It also can be seen that with increasing reaction temperature the peaks derived from coke precursors shift from low TPD temperature to high TPD temperature. Coke precursors formed at high reaction temperatures are more difficult to be removed than that of low reaction temperatures. Coke precursors become more stable and contribute to hard coke with increasing reaction temperature resulting in less integral area located at high TPD temperatures.

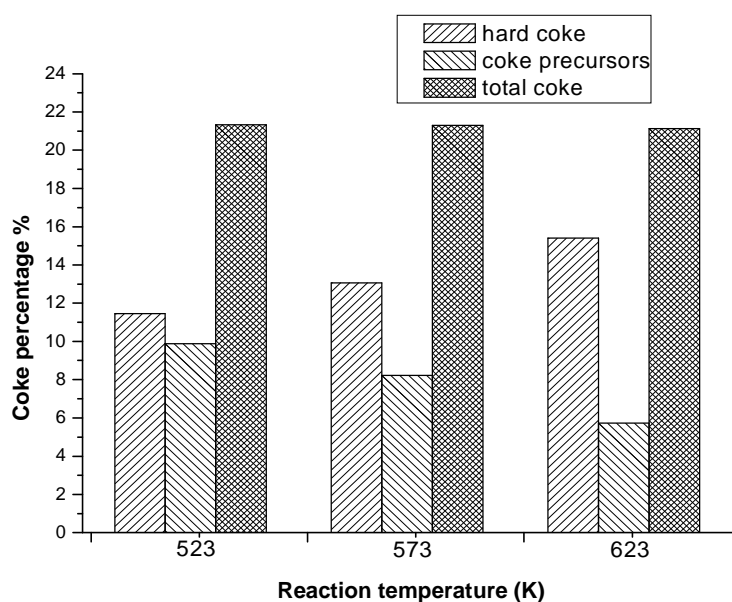


Figure 4-33 TGA-measured coke content of deactivated USHY zeolite coked during acid catalytic cracking reaction of 1-pentene at different reaction temperatures (TOS = 20 min).

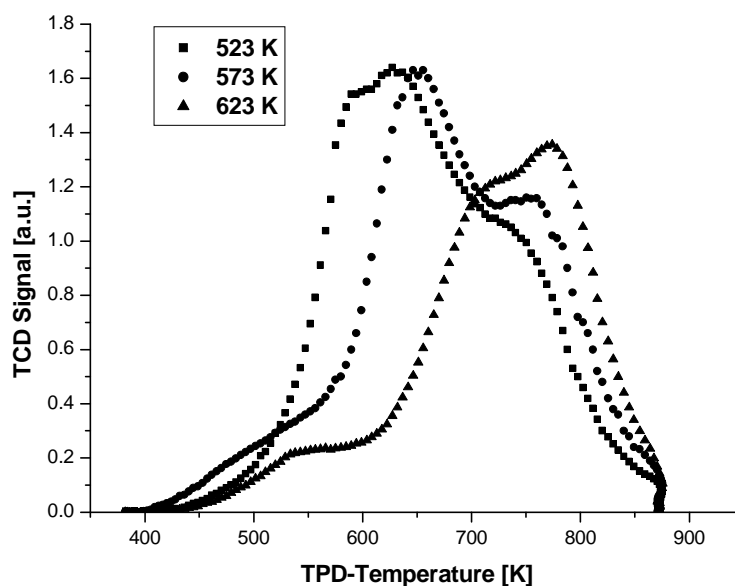


Figure 4-34 TPD without ammonia of deactivated USHY zeolite coked during 1-pentene reactions at different reaction temperatures (TOS = 20 min).

The free acid sites of the coked catalyst reacted at different temperatures (Figure 4-36) are calculated from the difference of corresponding first TPD (Figure 4-35) and TPD without NH_3 (Figure 4-34). There is not much difference among the three free acid sites curves. The amount of free acid sites agrees well with the amount of total coke (Figure 4-33). Moreover, the free acid sites distribution is very similar. Both coke precursors and hard coke contribute to acid sites deactivation. The effect of the slight increase of the concentration of hard coke with temperature is compensated by the slight decrease of the concentration of coke precursor. Hence, reaction temperature does not have a distinct effect on the amount of total coke and acid sites deactivation.

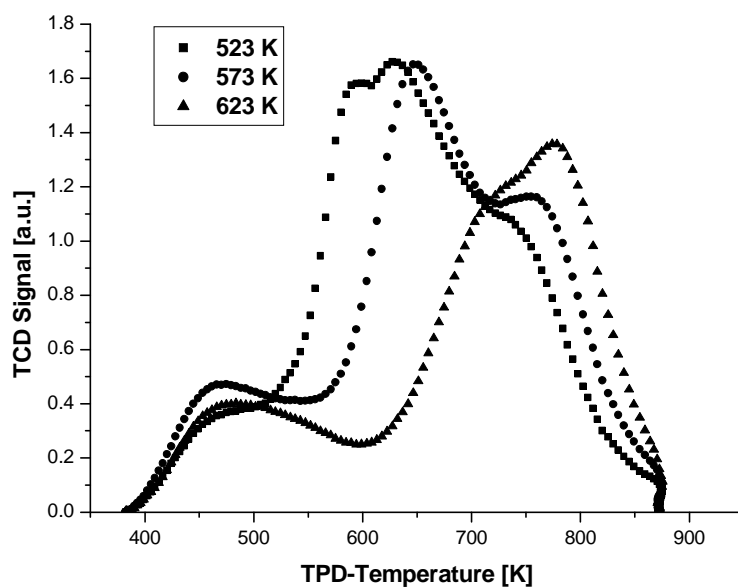


Figure 4-35 First TPD of deactivated USHY zeolite coked during 1-pentene reactions at different reaction temperatures (TOS = 20 min).

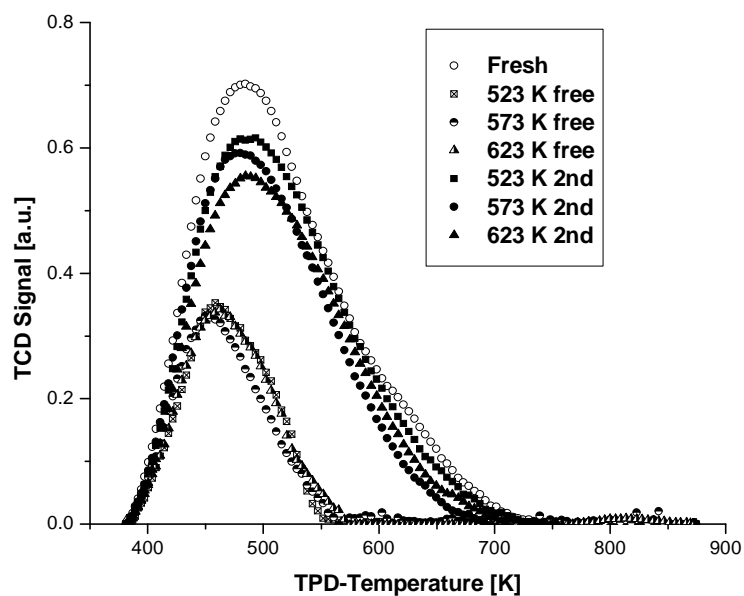


Figure 4-36 TPD of fresh catalyst, Free acid sites and Second TPD of deactivated USHY zeolite coked during 1-pentene reactions at different reaction temperatures (TOS = 20 min).

Figure 4-36 compares the acid sites of fresh catalyst, free acid sites of coked catalyst (first TPD minus TPD without NH_3 , i.e. free acid sites not blocked by coke precursors and hard coke), and second TPD (free acid sites not blocked by hard coke). The gap between the fresh and the second TPD, i.e. the acid sites inhabited only by hard coke, is mainly located at high TPD temperature area, suggesting strong acid site deactivation. On the other hand, the gap between the second TPD and free acid sites, i.e. that of acid sites only inhabited by coke precursors, lies preferentially at relatively strong acid sites too. Furthermore, the area of acid sites blocked by coke precursors is larger than that of hard coke, in contrast to the corresponding TGA results (Figure 4-33), where the weight of hard coke is higher than that of coke precursors. This means that the number of acid sites blocked per mass unit of coke components is higher for coke precursors than for hard coke. This is in good agreement with the fact that hard coke molecules are more aromatic and bigger than coke precursors. Thus, even though the molar amount of hard coke is lower than that of coke precursors, its weight is larger than that of coke precursors.

4.4 THE ROLE OF STRONG ACID SITES ON HYDROCARBON REACTIONS

In the work reported in this chapter, 1-pentene reactions were carried out over USHY zeolite whose strong acid sites were selectively poisoned by hard coke in order to study the role of these strong zeolitic acid sites on hydrocarbon conversions. We show conclusively that strong acid sites are responsible for

cracking and hydride transfer reactions as well as strong coke formation while weak acid sites can only catalyse double bond isomerisation. Furthermore, we clarify the question of the prolongation of the phase of rapid decline of cracking and hydride transfer reactions and unequivocally show that this is not due to hydrogen release delay.

4.4.1 Catalyst Preparation

The USHY zeolite was calcined in an oven with 10 K/min heating rate to 873 K for 12 hours. This is fresh catalyst for the reaction.

The selective poisoning of strong catalytic acid sites was carried out over fresh catalyst with 1-pentene reactions ($P_{1\text{-pentene}} = 0.2$ bar, $P_{N_2} = 0.8$ bar) in a fixed-bed reactor at different experimental conditions:

- 1) 573 K for 20 min of TOS, and
- 2) 623 K for 300 min of TOS respectively.

After each reaction run, the coked catalyst was collected and thermally treated at the TGA equipment at 873 K (10K/min) for 30 min in nitrogen flow to completely remove the coke precursors. We call these two catalyst samples produced at conditions 1 and 2 as pre-coked sample 1 (PCS1) and pre-coked sample 2 (PCS2) respectively. Using the above described coke classification method, the contents of coke precursors and hard coke of PCS1 and PCS2 are shown in Table 4-3.

Table 4-3 Coke content of PCS1 and PCS2 under the specified reaction conditions.

$\% = \text{g coke} / 100\text{g zeolite}$	Coke precursors %	Hard coke %	Total coke %
PCS1 (573 K, TOS = 20min)	6.7 (removed)	11.9	18.6
PCS2 (623 K, TOS = 300min)	4.2 (removed)	17.7	21.9

The amount of total coke and hard coke is larger at higher reaction temperature and longer TOS while this of coke precursors is smaller (Wang and Manos, 2007b). Furthermore, the change of total coke amount is not comparable to that of hard coke which can be explained by previous work, fast transformation of coke precursors into hard coke compared to the much slower formation of reactant into coke precursors (Wang and Manos, 2007b). Since coke precursors have been removed in PCS1 and PCS2, only hard coke remained deposited on these samples which cannot be removed during the reaction experiments as the reaction temperature was 573 K much below 873 K. Using the above described TPD method (described in 3.1.6) the free acid sites of fresh catalyst, PCS1 and PCS2 were determined and presented in Figure 4-37. The acid sites of PCS2 were deactivated much more than those of PCS1.

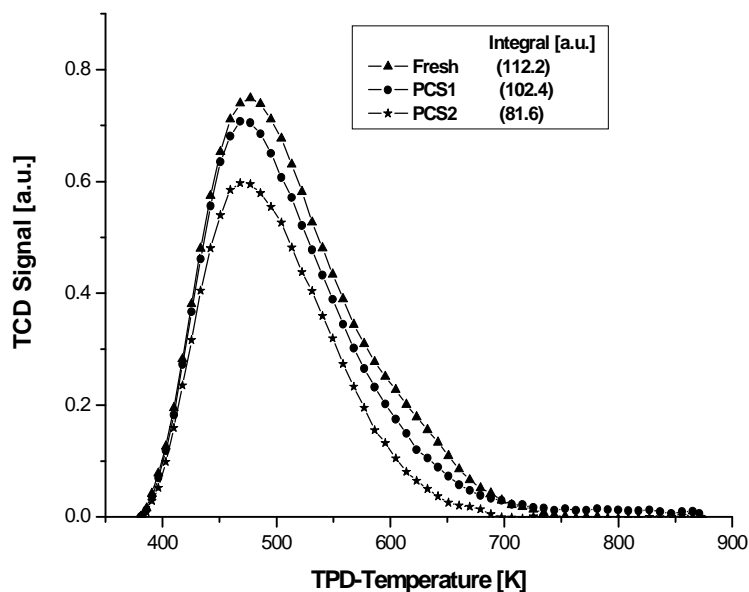


Figure 4-37 Acid sites distribution of fresh catalyst, PCS1 (pre-coked catalyst, deactivated at 573 K for 20 min with coke precursors removed- only hard coke remaining) and PCS2 (pre-coked catalyst, deactivated at 623 K for 300 min with coke precursors removed- only hard coke remaining).

In order to further look inside strong and weak sites, the NH_3 -TPD thermogram of the fresh catalyst was deconvoluted using the digital deconvolution method of Micromeritics software. The correspondent deconvoluted curves of fresh catalyst are shown in Figure 4-38. The original desorption curve starts from 380 K and ends at 780 K. Two deconvoluted peaks are located at 473 K and 635 K representing weak and strong acid sites respectively. The concentration of strong acid sites is much lower than that of weak acid sites. In the same figure the weak and strong acidity curves of PCS1 and PCS2 are also shown. For PCS1 and PCS2, we made the reasonable assumption that the weak/strong acid sites are a fraction of the weak/strong acid sites of fresh catalyst. We fitted the weak/strong sites

fractions so that the sum of the curves of weak and strong sites shows the lowest deviation from the actual TPD curve of the corresponding sample. About 60 % of strong acid sites remained in PCS1 while PCS2 has very few strong acid sites (10 %). The corresponding weak site fractions are 95 % for PCS1 and 80 % for PCS2.

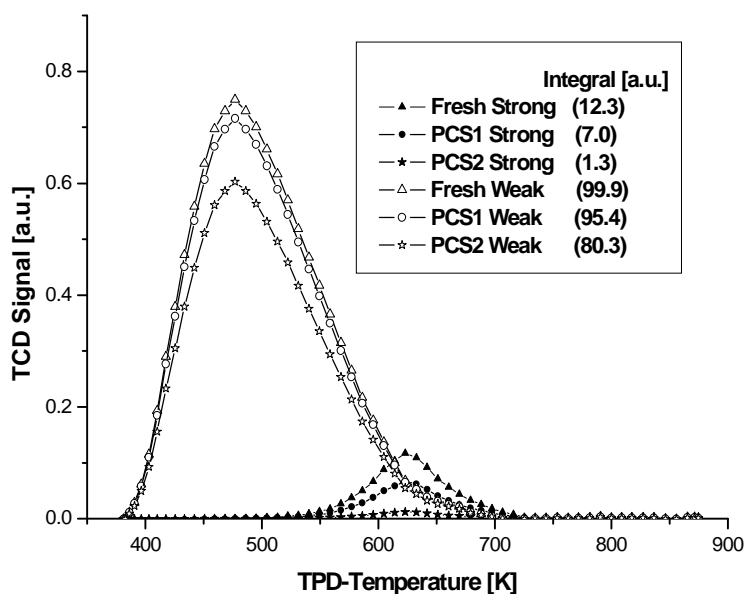


Figure 4-38 Deconvolution into weak and strong acid sites distribution of fresh catalyst, PCS1 (coked catalyst, deactivated at 573 K for 20 min with coke precursors removed- only hard coke remaining) and PCS2 (coked catalyst, deactivated at 623 K for 300 min with coke precursors removed- only hard coke remaining).

4.4.2 Reaction Experiments

Catalytic reactions of 1-pentene over fresh catalyst, PCS1 and PCS2 were carried out at temperature of 573 K and atmospheric pressure, in a stainless steel tubular

fixed-bed reactor. To ensure the same amount of pure USHY zeolite, 0.65g of fresh catalyst, 0.73 g (0.65 g USHY + 0.08 g hard coke) of PCS1 and 0.77 g (0.65 g USHY + 0.12 g hard coke) of PCS2 were used in each experiment. In these experiments, the reactant partial pressure was $P_{1\text{-pentene}} = 0.2$ bar ($P_{N_2} = 0.8$ bar), the weight hour space velocity was $WHSV = 21.553 \text{ h}^{-1}$, and the residence time was $\tau_{573K} = 0.057s$

4.4.3 Results and Discussion

4.4.3.1 Product Distribution and Conversion

As discussed in chapter 4.1.1, the major products of 1-pentene reactions over different catalysts according to the type of reaction were

- (1) propene ($C_3=$) and isobutene (iso- C_4) produced by cracking (Cr),
- (2) n-pentane (n- C_5) and 2-methylbutane (2-m- C_4) produced by hydride transfer (HT),
- (3) 2-methyl-2-butene (2-m-2- $C_4=$) and 2-methyl-1-butene (2-m-1- $C_4=$) produced by skeletal isomerisation (SkI), and
- (4) trans-2-pentene (trans-2- $C_5=$), cis-2-pentene (cis-2- $C_5=$) produced by double bond isomerisation (DbI).

A reaction network was suggested based on the product distribution as shown in Figure 4-4.

Product profiles with TOS according to reaction over all three catalyst samples are presented in Figure 4-39, Figure 4-40, Figure 4-41 and Figure 4-42.

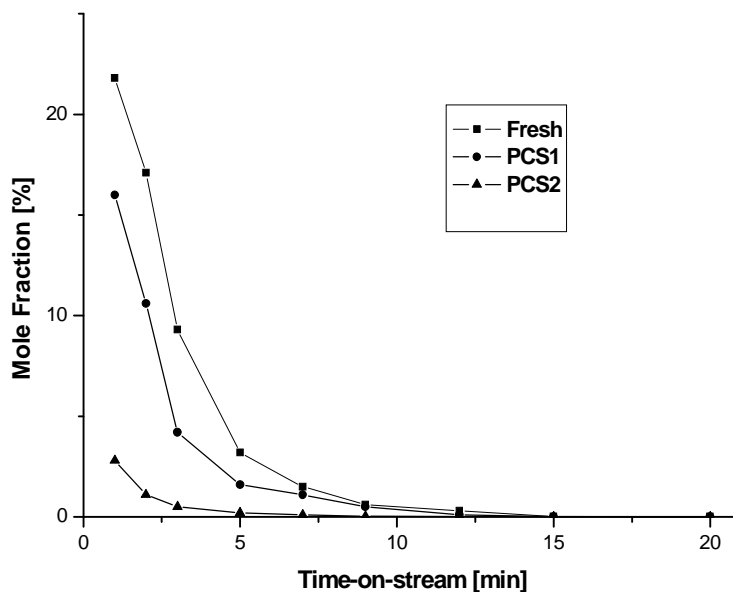


Figure 4-39 Cracking products ($C_3=$ + iso- C_4) of 1-pentene reaction over different catalyst at 573 K for 20 min.

The total amount of cracking products (Figure 4-39) over all three different catalysts decreases with TOS. More profoundly over fresh catalyst and PCS1 whose strong acid sites were only partially poisoned to a relatively low degree. These products decreased drastically during the initial stage, indicating a fast deactivation of cracking reaction. These phenomena concerning the decrease of cracking products can be explained by a rapid coke formation which takes place on strong acid sites resulting into strong acid site deactivation at the beginning of catalyst exposure to the reaction mixture (Brillis and Manos, 2003). During the reaction over PCS2 whose strong acid sites have been almost completely poisoned, only 2.7 % of cracking products were produced at 1 min TOS compared to 21.8 % formed over fresh catalyst. Stronger acid sites are expected to be more active for cracking proportionally to their strength (Williams et al., 1999).

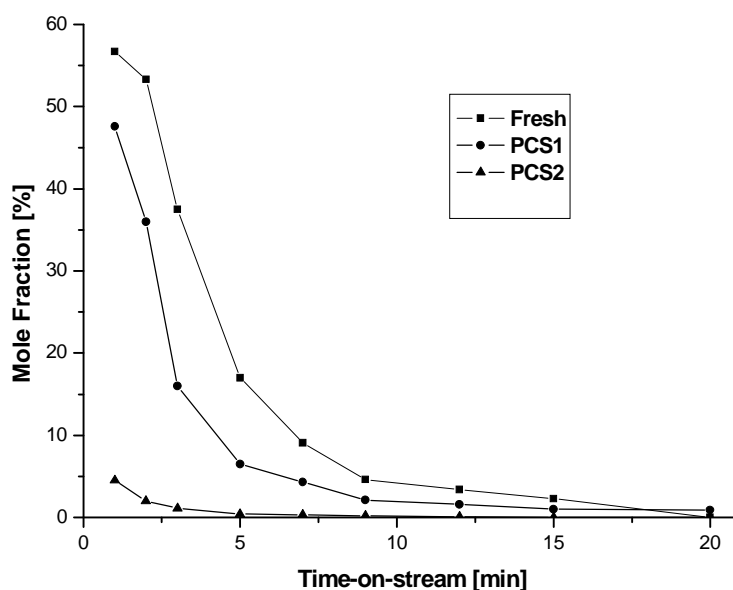


Figure 4-40 Hydride transfer products ($n\text{-C}_5 + 2\text{-m-C}_4$) of 1-pentene reaction over different catalyst at 573 K for 20 min.

Figure 4-40 shows that hydrogen transfer was initially the predominant reaction, accounting for 56.6% over fresh catalyst and 47.6 % over PCS1 at 1 min TOS respectively. However, much less hydrogen transfer products were formed over PCS2 (4.5 %) than the other two systems at 1 min. Furthermore, hydrogen transfer products show a similar pattern as cracking products. Then they decrease drastically with TOS, due to rapid coke formation at initial stage of the reaction (Brillis and Manos, 2003; Wang and Manos, 2007b). The composition of coke is aromatics (Henriques et al., 1997b) whose carbon to hydrogen ratio (C/H) is much larger than that of paraffins. Coke components are hydrogen poor with a carbon to hydrogen ratio (C/H) much larger than this of the reactant. During coking, hydrogen is transferred from coke to olefinic surface species which desorb as paraffinic products. Formation of paraffins – n-pentane, 2-methyl-butane and isobutane – in these reactions, is enhanced by hydride transfer from these free

hydrogens at initial TOS. As this hydrogen was consumed in conjunction with a sharp decrease of coking rate, no more hydrogen was available for hydride transfer to form paraffins resulting in a sharp drop of the yield of n-pentane, 2-methyl-butane and isobutane from 1-pentene.

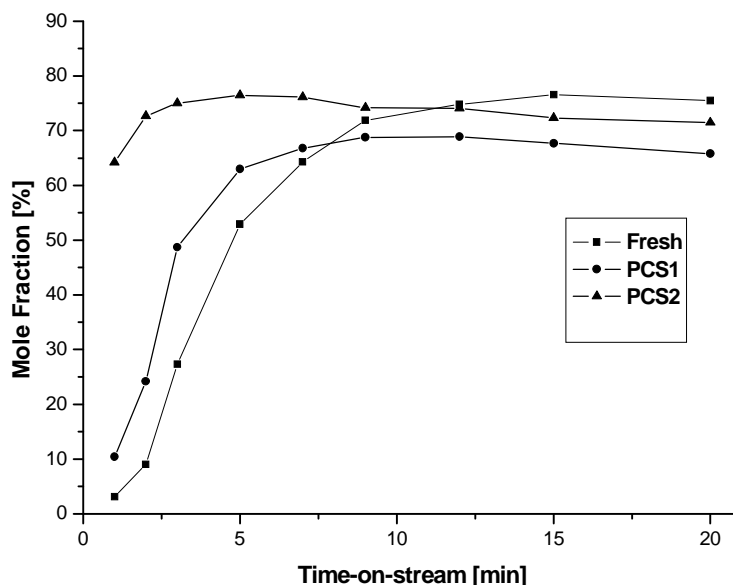


Figure 4-41 Double bond isomerisation products (trans-2-C₅= + cis-2-C₅=) of 1-pentene reaction over different catalyst at 573 K for 20 min.

For double bond isomerisation shown in Figure 4-41, the mole fraction of trans- and cis-2-pentene increases rapidly from less than 10 % at 1 min TOS to more than 60 % at 7 min followed by a plateau at considerable high level until 20 min over fresh catalyst and PCS1. From these profiles it seems that trans- and cis-2-pentene isomers are intermediate products formed by 1-pentene and reacting further to cracking and hydride transfer reactions. The activity of cracking and hydride transfer decrease rapidly due to rapid coking of strong acid sites, while isomerisation maintains high activity resulting in an increase of the mole fraction

of 2-pentene isomers (trans- and cis-2-pentene). It can be deduced that the predominant reaction taking place after 7 min is double bond isomerisation due to the fast initial deactivation of strong acid sites. A confirmation is provided by the profile over PCS2 where double bond isomerisation was the main reaction even at the beginning. Since almost no cracking or hydride transfer occurs over PCS2 due to the poisoning of strong acid sites, trans- and cis-2-pentene do not react further. As a result the increase of their mole fractions takes place much earlier than over fresh and PCS1. For the same reason the increase of trans- and cis-2-pentene takes place earlier over PCS1 than fresh due to availability originally of less strong sites which deactivate faster allowing double bond isomerisation to become the dominant reaction earlier.

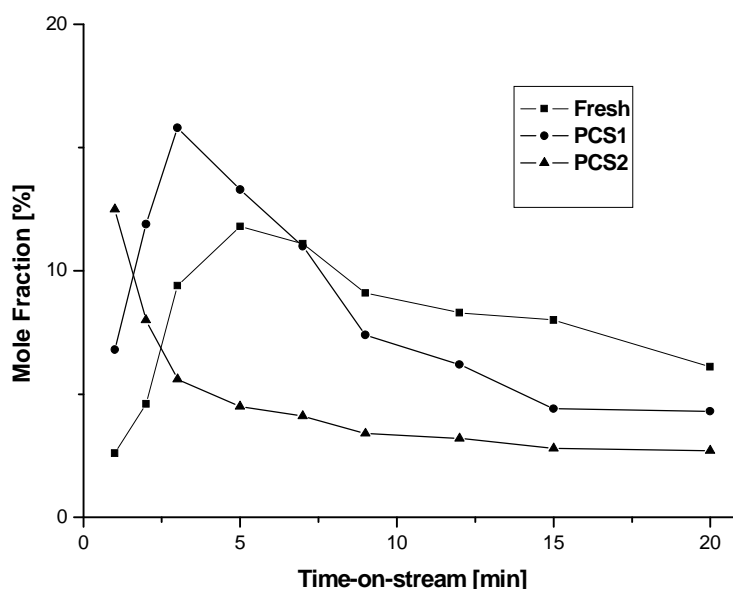


Figure 4-42 Skeletal isomerisation products (2-m-1-C₄= + 2-m-2-C₄=) of 1-pentene reaction over different catalyst at 573 K for 20 min.

Figure 4-42 reveals a maximum in the skeletal isomerisation products over fresh catalyst and PCS1, which indicates that skeletal isomerisation products are also intermediates being formed by 1-pentene and undergoing further cracking/hydride transfer. The fact that the decline of the mole fractions of these products with TOS after they reached their maximum is faster than the corresponding decline of double bond isomerisation products (Figure 4-41) means that strong acid sites contribute a lot to the formation of these products. However, the fact that over PCS2 skeletal isomerisation products have a higher mole fraction than cracking/hydride transfer products means that the acid strength needed for skeletal isomerisation is not as high as the one needed for cracking/hydride transfer.

Generally, the acid strength required for these reactions decreases in the order: cracking \approx hydride transfer $>$ skeletal isomerisation \gg double bond isomerisation (Corma and Wojciechowski, 1982). According to this, strong acid sites will promote cracking and hydride transfer reactions, while weak acid sites will be more selective towards skeletal isomerisation. However, when the acidity is too low, the activity of the catalyst is only sufficient for double bond isomerisation (Hochtl et al., 2001). Moreover, since the order of strong acid sites of these three catalysts is

Fresh $>$ PCS1 $>$ PCS2 (almost no strong sites)

at the beginning of the reaction, 1 min TOS, the selectivity of cracking products (fresh catalyst: 21.8 %, PCS1: 16.0 %, PCS2: 2.8 %) and hydride transfer (fresh catalyst: 56.7 %, PCS1: 47.5 %, PCS2: 4.5 %) decreases with decreasing concentration of strong acid sites while double bond isomerisation (fresh catalyst:

3.1 %, PCS1: 10.4 %, PCS2: 64.2 %) and skeletal isomerisation (fresh catalyst: 2.6 %, PCS1: 6.8 %, PCS2: 12.5 %) increase.

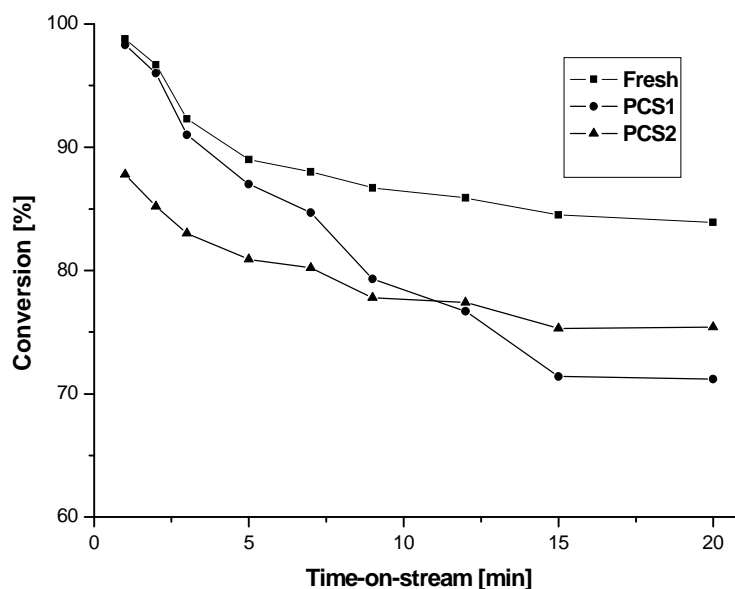


Figure 4-43 Conversion over fresh catalyst, PCS1 (coked catalyst, deactivated at 573 K for 20 min with coke precursors removed- only hard coke remaining) and PCS2 (coked catalyst, deactivated at 623 K for 300 min with coke precursors removed- only hard coke remaining).

The conversions of 1-pentene versus TOS are shown in Figure 4-43 for the three different catalysts. As expected the conversion eventually decreased at all catalysts due to catalyst deactivation. During the initial period, the reaction was accompanied by a deactivation phase, which was stronger over PCS1 compared to fresh catalyst. Initially the conversion was almost 100 % over fresh catalyst and PCS2. As discussed above, during the first minute of TOS the conversion was exclusively due to hydride transfer/cracking reactions and strong coking on strong acid sites, while later it was due to isomerisation reactions. Since almost all strong

acid sites of PCS2 have been poisoned, the conversion is lower than that of fresh catalyst. The catalytic activity decreases with reducing catalyst acidity.

4.4.3.2 Purge with Nitrogen in order to Test Hydrogen Release Delay

Another question that arises regarding catalytic hydrocarbon reactions is one related to the initial fast deactivation in conjunction with the appearance of components produced by secondary reactions into the gas product spectrum. More specifically, the question tested is the following. Is the initial deactivation extremely rapid (almost instantaneous) with the result of an immediate complete decline of cracking/hydride transfer reactions? In this scenario hydride transfer products would be belatedly released due to hydrogen release delay. The alternative scenario would be that the fast initial deactivation is not extremely rapid and the decline of the cracking/hydride transfer products simply follows the catalyst deactivation.

In order to clarify this question, a reaction of 1-pentene over fresh USHY was carried out at the same temperature of 573 K. The reaction conditions and procedure were the same as described in the experimental section with the following modification. After collecting the first sample, the feeding of reactant 1-pentene stopped at TOS=1.5 min and the fixed bed reactor was purged with pure nitrogen for 2 min. The choice of the purge timing was justified as follows. Since coke formation rate was at its highest before 1 min TOS (Wang and Manos, 2007b), the nitrogen purge was carried out after the first sample was collected at 1

min TOS. From previous work with TGA and TPD analysis, there is no profound change in coke content and character if the coked catalyst is purged in nitrogen at 573 K for only 2 min. After nitrogen purging finished (original TOS=3.5 min), reactant continued to be fed into the bed and the reactor started to operate in reaction mode again. Reaction mixture sampling continued as usual. The results of product distribution during this experiment were compared with the product distribution of the original experiment. For comparison reasons we would like to distinguish between original TOS and modified TOS. Original TOS is the experimental time counting from the original start of the experiment when reactant was fed into the catalyst bed for the first time. Until 1.5 min the modified TOS is the same as the original one. After 3.5 min, i.e. after finish of nitrogen purging, modified TOS is equal to the original one reduced by 2 min, i.e. the time period of the nitrogen purging. The sampling during this experiment took place at:

Modified TOS: 1, 2, 3, 5, 7, 9, 12, 15, 20 min

Original TOS: 1, 4, 5, 7, 9, 11, 14, 17, 22 min

The product distribution of this experiment at the modified TOS should compare with this of the original experiment at the original TOS. Are the product distribution profiles almost the same, then there is no hydrogen release delay taking place. If not, then hydrogen release delay distorts the picture of product distribution.

The product distributions of 1-pentene reaction over fresh USHY zeolite without and with nitrogen purging are presented in Figure 4-44 and Figure 4-45 respectively. It can be seen that there are no significant differences in distribution of all products after purging with nitrogen. This means that the decline of the yield

of cracking/hydride transfer products follows the initial strong decrease of the catalyst activity rather than being released belatedly due to hydrogen release delay.

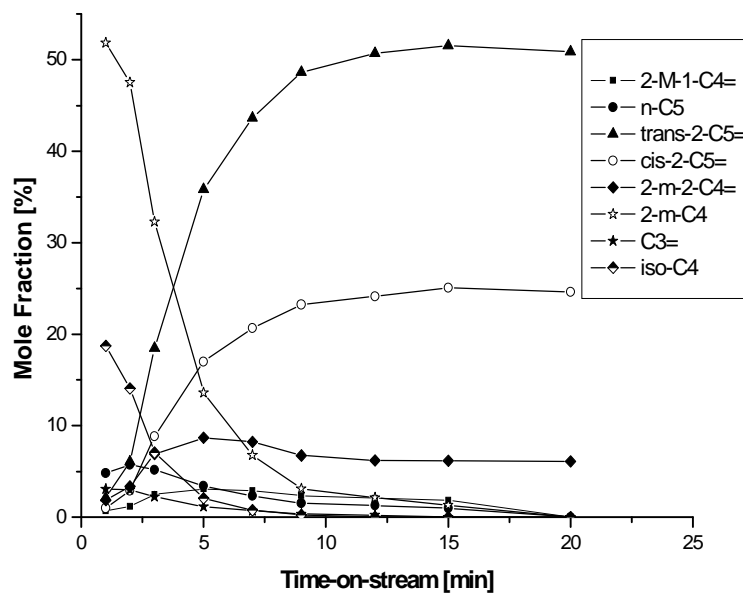


Figure 4-44 Product distribution vs TOS during 1-pentene reactions over fresh USHY catalyst at 573 K.

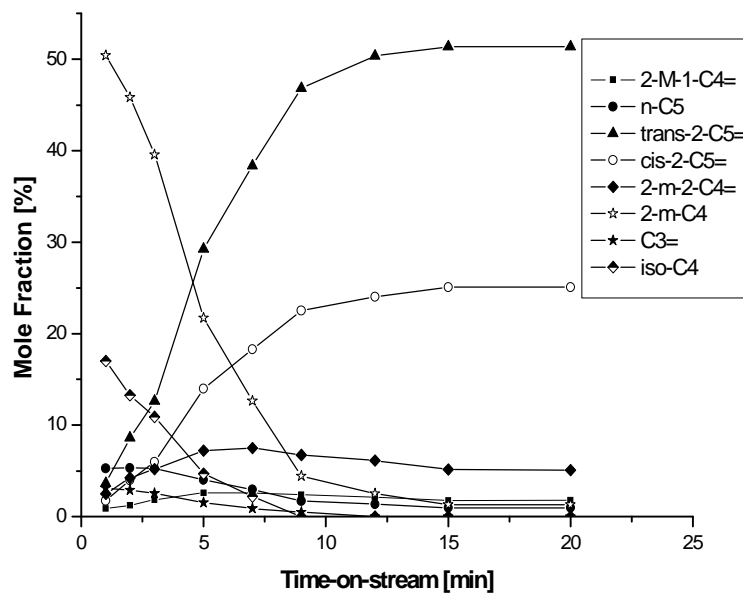


Figure 4-45 Product distribution vs TOS during 1-pentene reactions over fresh USHY catalyst with purging N₂ at 573 K.

Furthermore, we have explained the effect of the nitrogen purge on coke component concentration. After 20 min of the reaction, the coked catalyst was analysed by TGA and the result is displayed in Table 4-4.

Table 4-4 Content of coke formed over fresh catalyst, PCS1 and PCS2 at 573 K and TOS=20 min (additionally formed hard coke for PCS1 and PCS2).

$\% = \frac{\text{g coke}}{100\text{g zeolite}}$	Coke precursors %	Hard coke %	Total coke %
Fresh	6.7	11.9	18.6
Fresh with N ₂ purging	6.6	11.7	18.3
PCS1	5.1	4.7	9.8
PCS2	3.3	2.8	6.1

The concentrations of coke precursors, hard coke and total coke formed over USHY zeolite during the N₂ purge experiment are practically identical to those formed over USHY zeolite during a standard experiment. N₂ purging had no effect on coke formation either.

4.4.3.3 Coke Formation and Acid Site Characterisation

Table 4-4 shows also the content of coke precursors, hard coke and total coke over fresh catalyst, PCS1 and PCS2 after their deactivation. We would like to clarify that for the pre-coked samples, PCS1 and PCS2, these coke amounts refer to additional coke components formed during the respective experiments and they do not include the hard coke which was already formed during catalyst preparation. Both coke precursor and hard coke concentrations decrease with decreasing

catalyst acidity. Strong acid sites favour cracking and hydride transfer reactions as well as coking (Williams et al., 1999).

The coke precursor distribution taken from a TPD without NH_3 can be seen in Figure 4-46 where the peaks from the TCD output are due to coke precursors in the carrier gas. Since the TCD signal response factors of different coke precursors are not profoundly different, the integral TPD area of the different catalyst systems is in the same order as the coke precursors content measured by TGA. Moreover, the TPD signal of coke precursors formed on fresh catalyst shows a wide distribution whereas coke precursors formed on PCS1 and PCS2 locate within that of fresh catalyst. In previous work, we further classified coke precursors into large/stable coke precursors – showing a peak at high temperature – and small/unstable coke precursors – showing a peak at low temperatures. From Figure 4-46, we can see there are two peaks located at 650 K and 750 K correspondingly in TCD curves of fresh catalyst and PCS1, which are due to small/unstable coke precursors and large/stable coke precursors respectively. While the peaks corresponding to small/unstable coke precursors have declined relatively little at PCS1 and PCS2, the decline of the large/stable coke precursors peak is profound for both samples (considerably more for PCS2 than for PCS1), indicating that lack of strong acidity slows down coke growth much more than coke precursor formation. Additionally hard coke formed over PCS1 is lower than over fresh catalyst and even lower over PCS2.

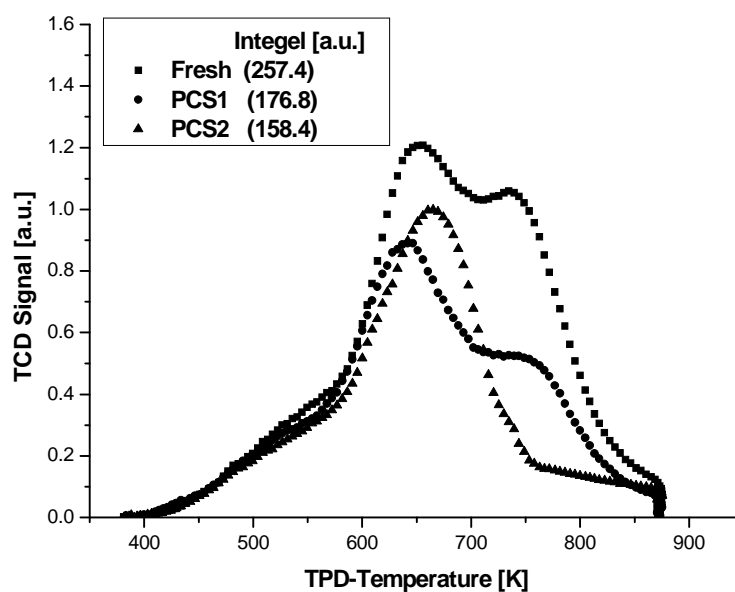


Figure 4-46 TPD without ammonia of deactivated USHY zeolite coked over different catalyst ($T = 573$ K, TOS = 20 min).

We are going to employ the assistance of a model of acid site deactivation shown in Figure 4-47 to explain this.

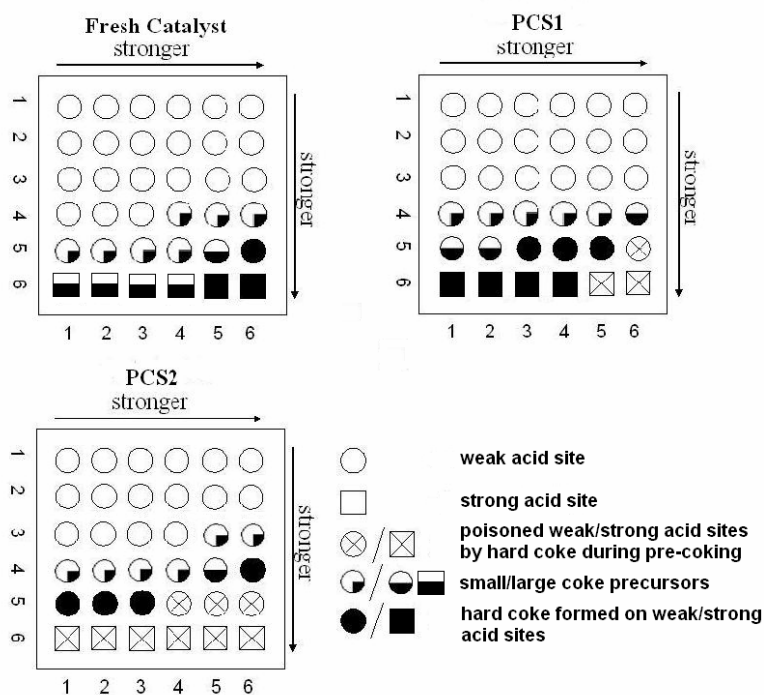


Figure 4-47 Acid sites deactivation model.

In the model all strong acid sites of PCS2 have been blocked as well as some of its weak sites, while for PCS1 only a small part of strong and weak sites has been blocked, in order to approach the picture of free strong and weak acid sites for all catalysts (Figure 4-38). There is only one peak in the PCS2 curve (670 K) arising from small/unstable coke precursors formed on weak acid sites. Furthermore, since there are more free acid sites in fresh catalyst than in PCS1, more large/stable coke precursors are formed over fresh catalyst than over PCS1. Hence, more coke precursors are removed at high TPD-temperature from fresh catalyst than from PCS1. This agrees well with coke being formed preferentially on the strongest acid sites (M Guisnet and P Magnoux, 1994).

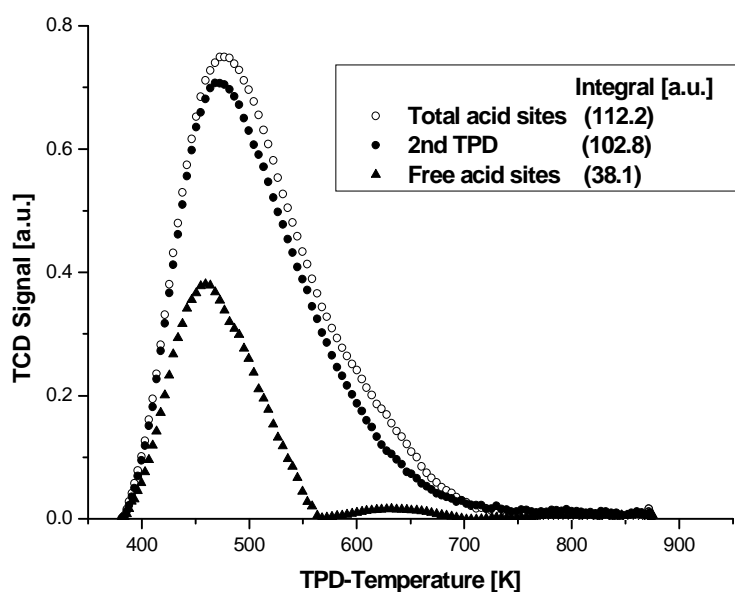


Figure 4-48 TPD of Total acid sites, Free acid sites and Second TPD of deactivated fresh catalyst coked during 1-pentene reactions at 573 K and TOS = 20 min.

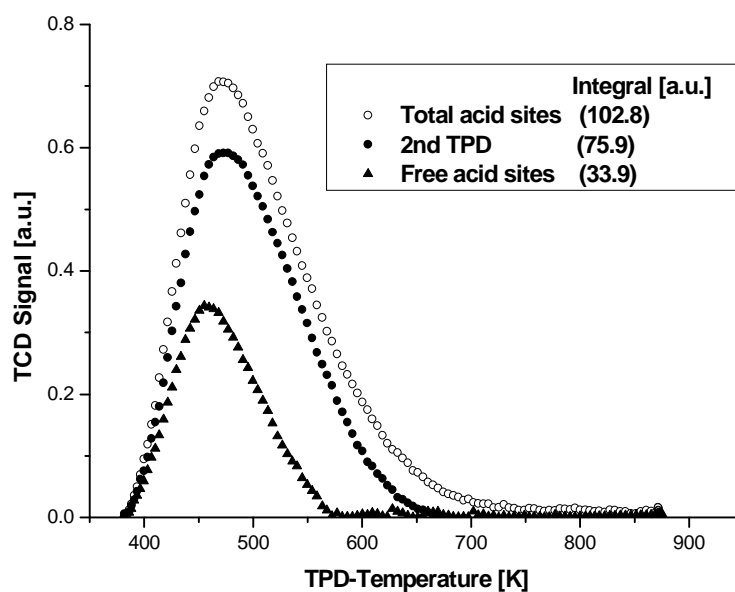


Figure 4-49 TPD of Total acid sites, Free acid sites and Second TPD of deactivated PCS1 coked during 1-pentene reactions at 573 K and TOS = 20 min.

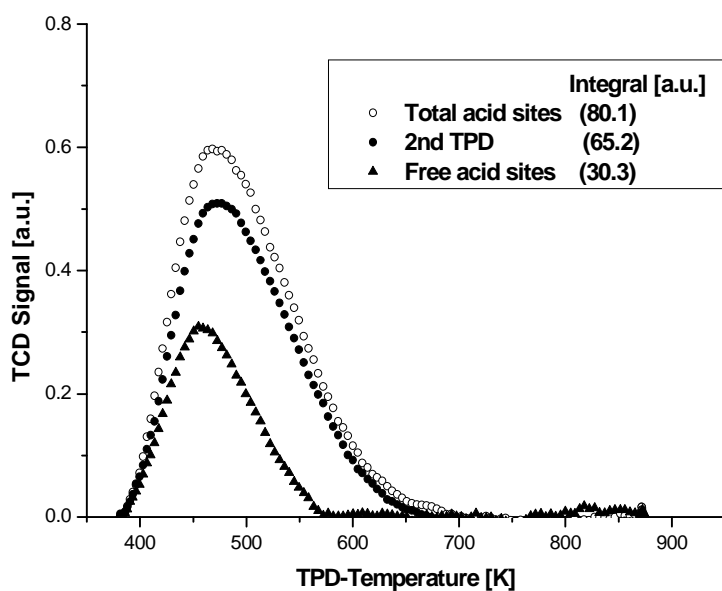


Figure 4-50 TPD of Total acid sites, Free acid sites and Second TPD of deactivated PCS2 coked during 1-pentene reactions at 573 K and TOS = 20 min.

Figure 4-48, Figure 4-49 and Figure 4-50 present the original available total acid sites, Second TPD (free acid sites not blocked by hard coke) and free acid sites of the three catalyst systems respectively. The gap area between total acid sites and Second TPD is proportional to the concentration of acid sites inhabited by the additionally formed hard coke. The gap area between Second TPD and free acid sites is the concentration of acid sites occupied by coke precursors. For all three systems, the integral area of acid sites due to hard coke poisoning is less than that of coke precursors. However, from the TGA results in Table 4-4, the content of hard coke is larger than that of coke precursors over fresh catalyst. If we set

$$\alpha = \frac{\text{Number of acid sites occupied by hard coke}}{\text{weight content of hard coke}} \propto \frac{\text{Area of Total} - \text{Area of 2nd TPD}}{\text{g}_{\text{hard coke}}/100\text{g}_{\text{zeolite}}}$$

$$\beta = \frac{\text{Number of acid sites occupied by coke precursors}}{\text{weight content of coke precursors}} \propto \frac{\text{Area of 2nd TPD} - \text{Area of Free}}{\text{g}_{\text{coke precursors}}/100\text{g}_{\text{zeolite}}}$$

then: α_{fresh} (0.79) , α_{cat2} (5.36) , α_{cat1} (5.74) , β_{fresh} (9.66) β_{cat1} (8.22) , and β_{cat2} (10.58).

The α -values indicate hard coke which is formed over very strong sites on fresh catalyst [coordinate (5,6) and (6,6) in Figure 4-47] are much larger/heavier than hard coke formed over precoked samples, PCS1 and PCS2, even much larger and heavier than coke precursors formed on weak acid sites.

From β -values, we can conclude that the acid sites occupied by coke precursors are comparable to the content of coke precursors, which suggests that coke precursors deposited on weaker acid sites of each catalyst are relatively uniform. The difference may come from the different types of coke precursors which may not have significantly different molecular weight.

5 CONCLUSION AND FUTURE WORK

5.1 CONCLUSIONS

- During 1-pentene conversion over USHY zeolite, cracking and hydride transfer were predominant reactions only in the first couple of minutes experiencing a rapid deactivation, giving rise afterwards to isomerisation reactions, especially double bond isomerisations. The main products after three minutes of TOS were trans- and cis-2-pentene.
- The conversion was higher at higher reaction temperatures as expected. The temperature dependence of conversion could be explained by the Arrhenius relationship.
- Coke formation was an extremely rapid process at the beginning of catalyst exposure to the reaction mixture. The gradient of total coke content was particularly high during the first minute of TOS while it became much flatter afterwards. The amount of total coke decreased with increasing reaction temperature at first minute while it was not significantly different among various reaction temperatures at 20 minutes.
- At all conditions more hard coke was formed than coke precursors. Both hard coke and coke precursors increased with TOS and both showed a fast coke formation in the first minute and linear dependence after one minute. At 20 minute TOS, the total amount of coke nearly did not change with reaction

temperature, the amount of coke precursors decreased with increasing reaction temperature due to higher desorption of coke precursors into gas phase while hard coke amount increased with temperature as expected from an activated process.

- The initial hydride transfer products were formed due to the release of hydrogen during the transformation of hydrogen rich gas phase reaction components to hydrogen poor coke components on the catalyst surface.
- Different reactant composition had not much effect on the preferential initial coking of the strong acid sites, which shows pseudo-zeroth-order behaviour with regard to the reactant composition.
- The thermogravimetric method provides insight into the chemical character of coke precursor components in terms of the mode their removal in an inert atmosphere and allows further classification of coke precursors into small and large coke precursors. Furthermore, it reveals a maximum in the mass fraction of large coke precursors with TOS due to their fast conversion to hard coke over strong acid sites compared with their much slower formation from small coke precursors over weak acid sites. The method also clearly reveals differences in coke precursors formed by different reactants (i.e., paraffins, olefins, and aromatics), as well as different reaction temperatures and TOS.
- The apparent activation energy of coke precursors removing from USHY zeolite was estimated by Ozawa method using thermogravimetric analysis.

The deviation of the apparent activation energy values reveals the existence of different types of coke precursors.

- The temperature programmed desorption (TPD) method using mild temperature pre-treatment and combining of TPD without and with ammonia allows us to quantitatively measure the free acid sites of coked and fresh solid acid catalyst as well as their strength distribution. The method also provides information of acid sites deactivation caused by hard coke only. Furthermore, the amount of coke precursors as well as coke precursors stability can be determined by TPD without ammonia. Since coking is of great interest to the petroleum refineries that use commercial FCC catalysts in large quantities, the application of the method on industrial catalysts would give a better understanding on the effect of coking on catalyst deactivation and will help the design of tailored made catalysts with fewer coking problems.
- The USHY zeolite suffered a strong reduction of free acid sites especially at the initial stage during 1-pentene reaction while it slowed considerably afterwards. The concentration of free acid sites is inversely correlated well with the total concentration of coke. Coke was formed preferentially on the strongest acid sites and caused their deactivation. The initial deactivation effect of coke was more pronounced than it would have been if all of the acid sites were of the same strength. Coke precursors become more stable with time-on-stream and increasing reaction temperatures.

- Cracking and hydride transfer are catalysed by strong acid sites while weak acid sites catalyse only double bond isomerisation. On the other hand, strong acid sites play significant role in coke formation. Moreover, coke formed on strong acid sites is much heavier than that on weak acid sites.

5.2 FUTURE WORK

It is believed that in order to confirm some of the conclusions drawn and explain certain phenomena behind the trends observed, further investigation is required.

Some suggestions on further work are the following:

Based on the above methods, the effect of residence time on products distribution, conversion and coke character will be investigated in future work. Various residence times will be achieved by altering the total flow rate as well as the amount of catalyst.

The catalyst bed profile will be measured to further illuminate the process of coke formation.

Availability of GC/MS or HPLC/MS instruments coupled to TGA rig could characterise the molecular composition of the coke components removed during the TGA thermal treatment.

Furthermore, availability of MS coupled with TPD possibly could differentiate the signal of NH_3 and coke components and draw a direct acid site picture of coked catalysts.

REFERENCES

Abbot J., Wojciechowski B. W., 1987, Kinetics of reactions of c-8 olefins on HY zeolite, *Journal of Catalysis*, 108, 346-355.

Abbot J., Wojciechowski B. W., 1988, Catalytic reactions of branched paraffins on HY zeolite: *Journal of Catalysis*, 113, 353-366.

Brillis A., Manos G., 2003, Coke formation during catalytic cracking of C8 aliphatic hydrocarbons over ultrastable Y zeolite, *Industrial & Engineering Chemistry Research*, 42, 2292-2298.

Babitz S. M., Kuehne M. A., Kung H. H., Miller J. T., 1997, Role of Lewis acidity in the deactivation of USY zeolites during 2-methylpentane cracking, *Industrial & Engineering Chemistry Research* 36, 3027-3031.

Barbier J., 1986, Deactivation of reforming catalysts by coking - A Review, *Applied Catalysis*, 23, 225-243.

Bartley B. H., Emmett P. H., 1984, Catalytic cracking of n-hexadecane .6. C-14 tracer studies of secondary reactions over amorphous silica-alumina and zeolite catalysts, *Journal of Catalysis*, 89, 442-451.

Bennett J. M., Blackwell C. S., Cox D. E., 1983, *Interzeolite Chemistry*, Washington, D. C., Am. Chem. Soc. Symp. Ser. 218, American Chemical Society.

- Besset E., Meloni D., Martin D., Guisnet M., and Schreyeck L., 1999, Multitechnique determination of the location of coke formed during n-heptane cracking on a H-MWW zeolite, *Catalyst Deactivation*, 171.
- Best D., Wojciechowski B. W., 1977, Identifying primary and secondary products of catalytic cracking of cumene, *Journal of Catalysis*, 47, 11.
- Beyerlein R. A., Mcvicker G. B., Yacullo L. N., and Ziemia k J. J., 1988, Influence of framework and nonframework aluminum on the acidity of high-silica, proton-exchanged FAU-framework zeolites, *Journal of Physical Chemistry*, 92, 1967.
- Biswas J., Gray P. G., and Do D. D., 1987, The reformer lineout phenomenon and its fundamental importance to catalyst deactivation, *Applied Catalysis*, 32, 249.
- Bjorgen M., Olsbye U., and Kolboe S., 2003, Coke precursor formation and zeolite deactivation: mechanistic insights from hexamethylbenzene conversion, *Journal of Catalysis*, 215, 30.
- Boronat M., Viruela P., Corma A., 1998, Theoretical study of the mechanism of zeolite-catalyzed isomerization reactions of linear butenes, *Journal of Physical Chemistry* 102, 982.
- Breck D. W., Breck D. W., 1974, *Zeolite Molecular Sieves - Structure, Chemistry and Use*, New York, John Wiley & Sons.
- Brown H. C., Pearsall H. W., 1952, The action of the catalyst couple aluminum chloride-hydrogen chloride on toluene at low temperatures - the nature of friedel-crafts complexes, *Journal of the American Chemical Society*, 74, 191.

- Brown H. C., Wallace W. J., 1953, Complexes of hydrogen bromide aluminum bromide with aromatic hydrocarbons, *Journal of the American Chemical Society*, 75, 6268.
- Buchanan J. S., Santiesteban J. G., and Haag W. O., 1996, Mechanistic considerations in acid-catalyzed cracking of olefins, *Journal of Catalysis*, 158, 279.
- Butt J. B., and Petersen E. E., 1988, *Activation, deactivation and poisoning of catalysts*, Academic Press.
- Butt J. B., 1980, *Reaction Kinetics and Reactor Design*, NJ, Prentice-Hall.
- Bystrov D. S., 1992, A usual explanation of the unusual mechanism of Lewis acidity manifestation in HZSM-5 zeolites, *Zeolites*, 12, 328.
- Campbell D. R., Wojciech. B , 1971, Catalytic cracking of cumene on aging catalysts .1. Mechanism of reaction, *Journal of Catalysis*, 20, 217.
- Carvajal R., Chu P. J., and Lunsford J. H., 1990, The role of polyvalent cations in developing strong acidity - A study of lanthanum-exchanged zeolites, *Journal of Catalysis*, 125, 123.
- Cavell K. J., Masters A. F., and Wilshier K. G., 1982, ^{29}Si N.M.R. of aqueous tetrapropylammonium silicate solutions, *Zeolites*, 2, 244.
- Cerqueira H. S., Ayrault P., Datka J., and Guisnet M., 2000a, Influence of coke on the acid properties of a USHY zeolite, *Microporous and Mesoporous Materials* 38, 197.

Cerqueira H. S., Ayrault P., Datka J., Magnoux P., and Guisnet M., 2000b, m-xylene transformation over a USHY zeolite at 523 and 723 K: Influence of coke deposits on activity, acidity, and porosity, *Journal of Catalysis*, 196, 149.

Chen, S., Manos G., 2004, Study of coke and coke precursors during catalytic cracking of n-hexane and 1-hexene over ultrastable Y zeolite: *Catalysis Letters*, 96, 195.

Chen S., Manos G., 2004, In situ thermogravimetric study of coke formation during catalytic cracking of normal hexane and 1-hexene over ultrastable Y zeolite, *Journal of Catalysis*, 226, 343-350.

Corma, A., Richard C., Catlow A., and Sastre G., 1998, Diffusion of linear and branched C7 paraffins in ITQ-1 zeolite. A molecular dynamics study, *Journal of Physical Chemistry B*, 102, 7085.

Corma, A., and Wojciechowski B. W., 1979, Comparison of hy and lay cracking activity in cumene dealkylation, *Journal of Catalysis*, 60, 77.

Corma, A., and Wojciechowski B. W., 1982, The catalytic cracking of cumene, *Catalysis Reviews-Science and Engineering*, 24, 1.

Costa, C., Lopes J. M., Lemos F., and Ribeiro F. R., 1999a, Activity-acidity relationship in zeolite Y Part 1. Transformation of light olefins, *Journal of Molecular Catalysis A-Chemical*, 144, 207.

Costa, C., Lopes J. M., Lemos F., and Ribeiro F. R., 1999b, Activity-acidity relationship in zeolite Y Part 2. Determination of the acid strength distribution by

temperature programmed desorption of ammonia, *Journal of Molecular Catalysis A-Chemical*, 144, 221.

Covini, R., and Pines H., 1965, Alumina - catalyst and support .22. Effect of intrinsic acidities of aluminas in molybdena-alumina catalysts upon hydrogenolysis and isomerization of alkylbenzenes, *Journal of Catalysis*, 4, 454.

Csicsery S. M., 1969, Catalytic reactions of n-pentylbenzene and 2-phenylpentane, *Journal of Catalysis*, 15, 111.

de Lucas, Canizares A., P., Duran A., and Carrero A., 1997, Coke formation, location, nature and regeneration on dealuminated HZSM-5 type zeolites, *Applied Catalysis A: General*, 156, 299-317.

Decanio S. J., Sohn J. R., Fritz P. O., and Lunsford J. H., 1986a, Acid catalysis by dealuminated zeolite-Y .1. methanol dehydration and cumene dealkylation: *Journal of Catalysis*, 101, 132-141.

Dedecek J., Capek L., and Wichterlova B., 2006, Nature of active sites in decane-SCR-NO_x and NO decomposition over Cu-ZSM-5 zeolites, *Applied Catalysis A: General*, 307, 156-164.

Dietz W.A., 1967, Response factors for gas chromatographic analyses, *Journal of Gas Chromatography*, 5, 68.

Doyle C D, 1961, Kinetics analysis of thermogravimetric data, *J Appl Polym Sci*, 5, 285.

Engelhardt J., Onyestyak G., and Hall W. K., 1995, Induced catalytic activity of fluorided alumina in the reactions of isobutane, *Journal of Catalysis*, 157, 721-729.

- Farooq M.A., Lemos F., Deactivation by coking of USHY zeolites, 1998. South Bank University.
- Flanigen E. M., Ribeiro F. R., and Rodrigues A. E., 1984, Zeolites, Science and Technology, Martinus Nijhoff, The Hague.
- Gates B.C., 1992, Catalytic Chemistry, Wiley.
- Gayer F. H., 1933, The catalytic polymerization of propylene, *Industrial & Engineering Chemistry Research*, 25, 1122-1127.
- Gil B., Mierzynska K., Szczerbinska M., and Datka J., 2007, In situ IR and catalytic studies of the effect of coke on acid properties of steamed zeolite Y: *Microporous and Mesoporous Materials*, 99, 328-333.
- Goldfarb Y. Y., Katsobashvili Y. R., and Rozental A. L., 1977, Ratio of rates of n-decane and methylnonane reactions in hydrocracking of hydrocarbons on an aluminum-nickel-molybdenum catalyst .2: *Kinetics and Catalysis*, 18, 370-373.
- Goovaerts F., Vansant E. F., Philippaerts J., Dehulsters P., and Gelan J., 1989, Initial cracking properties and physicochemical characterisation of acid-leached small-pore (Sp) and large-pore (Lp) mordenites by pulse normal-hexane cracking, infrared and Al-27 magic angle spinning nuclear magnetic-resonance spectroscopy, *Journal of the Chemical Society-Faraday Transactions I*, 85, 3675-3685.
- Gorte R. J., 1999, What do we know about the acidity of solid acids, *Catalysis Letters*, 62, 1-13.
- Greensfelder B. S., Voge H. H., and Good G. M., 1949, Catalytic cracking of pure hydrocarbons, *Industrial and Engineering Chemistry*, 41, 2573.

Greensfelder B. S., Voge H. H., and Good G. M., 1945, Catalytic cracking of pure hydrocarbons - aromatics and comparison of hydrocarbon classes, *Industrial and Engineering Chemistry*, 37, 1168-1176.

Guisnet M., and Magnoux P., 1992, composition of the carbonaceous compounds responsible for zeolite deactivation. Modes of formation, in E. G. Derouane et al. ed., *Zeolite Microporous Solids; Synthesis, Structure and Reactivity*: Kluwer Academic Publishers, 437.

Guisnet M., and Magnoux P., 1989, Coking and deactivation of zeolites - influence of the pore structure, *Applied Catalysis*, 54, 1-27.

Guisnet M., and Magnoux P., 1997a, Deactivation by coking of zeolite catalysts. prevention of deactivation. optimal conditions for regeneration, *Catalysis Today*, 36, 477-483.

Guisnet M., and Magnoux P., 1997b, Roles of acidity and pore structure in the deactivation of zeolites by carbonaceous deposits, *Catalyst Deactivation*.

Guisnet M., and Magnoux P., 2001, Organic chemistry of coke formation: *Applied Catalysis A: General*, 212, 83-96.

Guisnet M. R., 1990, Model reactions for characterizing the acidity of solid catalysts, *Accounts of Chemical Research*, 23, 392-398.

Guisnet M, and Magnoux P, 1994, Fundamental description of deactivation and regeneration of acid zeolites, *Stud.Surf.Sci.Catal*, 88, 53.

Haag W. O., Lago R. M., and Weisz P. B., 1984, The active-site of acidic aluminosilicate catalysts, *Nature*, 309, 589-591.

- Hansford R. C., 1947, A mechanism of catalytic cracking, *Industrial & Engineering Chemistry Research*, 39, 849-852.
- Hansford R. C., Waldo P. G., Drake L. C., and Honig R. E., 1952, Hydrogen exchange between deuterium oxide and hydrocarbons, *Industrial & Engineering Chemistry Research*, 44, 1108.
- Hatch L. F., 1969, A chemical view of refining, *Hydrocarbon Processing*, 77.
- Henriques C. A., Afonso J. Magnoux C., P., Guisnet M., and Monteiro J. L. F., 1997a, Temperature effects on deactivation rate and on nature of coke formed from propene over mordenites.
- Henriques C. A., Monteiro J. L. F., Magnoux P., and Guisnet M., 1997b, Characterization of the coke formed during o-xylene isomerization over mordenites at various temperatures, *Journal of Catalysis*, 172, 436-445.
- Hochtl M., Jentys A., and Vinek H., 2001, Isomerization of 1-pentene over SAPO, CoAPO (AEL, AFI) molecular sieves and HZSM-5, *Applied Catalysis A: General*, 207, 397-405.
- Holmes S. M., Garforth A., Maunders B., and Dwyer J., 1997, A solvent extraction method to study the location and concentration of coke formed on zeolite catalysts, *Applied Catalysis A: General*, 151, 355-372.
- Hopkins P. D., Miller J. T., Meyers B. L., G. J. Ray, Roginski R. T., Kuehne M. A., and Kung H. H., 1996, Acidity and cracking activity changes during coke deactivation of ultrastable Y zeolite: *Applied Catalysis A: General*, 136, 29-48.

Humphries A., Harris D. H., and Oconnor P., 1993, The nature of active-sites in zeolites - influence on catalyst performance, *Studies in Surface Science and Catalysis*, 76, 41-82.

Jacobs P. A., Martens J. A., Weitkamp J., and Beyer H. K., 1981, Shape-selectivity changes in high-silica zeolites: *Faraday Discussions*, 72, 353-369.

Jolly S., Saussey J., and Lavalley J. C., 1994, Ft-IR characterization of carbenium ions, intermediates in hydrocarbon reactions on H-ZSM-5 zeolites, *Catalysis Letters*, 24, 141-146.

Kao H. M., Grey C. Pitchumani P., K., Lakshminarasimhan P. H., and Ramamurthy V., 1998, Activation conditions play a key role in the activity of zeolite CaY: NMR and product studies of Bronsted acidity, *Journal of Physical Chemistry A*, 102, 5627-5638.

Kazansky V. B., and Senchenya I. N., 1989, Quantum chemical study of the electronic structure and geometry of surface alkoxy groups as probable active intermediates of heterogeneous acidic catalysts: What are the adsorbed carbenium ions?, *Journal of Catalysis*, 119, 108-120.

Kissin Y. V., 1994, Degenerate nonprimary products in catalytic cracking of isoalkanes, *Journal of Catalysis*, 146, 358-369.

Kissin Y. V., 2001, Chemical mechanisms of catalytic cracking over solid acidic catalysts: Alkanes and alkenes, *Catalysis Reviews-Science and Engineering*, 43, 85-146.

- Kissin Y. V., 1998, Kinetics of alkane adsorption on a solid cracking catalyst: *Journal of Molecular Catalysis A: Chemical*, 132, 101-112.
- Lange J. P., Gutsze A., Allgeier J., and Karge H. G., 1988, Coke formation through the reaction of ethene over hydrogen mordenite .3. Ir and C-13-Nmr Studies, *Applied Catalysis*, 45, 345-356.
- Liu K., Fung S. C., Ho T. C., and Rumschitzki D. S., 1997, Identification of coke precursors in heptane reforming with a multioutlet fixed-bed reactor and a novel vibrational microbalance, *Journal of Catalysis*, 169, 455-468.
- Lopez G., Perot G., Gueguen C., and Guisnet M., 1977, Isomerization and cracking of saturated-hydrocarbons on hydrogen-mordenite and platinum-hydrogen-mordenite catalysts, *Acta Physica et Chemica*, 24, 207-213.
- Magnoux P, Roger C, and Guisnet M, 1987, New technique for the characterization of carbonaceous compounds responsible for zeolite, *Stud. Surf. Sci. Catal*, 34, 317.
- Manos G., and Hofmann H., 1990, Disproportionation of ethylbenzene on an ultrastable Y-zeolite, Investigation of the coking mechanism in an integral reactor, *Chem.Ztg.*, 114, 183.
- March J., 1985, March, J. *Advanced Organic Chemistry*: New York, Wiley.
- Martens J. A., Jacobs P. A., and Weitkamp J., 1986, Attempts to rationalize the distribution of hydrocracked products .1. qualitative description of the primary hydrocracking modes of long-chain paraffins in open zeolites, *Applied Catalysis*, 20, 239-281.

Marziano N. C., Tortato C., Ronchin L., and Bianchi C., 1998, On the acidity of liquid and solid acid catalysts: Part 1. A thermodynamic point of view, *Catalysis Letters*, 56, 159-164.

Matsushita K., Hauser A., Marafi A., Koide R., and Stanislaus A., 2004, Initial coke deposition on hydrotreating catalysts. Part 1. Changes in coke properties as a function of time on stream: *Fuel*, 83, 1031-1038.

Mccaulay D. A., and Lien A. P., 1951, Relative basicity of the methylbenzenes: *Journal of the American Chemical Society*, 73, 2013-2017.

Moljord K., Magnoux P., and Guisnet M., 1995, Coking, aging and regeneration of zeolites .15. influence of the composition of HY zeolites on the mode of formation of coke from propene at 450-degrees-C, *Applied Catalysis A-General*, 122, 21-32.

Mori N., Nishiyama S., Tsuruya S., and Masai M., 1991, Deactivation of zeolites in n-hexane cracking, *Applied Catalysis*, 74, 37-52.

N. Y. Chen, William E. Garwood, and Francis G. Dwyer, 1996, Shape selective catalysis in industrial applications, Marcel Dekker, Inc. New York.

Nace D. M., 1969, Catalytic cracking over crystalline aluminosilicates. 2. application of microreactor technique to investigation of structural effects of hydrocarbon reactants, *Industrial & Engineering Chemistry Product Research and Development*, 8, 31-&.

Olah G., Kuhn S., and Pavlath A., 1956, Isolation of the stable boron trifluoride-hydrogen fluoride complexes of the methylbenzenes - onium salt (Or sigma-complex) Structure of the friedel-crafts complexes, *Nature*, 178, 693-694.

Olah G., and Molnar A., 1995, *Hydrocarbon Chemistry*, New York, Wiley.

Olah G. A., Halpern Y., Shen J., and Mo Y. K., 1971, Electrophilic reactions at single bonds .3. Hydrogen-deuterium exchange and protolysis (Deuterolysis) Of alkanes with superacids - mechanism of acid-catalyzed hydrocarbon transformation reactions involving omicron electron pair donor ability of single bonds [Shared electron pairs) Via 3-center bond formation, *Journal of the American Chemical Society*, 93, 1251-&.

Olah G. A., and Kuhn S. J., 1959, Aromatic substitution .4. Protonated and deuterated alkylbenzene tetrafluoroborate complexes, *Journal of the American Chemical Society*, 80, 6535-6539.

Olah G. A., Mateescu G. D., Schlosbe. R. H, Mo Y. K., Porter R. D., and Kelly D. P., 1972, Stable carbocations .124. Benzenium ion and monoalkylbenzenium ions, *Journal of the American Chemical Society*, 94, 2034-&.

Ozawa T., 1965, A new method of analysing thermogravimetric data, *Bull Chem Soc Jpn*.

Paweewan B., Barrie P. J., and Gladden L. F., 1998, Coking during ethene conversion on ultrastable zeolite Y, *Applied Catalysis A: General*, 167, 353-362.

Plank C. J., and Nace D. M., 1955, Coke formation and its relationship to cumene cracking, *Industrial and Engineering Chemistry Research*, 47, 2374-2379.

- Poutsma M. L., 1976, *Zeolite Chemistry and Catalysis*, Washington, DC, American Chemical Society.
- Quann R. J., Green L. A., Tabak S. A., and Krambeck F. J., 1988, Chemistry of olefin oligomerization over ZSM-5 catalyst, *Industrial & Engineering Chemistry Research*, 27, 565-570.
- Rabo J. A., 1976, *Zeolite chemistry and catalysis*, Washington, D. C., Am. Chem. Soc. Monogr. 171, American Chemical Society.
- Robert C. Reid, John M. Prausnitz, and Bruce E. Poling, 1987, *The Properties of Gases & Liquids*: New York, McGraw-Hill Co.
- Satterfield C. N., 1980, *Heterogeneous Catalysis in Practice*: New York, McGraw Hill.
- Schraut A., Emig G., and Sockel H. G., 1987, Composition and Structure of Active Coke in the Oxydehydrogenation of Ethylbenzene, *Applied Catalysis*, 29, 311-326.
- Selli E., and Forni L., 1999, Comparison between the surface acidity of solid catalysts determined by TPD and FTIR analysis of pre-adsorbed pyridine, *Microporous and Mesoporous Materials*, 31, 129-140.
- Sie S. T., 1993, Acid-Catalyzed Cracking of Paraffinic Hydrocarbons .2. Evidence for the Protonated Cyclopropane Mechanism from Catalytic Cracking Experiments, *Industrial & Engineering Chemistry Research*, 32, 397-402.
- Smith G. C., 1993, *Catalytic Cracking of n-Alkanes and n-Alkylbenzenes over H-ZSM-5 Zeolite*: PhD, MIT.

Stepanov A. G., Luzgin M. V., Romannikov V. N., and Zamaraev K. I., 1994, Carbenium ion properties of octene-1 adsorbed on zeolite H-ZSM-5, *Catalysis Letters*, 24, 271-284.

Subhash Bhatia, 1990, *Zeolite Catalysis: principles and applications*: CRC Press, Inc.

Thomas C. L., 1949, *Chemistry of Cracking Catalyst*, *Industry & Engineering Chemistry Research*, 41, 2564.

Turkevich J., and Smith R. K., 1948, Catalytic Isomerization of 1-Butene to 2-Butene, *Phys. Chem.*, 16, 466.

Vasques M. H., Ribeiro F. R., Gnep N., and Guisnet M., 1989, Effects of Steaming on the Shape Selectivity and on the Acidity of HZSM-5, *Reaction Kinetics and Catalysis Letters*, 38, 301-306.

Wang B., and Manos G., 2007a, Acid Site Characterization of Coked USHY Zeolite Using Temperature Programmed Desorption with a Component-Nonspecific Detector, *Industrial & Engineering Chemistry Research*, 46, 7977-7983.

Wang B., and Manos G., 2007b, A novel thermogravimetric method for coke precursor characterisation, *Journal of Catalysis*, 250, 121-127.

Whitemore F. C., 1932, The Common Basis of Intramolecular Rearrangements, *Journal of the American Chemistry*, 54, 3274.

Whitemore F. C., 1934, Mechanism of the Polymerization of Olefins by Acid Catalysts, *Ind. & Eng. Chem.*.

Williams B. A., Babitz S. M., Miller J. T., Snurr R. Q., and Kung H. H., 1999, The roles of acid strength and pore diffusion in the enhanced cracking activity of steamed Y zeolites, *Applied Catalysis A-General*, 177, 161-175.

Wojciechowski B. W., 1998, The reaction mechanism of catalytic cracking: Quantifying activity, selectivity and catalyst decay, *Catalysis Review- Science and Engineering*, 40, 209.

Wolf E. E., and Alfani F., 1982, Catalysts Deactivation by Coking, *Catalysis Reviews-Science and Engineering*, 24, 329-371.

Zhu X., Liu S., Song Y., Xie S., and Xu L., 2005, Catalytic cracking of 1-butene to propene and ethene on MCM-22 zeolite, *Applied Catalysis A: General*, 290, 191-199.

APPENDIX 1

Publications

- B. Wang, G. Manos, Acid site characterisation of coked USHY zeolite using TPD with a component non-specific detector, *Ind. Eng. Chem. Res.* 46 (2007) 7977.
- B. Wang, G. Manos, A novel thermogravimetric method for coke precursor characterization, *J. Catal.* 250 (2007) 121.
- B. Wang, G. Manos, Deactivation Studies during Catalytic Cracking of 1-Pentene over USHY Zeolite (submitted in *Chem. Eng. J.*)
- B. Wang, G. Manos, The Role of Zeolitic Strong Acid Sites on Hydrocarbon Reactions (submitted to *Ind. Eng. Chem. Res.*)
- S. Chen, B. Wang, G. Manos, Study of Acidity of Coked Zeolites Using Temperature Programmed Desorption of Ammonia (submitted to *Catal. lett.*)

Conference Proceedings

- B. Wang, G. Manos, Product Selectivity Effects and Deactivation Study during 1-Pentene Reaction over USHY Zeolite, 15th International Zeolite Conference (2007), 211.
- S. Chen, B. Wang & G. Manos, A Novel Classification Method for Coke Components and Acidity Characterisation of Coked Zeolite, 10th International Symposium on Catalyst Deactivation (2006), 136

- B. Wang, G. Manos, Hydrocarbon Conversion on Zeolite and Catalyst Deactivation, AIChE annual meeting, 11. 2007, Utah, USA.

Conference Presentations

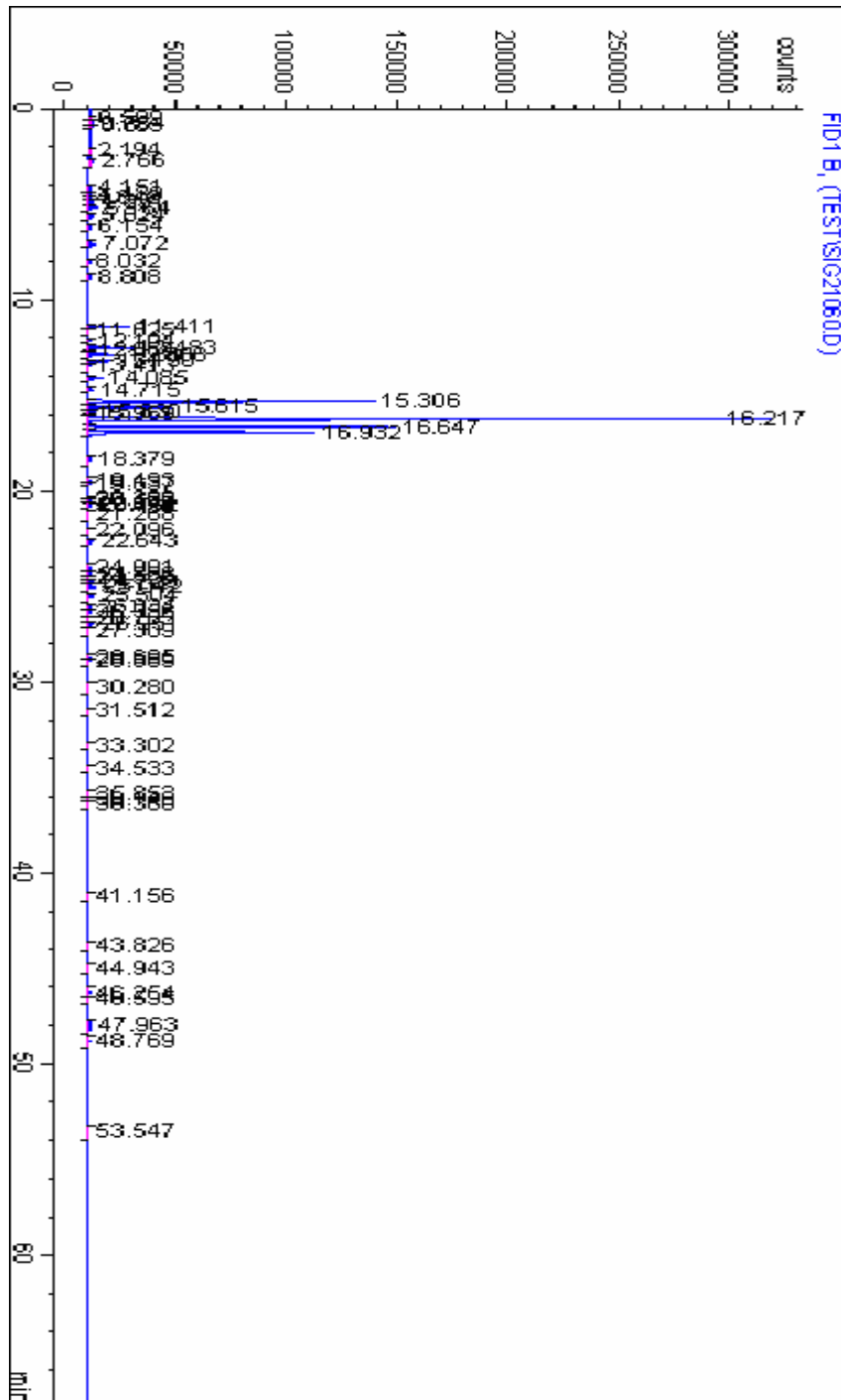
- A novel classification method for coke components and acidity characterisation of coked zeolite, 10th International Symposium on Catalyst Deactivation, 02.2006, Berlin.
- Hydrocarbon Conversion on Zeolite and Catalyst Deactivation, AIChE annual meeting, 11. 2007, Utah, USA

Conference Poster

- Product selectivity effects and deactivation study during 1-pentene reaction over USHY zeolite, 15th International Zeolite Conference, 08.2007, Beijing, China

APPENDIX 2

GAS CHROMATOGRAPH



APPENDIX 3

TEMPERATURE PROGRAMMED DESORPTION

US-Y in nh3.

WIN2910 V5.01

Unit 1

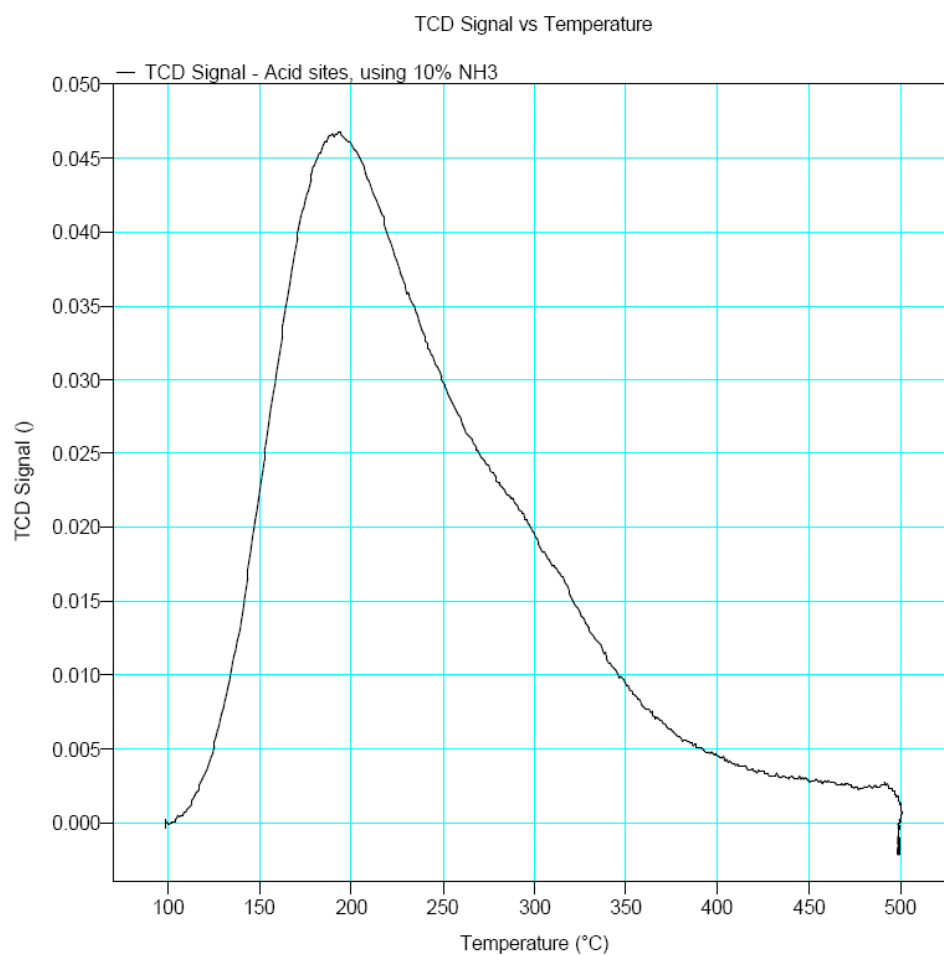
Serial # 309

Page 18

Sample: US-Y in NH3/new prog.
Operator: Baodong
Submitter: Baodong
File Name: C:\WIN2910\DATA\JULIAN\000-298.SMP

Started: 4/14/05 9:34:57AM Sample Weight: 0.0820 g
Completed: 4/14/05 3:22:32PM Report Time: 4/14/05 3:22:32PM

US-Y in nh3 nnamso/new prog.



APPENDIX 4**THERMOGRAVIMETRIC ANALYSIS**